

Emergency Meal Kitchen Services

submitted to the Faculty
of the
WORCESTER POLYTECHNIC INSTITUTE
in partial fulfillment of the requirements for the
Degree of Bachelor of Science

by

Cailah DeRoo

Ivana Indruh

April 28, 2011

Prof. M. S. Fofana, Advisor
Department of Mechanical Engineering
Prof. Erkan Tüzel, Advisor
Department of Physics

ABSTRACT

The goal of this MQP project was to create a design for a portable and compact kitchen unit that could provide three days' worth of food and water for at least 500 people, in any disaster location. This Emergency Meal Kitchen Services (EMKS) unit will help distribute food and water that is necessary in times of need. The EMKS is designed to fit inside an 8 x 15 x 8 foot container and use a range of on-board energy sources. Models describing the geometry of the EMKS and dynamic motion were constructed. The models were constructed in terms of design and stability criteria relating to the weight, transportability, and food preparation capabilities. We created a CAD model of the EMKS to illustrate the three-dimensional layout. Studies have shown that similarly sized units are subjected to uncontrollable excitations during transportation as a helicopter sling load. These excitations cause unsafe flight conditions and induce instability that causes the kitchen unit to swing uncontrollably. In an effort to study these excitations, we modeled the EMKS in a sling load as a pendulum. We used both linear and nonlinear models, for simple and double pendulums, to study the effect of various initial angles on the EMKS' swinging motion. To reduce these oscillations, we proposed a control mechanism utilizing racks and pinion gears. This control mechanism provides control forces acting on the pendulum's pivot point so as to effectively reduce and dampen out the oscillations with the help of a phase delay. Utilizing this mechanism will reduce the uncontrollable swinging, thus making the EMKS easier and safer to transport by a helicopter sling load. Our design of the kitchen will be applicable to not only disaster relief situations, but could also be adapted in military operations.

TABLE OF CONTENTS

<i>Abstract</i>	<i>i</i>
<i>Table of Contents</i>	<i>ii</i>
<i>List of Figures</i>	<i>iii</i>
<i>List of Tables</i>	<i>iv</i>
<i>ACcknowledgements</i>	<i>v</i>
CHAPTER 1. INTRODUCTION	1
CHAPTER 2. BACKGROUND	3
2.1 Disaster Relief	3
2.2 Mobile Kitchens	5
2.3 Commercial Airplane Kitchen Units	7
CHAPTER 3. THE EMERGENCY MEAL KITCHEN SERVICES UNIT	10
3.1 Design Process	10
3.2 Appliance Selection.....	11
3.3 Designing the Layout.....	14
3.4 EMKS Design	19
CHAPTER 4. EXISTING VIBRATION MODELS	23
4.1 Helicopter Sling Load Systems	23
4.2 Crane Dynamics	25
CHAPTER 5. EMKS TRANSPORTATION ANALYSIS	29
5.1 Model Development	30
5.2 Simple Pendulum	31
5.3 Double Pendulum	36
5.4 Control Strategy	46
CHAPTER 6. CONCLUSIONS	53
APPENDIX A. Refrigerator Spec Sheet.....	56
APPENDIX B. Heating Cabinet Spec Sheet	58
APPENDIX C. SolidWorks Drawings and Models.....	60
Appendix D. Simple Pendulum MATLAB Code.....	74
Appendix E. Double Pendulum MATLAB Code	76
APPENDIX F. Driven Pendulum MATLAB Code	78
REFERENCES.....	80

LIST OF FIGURES

Figure 1. Various organizations distribute food for disaster relief.....	3
Figure 2. Ruined house from Hurricane Katrina, a map of countries affected by the Indian Ocean tsunami, and a flooded building in Indonesia.....	4
Figure 3. Humanitarian daily rations being airdropped and collected on the ground by people in need ...	4
Figure 4. Nationwide Mobile kitchen unit and inside appliances and layout.....	5
Figure 5. Deployed Resources' Containerized Kitchen Unit and inside appliances and layout.....	5
Figure 6. An Army CK with soldiers waiting for a meal and being served inside.....	6
Figure 7. Typical methods of container transportation.....	7
Figure 8. Sling load configurations.....	7
Figure 9. Preparing airline meals on the ground, loading them onto the plane, and an airplane galley.....	8
Figure 10. EMKS refrigerator, heating cabinet, griddle, and sink.....	14
Figure 11 Two-dimensional layout of kitchen.....	20
Figure 12. CAD model of EMKS inside from an isometric view and outside serving window.....	21
Figure 13. Simplified pendulum model of sling load and animation of helicopter and load motion.....	24
Figure 14. Proposed fin attached to the CONEX cargo container.....	25
Figure 15. Gantry crane, tower crane, and a ship-mounted crane.....	26
Figure 16. Quay-side container crane model and simplified pendulum mode.....	27
Figure 17. Sling load sketch and EMKS container FBD.....	30
Figure 18. Simple pendulum model and FBD of the container.....	31
Figure 19. Plot of simple pendulum angular displacement for initial angles of 1°, 20°, and 90°.....	35
Figure 20. Phase space portraits for simple pendulum with initial angles of 1° and 90° for 50 seconds...	36
Figure 21. Double pendulum model and FBDs for the hook and EMKS load.....	36
Figure 22. Angular displacement plots for initial angles of $\theta_1=1^\circ$ and $\theta_2=2^\circ$ for the hook and the load....	39
Figure 23. Load angular velocity and acceleration plots for initial angles of $\theta_1=1^\circ$ and $\theta_2=2^\circ$	40
Figure 24. Load phase portraits for initial angles of $\theta_1=1^\circ$ and $\theta_2=2^\circ$ at 1 sec and 20 sec.....	41
Figure 25. Angular displacement plots for initial angles $\theta_1=25^\circ$ and $\theta_2=30^\circ$ for the hook and the load....	42
Figure 26. Load angular velocity and acceleration plots for initial angles of $\theta_1=25^\circ$ and $\theta_2=30^\circ$	43
Figure 27. Phase portrait for initial angles of $\theta_1=25^\circ$ and $\theta_2=30^\circ$ at 25 sec and 100 sec.....	44
Figure 28. Angular position plots with initial angles of $\theta_1 = \theta_2 = 15^\circ$ for the hook and the load.....	44
Figure 29. Load angular velocity and acceleration plots for initial angles of $\theta_1=\theta_2=15^\circ$	45
Figure 30. Load phase portrait for initial angles of $\theta_1=\theta_2=15^\circ$ at 6 sec and 30 sec.....	46
Figure 31. Schematic of control mechanism.....	47
Figure 32. Simplified control mechanism and pendulum representation.....	48
Figure 33. Plots of the load angular position and phase portrait for zero external forces.....	51
Figure 34. Plots of the load angular position and phase portrait with a driving force.....	51

LIST OF TABLES

Table 1. EMKS appliance specifications	12
Table 2. Anthropometric measurements, from [18]	15
Table 3. Dimensions of cabinets and shelving units	18
Table 4. Parameters used in modeling the sling load	30
Table 5. Description of code used to model simple pendulum	34
Table 6. Periods for simple pendulum for different initial angles	34
Table 7. Description of code used to model double pendulum	38

ACKNOWLEDGEMENTS

We would like to thank Professor Fofana of the Mechanical Engineering Department for giving us the opportunity to work with him on this project. In addition we would like to thank him for all of his assistance and support throughout the project. We would also like to thank Professor Tüzel of the Physics Department for his continuous help, particularly with the use of MATLAB software. Both advisors provided us with valuable feedback and guidance throughout the year of working on this project. We would also like to thank Ivica Indruh of Brattle Works Inc. for his assistance in the making of our prototype. We thank him for allowing us the use of his facilities, as well as materials and all the time he took to help us make the prototype of the EMKS unit.

CHAPTER 1. INTRODUCTION

Natural disasters can strike anywhere in the world. Thousands of people are affected each year by disasters such as earthquakes, tsunamis, and hurricanes. These natural disasters cause immense damage to the area hit – building, homes, infrastructure, and vehicles can be demolished or permanently ruined beyond use. Without the usual comforts of home or access to stores, people can be left without clothing, food, water, sanitation, and medical supplies. Over 350,000 homes were severely damaged by Hurricane Katrina [1]. All of these people had to relocate, and many had to rely on Federal relief and donations to rebuild their lives.

Most countries have a government-run organization to aid in disasters; in the United States, we have the Federal Emergency Management Agency (FEMA). Additionally, there are numerous non-profit, non-governmental organizations (NGOs), such as the Red Cross and the Salvation Army, that help in disaster relief. These organizations raise money to donate to affected families and visit the disaster site to distribute supplies, reconnect separated family members, and provide medical assistance.

The goal of this project was to create a design for a portable and compact kitchen unit that provides three days' worth of food and water, for at least 500 people in any disaster location. This Emergency Meal Kitchen Services (EMKS) unit will help distribute food and water that is necessary in times of need. Although there are kitchen units that currently exist for disaster relief, they are typically large and difficult to transport. Most of them are also unable to be deployed worldwide, other than the current containerized kitchen (CK) unit used by the United States military. This military kitchen unit however, is used to supply hot meals to soldiers in battle, not for disaster relief. The CK has similar specifications and goals as our EMKS, so we designed our model to serve as an improvement of the current CK model. Ideally, the EMKS could be used for both disaster relief and, with a few small adjustments, supplying meals to our troops.

We researched existing mobile kitchens, as well as methods of supplying food to large groups of people, as is done on airplanes. After considering many layouts, we identified appliances that would fit two main criteria. First, the appliance had to have the adequate storage for three days' worth of food. Second, the appliance had to be small enough to fit into our desired space of the 8x8x15 ft container. We also considered the appliances' weight and energy consumptions in the final selection. We created simple two-dimensional sketches of different kitchen layouts. Once the final layout of the kitchen was selected, based on feasibility and ease of use, the CAD model was used to create a three-dimensional view of the EMKS.

In addition to improving the layout, storage and cooking capabilities, and serving method, we designed the EMKS to be more compact and easier to transport. The military currently has a problem with transporting CKs as helicopter sling loads because wind disturbances and vibrations cause the unit to oscillate out of control, causing premature release of the CK while in flight to preserve the helicopter. We researched existing control mechanisms, vibration analyses of helicopter sling loads, and crane dynamics. By studying the vibrations of the container, we hoped to identify a method to minimize the damage to the EMKS container and helicopter, as well as potentially eliminate the need to release the load while in flight. We created a mathematical model of the EMKS and derived its equations of motion. As a double pendulum, the sling load is modeled by two second-order, nonlinear differential equations. We completed a mathematical analysis of a simplified pendulum system and determined areas of stability. With this analysis, we identified the necessary damping and created a control system to help minimize the oscillations. This analysis was helpful in making the EMKS easier and safer to transport by helicopter. The EMKS can then be used for international disaster relief.

This report is comprised of six chapters. Chapter Two contains background information from our research on disaster relief, mobile kitchens, and commercial airplane kitchens. Chapter Three describes the design for our kitchen unit. In this chapter, you will find our project design process, the method for appliance selection, and the final layout and design of the Emergency Meal Kitchen Service EMKS. Chapter Four serves as a background section on the existing models of helicopter sling load motion and crane dynamics. Chapter Five describes our sling load transportation analysis. It begins with our simplest mathematical model and equations of motion, then is followed by a more complicated nonlinear model and double pendulum model. This chapter also describes our proposed control mechanism to reduce load swinging. Chapter Six serves as the concluding chapter in which the project objectives, methods, significant results, and future directions are summarized.

CHAPTER 2. BACKGROUND

In times of disaster and war, it can be difficult to find time to prepare meals, or even find food. However, food and water are necessary items for survival. We researched past and existing methods for food preparation and distribution, used for disaster relief and by the United States military. The successful methods described below helped provide us with ideas and improvements for our portable kitchen unit design.

2.1 Disaster Relief

Natural disasters are inevitable and can cause damage across the globe. People who have been affected by natural disasters such as tornadoes, hurricanes, volcanic eruptions, tsunamis, earthquakes, forest fires, and floods can lose their homes, personal property, vehicles, water supplies, and have various injuries. Natural disasters are stressful times for those affected, and it can be difficult to make a meal or even find food sometimes.

The Federal Emergency Management Agency (FEMA), the Red Cross, the Salvation Army, and similar organizations help to alleviate these problems by collecting donations and providing necessities to affected people, as seen in Fig. 1. The American Red Cross is most well-known for providing shelters, medical treatment, and food to disaster areas. They send trained teams and volunteers to affected areas to assess each disaster individually and distribute necessary services and supplies [2].



Figure 1. Various organizations distribute food for disaster relief, such as the Red Cross [3] (left), the military [4] (center), and the Salvation Army [5] (right).

Hurricane Katrina in 2005 caused over \$81 billion in property damage and took over 1800 lives along the Gulf Coast. Areas in Louisiana and Mississippi were particularly hard hit and had lingering floodwaters in houses for weeks. Approximately 350,000 homes were severely damaged [1], as shown by an affected house in Fig. 2. After evacuating and having their homes destroyed, some people displaced by the hurricane still have yet to rebuild their houses and lives. FEMA and volunteers helped in the immediate aftermath to provide supplies and search for survivors. They also provided trailer housing and paid for hotel costs. Additionally, non-governmental organizations collected over \$4.25 billion from

public donations to help in the rebuilding stage. The Red Cross assisted almost 1.5 million families by opening 1400 shelters, serving over 68 million hot meals and snacks, and distributing house clean up kits that contained mops and bleach to flooded houses [6]. The Salvation Army aided 1.7 million families and served over 5.7 million hot meals with their canteen feeding units and field kitchens [7].

Another recent and far-reaching natural disaster was the 2004 Indian Ocean earthquake, which resulted in the worst tsunami in history. The tsunami killed over 230,000 people in fourteen countries, and over 1.6 million people were displaced from their homes [8]. Roads and buildings were destroyed, and most drinking water sources were not useable because of contamination from the ocean's salt water or dead livestock and bodies. Countries and organizations from around the world came together to provide medical support, search and rescue missions, and supply distribution. Many people had to rely on help from these organizations to get food and supplies because their houses were flooded and completely ruined, as shown in Fig. 2.



Figure 2. Ruined house from Hurricane Katrina [9] (left), a map of countries affected by the Indian Ocean tsunami [10] (center), and a flooded building in Indonesia [11] (right)

Humanitarian food drops have been used for many years to distribute food and supplies to war zones and areas that are either unsafe or inaccessible. Food can be airdropped in pallets or individual packages, as shown in Fig. 3. The United States Department of Defense has used humanitarian daily rations (HDRs), which are individual packages of a full day's worth of food, since 1993. These meals are dropped from an aircraft onto a stretch of land and can last up to three years. FEMA also distributed these meals to aid in the Hurricane Katrina disaster recovery. The HDR program has been used successfully in over 24 countries suffering from natural disasters and war [12].



Figure 3. Humanitarian daily rations on a pallet [13] (left), being airdropped [14] (center), and being collected on the ground by people in need [13] (right)

2.2 Mobile Kitchens

There are many designs of mobile kitchens. They range from common ice cream trucks and hot dog stands to mobile trailers to large containerized units. These mobile kitchens have been used to provide food for the military, disaster relief, and special events like large concerts. These kitchens come in a variety of sizes and interior layouts, largely depending on their purpose and number of intended users. A couple of companies have successfully designed and employed mobile kitchens, although most units are large and cannot stand alone.

Nationwide Mobile Kitchens creates temporary structures and mobile modular trailers as various types of units. These units can be used for storage, rest rooms, dishwashing, food preparation, baking, or freezers. The mobile trailers can range in size from 16 to 53 ft long, and the modular trailers can be 30 x 8 ft up to 74 x 16 ft in size. They manufacture a standard 36' mobile kitchen unit with a serving window, shown in Fig. 4. This figure also shows the appliances and cooking area inside the kitchen. Multiple units together have been used on Army and Navy bases [15].



Figure 4. Nationwide Mobile kitchen unit (left) and inside appliances and layout (center, right) [15]

Containerized Kitchen Units, created by Deployed Resources, are kitchens inside connected ISO containers. A two-unit system can serve over 1500 people per meal. The units have their own power, hot water heater, and appliances; however, they do not produce any smaller units. Deployed Resources also has shower, bathroom, laundry, and office units. Figure 5 shows the containerized kitchen unit. These units have been used by the Department of Defense, for disaster relief, and for music festivals. A combination of these units were used as a base camp for First Responders and victims for Hurricane Katrina in 2005 and Hurricanes Ike and Gustav in 2008 [16].



Figure 5. Deployed Resources' Containerized Kitchen Unit (left) and inside appliances and layout (center, right) [16]

The United States military also currently uses a containerized kitchen (CK) unit during times of war overseas for the purpose of rapid food preparation. The CK is a single kitchen that can be deployed to the battalion level or to specific locations. The CK has the capability of preparing a minimum of 550 Army field meals (A-Ration, Heat and Serve Ration) up to three times per day. The CK was first used in 2001, and the Army plans to obtain 742 CK units in total [17].

The CK is equipped with appliances that allow the cooks to prepare A-Ration meals in less than three hours. The kitchen is operable in the range of temperatures from -25 °F to 120 °F and can be deployed nearly anywhere in the world. The CK does not need external power as it contains a generator to provide any needed electricity. The system weight without the trailer, fuel, or water is less than 14,000 lbs. All information that we have about this kitchen is from the Performance Specifications [18].



Figure 6. An Army CK with soldiers waiting for a meal [19] (left) and being served inside [20] (right)

The CK has a single kitchen to prepare food, and a food serving area inside the container that is protected from the elements. An ISO container was used as the shell because it is waterproof and easily transportable. ISO containers are frequently used as shipping containers and can hold up to 67,200 lbs of contents [21]. The kitchen is equipped with Government Furnished Equipment, and all appliances in the kitchen are of commercial food service quality and functionality. The CK has a single 10 kilowatt generator, a temperature control system, windows for natural light and ventilation, an exhaust system, a refrigerator with at least 40 cubic feet of storage, a heating cabinet, hand washing capabilities, floor drains, storage areas, weapons racks, and blackout capabilities.

The CK is transportable by the means of rail, fixed wing aircraft, helicopter slung load, and ground vehicles, as shown in Fig. 7. Forklifts and cranes are used to transfer the CK from one type of transportation to another. The fixed wing aircraft used to transport the CK are the Cargo Jet C-130 and larger Air Mobility Command (AMC) aircraft. The CK also has a trailer, which enables the unit to be towed by vehicles. In all means of transportation, the CK and its trailer are transportable without causing any damage to the CK, the trailer, or the mode of transportation.



Figure 7. Typical methods of container transportation, such as a C-130 [22] (left), a helicopter sling load [23] (center), and a ship-mounted crane [24] (right)

The military uses a Department of Defense Chinook 47D rotary winged helicopter to transport the CK as a suspended sling load. These helicopters can carry sling loads of up to 26,000 lbs and are used to transport shipping containers, humvees, and even smaller helicopters. Sling loads can be suspended using several different configurations shown in Fig. 8 [25]. One major problem of the CK as a sling load is that vibrations and wind disturbances can make the load oscillate during transport. These oscillations sometimes grow out of control and throw the helicopter off balance. When this occurs, the helicopter pilots need to release the CK while in air, destroying the kitchen. For more details on the transportation methods of the CK, refer to Performance Specifications, section 3.4.1 [18].

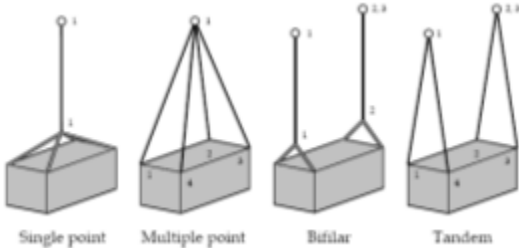


Figure 8. Sling load configurations [26]

A previous MQP studied the manufacturability of the CK [17]. Based on this study, several improvements were suggested and a new design for a thermal fluid containerized kitchen (TFCK) was proposed. The TFCK was a prototype design that used steam as a secondary means of heating in most appliances. The TFCK provided sanitary needs so that a separate sanitation center was not necessary. However, it had problems with an uneven weight distribution and parts becoming loose during transport, among others.

2.3 Commercial Airplane Kitchen Units

When considering the design for this project, we also researched the style of kitchen used on commercial airplanes. A Boeing 747-400 can seat 524 passengers in a 2-class seating arrangement [27], and an Airbus A380-800 can seat a maximum of 853 passengers in a single-class double deck

configuration [28]. Both of these large planes are used for long, international flights, on which at least one hot meal is served. Many commercial airplanes have the capability of serving one to two hot meals to a large number of people in a very limited space, as well as in a short amount of time. We primarily looked at the methods and means of food preparation to see if we could implement these methods of quick food preparation into our kitchen design.

Food is delivered to the airplane kitchen (which is located on the ground, not the plane) on a daily basis. Any food that needs to be cooked is cooked in this kitchen. If the food is immediately being transported to the aircraft, then the trays of cooked and prepared meals are placed in moveable heating or cooling storage containers, depending on the temperature needed. These storage containers are then transferred to the aircraft by delivery trucks equipped with hydraulic platforms that allow for easy offloading from the truck directly to the main gallery of the aircraft, as shown in Fig. 9. If the food is not going to be transported to the aircraft immediately, the cooked meals are frozen to a temperature below five degrees Celsius. Once the meals are on the aircraft, they are placed in heating cabinets, which thaw out the food and heat it to a desired temperature, until it is ready to be served.

Airplane galleys are very compact and make use of any available space. Everything also needs to be secured into place, especially during takeoff, landing, and turbulence. Since the meals are prepared on the ground, the airplane attendants just need to distribute the trays of meals on the airplane. No cooking or preparing is done on the plane, so these methods were not particularly helpful when considering our EMKS design and operation.



Figure 9. Preparing airline meals on the ground [29] (left), loading them onto the plane [30] (center) , and an airplane galley [27] (right)

Our emergency meal kitchen service (EMKS) will contain food and water that is necessary to survive. The EMKS will store food, cook food, and serve the prepared meals. It can be transported to almost any location and start serving hot meals within two hours. The kitchen was designed to be used in a variety of climates – from deserts to icy tundra to swamps to snow banks- so that it can be used

worldwide for emergency situations. The motivation behind this project was that no current kitchen model for disaster relief was small enough to be easily transported and used internationally. The EMKS was modeled loosely on the existing CK, with many improvements. Our design will help make providing meals easier, more efficient, and more widespread to disaster areas than current methods.

CHAPTER 3. THE EMERGENCY MEAL KITCHEN SERVICES UNIT

The goal of this project was to create a design for a portable and compact kitchen unit that provides three days' worth of food and water for at least 500 people in any disaster location. This kitchen will be called the Emergency Meal Kitchen Services or EMKS unit. As discussed in Chapter 2, there is no existing device with our same goal for the purpose of disaster relief, however there is a similar kitchen unit used to prepare meals for the military. Our redesign will be applicable to not only disaster relief, but could also be adapted with small changes to be used by the military. Our design will be an improvement over the military's existing model because it is scaled down; its smaller size and lighter weight will make it easier to transport. In this chapter, we discuss our design criteria, the process of selecting appliances, and creating a layout. We will then present our EMKS design, with the aid of sketches and CAD drawings.

3.1 Design Process

To accomplish our goal, we needed to satisfy the following design criteria:

- The size of the kitchen should be no greater than 8'D x 20'W x 8'H (a standard 20' long ISO container, currently used by the US military)
- Weigh less than 14,000 lb, not including the water or food supplies
- Capable of preparing 500 hot meals within three hours, three times a day
- Have a means for serving the food (i.e. a six foot long serving window)
- Need appliances to cook meals, hold warm food, and refrigerate/freeze unused food
- Need clear counters to prepare food that do not exceed 36" in depth
- Need adequate storage for spices, pots, utensils, first aid, fire extinguishers, etc.
- Needs to be transportable by air, land, and water to maximize its usefulness around the world

These design criteria will ensure that the EMKS will be functional and useful.

When designing our EMKS, we first researched various appliances. The best appliances were selected based on the criteria listed above. We created different layouts for the EMKS using scaled drawings, while trying to keep the weight balanced and creating two kitchen units and a serving area. Once we created a final layout, we created a three dimensional CAD model using SolidWorks. The following sections will describe in more detail each of these steps in our design process.

3.2 Appliance Selection

Initially, we researched standard household appliances to use in our EMKS. However, most of these appliances were too large and had a relatively small capacity. Commercial appliances were more suited to our needs and criteria. In all, we researched over fifty refrigerators and freezers, twenty heating cabinets, and twenty stovetops and grill tops, of a variety of brands. To create a layout for the kitchen, we needed to select appropriate appliances that satisfied the following criteria:

- Small enough to fit in container with other appliances and work space
- Large enough capacity for three days' worth of food
- Meet basic temperature requirements, as given by the FDA [31]
- Minimize weight
- Minimize energy usage

In order to store enough food for 4500 meals (1500 meals for 3 days), the kitchen needs to include refrigerators and freezers with a total capacity of at least 40 cubic feet. To be able to cook and serve 40-50 meals in 15 minutes (a total of 500 people in three hours), the EMKS needs at least one grill or stovetop, 1 heating cabinet or oven to cook food, 1 heating cabinet to hold warm food, and at least 1 sink. The heating cabinets need to hold at least 10 commercial standard, full size steam table pans. The sinks need to be a minimum of 10 inches deep and 1.2 cubic feet in volume. We used the minimum requirements for the military's CK because their values are known to work for their existing kitchen [18].

According to the FDA [31], refrigerators need to be able to hold food at temperatures of 38°F or lower and freezers need to keep food at temperatures lower than 0°F or lower. When cooking food (especially meat), it is important for the food to reach temperatures of at least 165 °F. Heating cabinets used to keep cooked food warm must maintain the food's temperature at no less than 135 °F.

The total weight of the kitchen, not including food and water, cannot exceed 14,000 lbs. When designing the kitchen, we selected appliances with the smallest weight after the size and capacity restrictions were satisfied. The lighter the kitchen, the easier it will be to transport. By minimizing the weight, the kitchen will be less likely to swing out of control.

When comparing appliances, we also considered the energy usage. The military's current kitchen uses one 10 kW generator to supply electricity to all the appliances and lights. When all of the appliances are on and operating, they cannot use more power than the generator can supply. Ideally, we were looking for Energy Star rated appliances to minimize power usage, but this was not always possible due to the other restrictions described above. If Energy Star appliances were not available, we selected the appliance with the lowest energy requirement once all of the other criteria were satisfied.

Table 1 shows a summary of the selected appliances and their specifications. Each of these appliances is described in the following subsections, and pictures are shown in Figure 10.

Table 1. EMKS appliance specifications

Appliance	Brand - Item #	D (in)	W (in)	H (in)	Weight (lb)
Fridge/freezer	GE Profile PSIC5RGXBV	28.75	35.75	72.125	394
Heating Cabinet	Doyon DPWI18	29.75	22.75	69	255
Grill Stovetop	Uniworld UGR-3E	19	25	14	65
Generator	Generac GP5500	33.5	26.5	27.5	167

Refrigerator

The GE Profile PSIC5RGXBV is a side-by-side refrigerator and freezer [32]. Table 1 has a summary of the refrigerator’s specifications. The main reason for selecting this specific refrigerator was that it had smallest dimensions out of all the refrigerators that met the capacity requirement. This refrigerator is Energy Star rated and uses 120 V, 60 Hz, and 15 A. The refrigerator can maintain temperatures of 34-46 °F, and the freezer can reach temperatures of -6 to 8 °F, both of which satisfy the FDA’s requirements. It has a refrigerator capacity 15.28 cubic ft and a freezer capacity of 9.32 cubic ft. With two refrigerators, we would have 49.2 cubic feet of total capacity, which exceeds the current capacity of the military’s CK. It will be beneficial to have two refrigerators so that each kitchen unit will have one, eliminating the need to walk from one end of the EMKS to the other. Two separate refrigerators also made it easier to balance the weight in the EMKS. See Appendix A for the manufacturer’s specification sheet.

Heating Cabinet

The Doyon DPWI18 is a dual-temperature insulated heating cabinet [33]; its specifications are listed in Table 1. This heating cabinet is more reasonable than an oven because it can both cook and hold warm food. We would need a heating cabinet to hold warm food if we had an oven, so this dual-temperature cabinet combines everything into one compact unit that is more space-efficient. This heating cabinet weighs less than the combination of a smaller holding cabinet and a separate electric range. It uses 2.3 kW of power to run. Additionally, this heating cabinet had the smallest dimensions to fit the space, while having a capacity to hold 18 standard sheet pans that are 18” x 26”. As with the refrigerators, having two heating cabinets will help in minimizing traveling between the two kitchen units. By having two of these cabinets, there will be a capacity for 36 standard sheet pans, which exceeds the military’s CK capacity of 10 sheet pans. The heating cabinet can be controlled to have

temperatures between 50 and 250 °F, so they meet the FDA's basic temperature requirements for both cooking and holding food. See Appendix B for the manufacturer's specification sheet.

Griddle

We selected the Uniworld UGR-3E electric griddle because we needed a stovetop without an oven [34]. This griddle fits on a countertop and allows for storage beneath the counter. This type of griddle will make it easy to cook many servings of food (say scrambled eggs or hotdogs) at once without the need of pans because of the special cooking surface. However, this griddle can still be used like a regular stovetop for heating pots up. It also has a dual thermostat control so that the griddle can cook two types of food at different temperatures.

Generator

The total energy required to run all of the appliances simultaneously is approximately 8.6 kilowatts. To accommodate this, we decided to select a generator that provided at least 10 kilowatts to be sure that all of the electric needs were satisfied. Most appliances require more energy to start up than their steady state operating requirements, so the extra energy supply will be most helpful when the kitchen is initially starting up. Care has to be taken since turning on all appliances at the same time may overload the generators. The generators should also not be run at 100% capacity all of the time because the wear and load will result in a shortened lifetime. Using a generator with a slightly higher power than the EMKS requires will help keep the average load below the 100% capacity.

We decided to use two Generac GP5500 generators, each of which provides 5500 watts of electricity [35]. By using two smaller generators, each kitchen unit can have its own power source. If one of the generators stops working, it will be helpful to have the second generator so that the EMKS can continue providing food, albeit at a slower pace. Having two generators also helped in maintaining weight balance of the EMKS. Although having two separate units weighed more than one 10 kilowatt generator, the other benefits outweigh this disadvantage. We selected this specific generator because of its size and energy output. The generator comfortably fits under a counter, and it provides more than enough power. A comparable 5 kW generator was slightly larger (and did not fit under a counter), so we selected the higher power generator. With all of the appliances running at once, the generator will be working at approximately 75% capacity. This generator's specifications are listed in Table 1 and further details in the specification sheets are in Appendix C.

Sink

The EMKS will have two Just SX-1719-A-GR sinks, shown in Figure 10. The sinks will be used for hand washing, cleaning food, draining food, and washing dishes. This sink is 17" D x 22" W x 10.5" H and weighs about 10 lbs. We selected this sink primarily because of its dimensions. Many other sinks were too large for our available counter space. The extra-deep basin will help make up for the fact that it is a smaller sink. This sink also satisfies the military's specifications that the sink be at least 10" deep. See Appendix D for the manufacturer's specification sheet.



Figure 10. EMKS refrigerator [32], heating cabinet [33], griddle [34], and sink [36]

3.3 Designing the Layout

Once we selected the best appliances based on the criteria listed in the previous section, we drew scaled sketches to create the kitchen's layout. When creating the layout, we kept several things in mind. We wanted to create at least two miniature kitchen areas in the unit. This would help create more workspace and allow four people to work simultaneously. If two people were working in each kitchen area, they would be less likely to get in the way or interfere with the other cooks. The individual cooking areas will minimize the need for travelling between units. Each cook should have access to each appliance in their individual cooking area to minimize travelling between units.

Similarly, the design of the layout should make cooking and preparing food as easy as possible. The layout was based on existing kitchens that are known to be usable. According to the CK Performance Specifications, walkways should be at least 27 in wide to accommodate most people [18]. Table 2 gives other anthropometric measurements that we used in designing the kitchen. When designing the two smaller kitchen units, we tried to keep the weight balanced throughout the container to make transportation easier. Ideally, the center of gravity should be in the center of the container. If it is significantly off-center, the helicopter will have a higher risk of losing control in flight.

Table 2. Anthropometric measurements, from [18]

Description	Dimensions	Application
Overhead reach	73 in (5 th percentile female)	Shelf height
Functional reach	32 in (5 th percentile female)	Counter depth
Stature	74 in (95 th percentile male, boots)	Head clearance
Shoulder breadth	27 in (95 th percentile male, bulky clothing)	Passage clearance
Weight	199 lb (in BDU)	Roof weight limits

To help mitigate the military’s problem with their current kitchen unit spinning while being transported as a helicopter sling load, we made the kitchen container smaller. Instead of a 20-foot long ISO container, we chose to use a similar container that is 15 ft long by 8 ft wide by 8 ft high. This container has 120 square ft of floor space that can be used for the kitchen’s layout.

A new addition to the EMKS that the military’s kitchen does not include is a bathroom. This improvement will be for the use of the cooks during their shifts. The bathroom will include a toilet and a hand-washing sink at minimum. This bathroom can be similar in size to airplane bathrooms. The toilet should use a minimum of water when flushing and will be connected to an appropriate water supply and waste treatment. By including a restroom, we eliminate the need for a separate restroom facility.

In our first attempts at sketching layouts, we found that our appliances (primarily the refrigerators) were too large to have multiple units fit in the available floor space. We concluded that having two kitchen units of approximately 8’ x 6’ would be better than having only one large kitchen or four smaller kitchens (one in each corner). We reselected smaller refrigerators that fit into the two-unit design. When arranging appliances, we kept six feet of one long side of the container open on the inside for the serving window.

Serving Window

The EMKS will have a serving window that will allow the personnel inside the kitchen to serve meals to the public outside of the container. The serving window is located on the long side of the container, between the two kitchen units. The window is 74.4 in long and 32 in high. In the closed position, the serving window is folded up and acts as part of the EMKS’s container wall. It is secured in place with several latches on the inside and outside of the container. In the open position, the serving window folds down from the container wall and is secured perpendicular to the container wall with support brackets. The window has a small lip along the outer edge to prevent food and serving containers from falling off the edges.

Because of its location in the center of the container, it was be easy for both kitchen areas to transfer cooked food to the serving area, minimizing traveling and foot traffic. One person, the server, can be in the serving area and be responsible for transferring cooked meals to the public through the serving window. The server can communicate with the other cooks about what food needs refills. The method of serving the food depends on the type of food being cooked. Meals can be presented to the public in individual meal packages or in large quantities of food, such as spaghetti, sauce, and salad. These large quantities could be supplied in serving pans that the public can help themselves to.

Bathroom

Within the EMKS there will be a bathroom unit that is to be used by the kitchen staff only. The entire bathroom is based on the compact design of an airplane. There is very limited information on the size of airplane bathrooms. JetBlue gives information about a bathroom on the aircraft that is approximately 37 in wide by 47 in deep, with a doorway entrance of approximately 19 inches [37]. The bathroom of the EMKS, much like airplane bathrooms, will have a sink, a vacuum-flush toilet, and a trash receptacle, including storage for all the necessary items for the bathroom.

Heating System

One complaint of soldiers using the CK in cold environments is that the CK can get very cold. They put cardboard on the floor to help insulate the bottom and make it more bearable to stand on the freezing metal. To help solve this problem, we considered a variety of mechanisms to provide heat and insulation for our EMKS.

Many households have gas or oil furnaces to provide heat. These would not be practical for the EMKS due to the size and weight. Steam radiators are not very efficient and they require more water than the EMKS could hold. Electric resistance heaters are expensive and would use electricity from the generators that need to power the appliances. The main drawback to active solar heating is that sunlight is required. This could be used as a secondary heating means, but a primary method would be needed that could work regardless of the weather outside.

We concluded that a pellet stove would be a good method for heating the EMKS. They are more efficient than wood stoves with an 85% efficiency (compared to 50% for oil furnaces). The pellets used for fuel are made of recycled and scrap wood that has a cleaner burn than regular wood. This means there is less of a buildup in the flue and a smaller fire hazard. Pellet stoves are also cheaper than wood stoves and need to be refueled less often. Additionally, the pellet stoves could provide and distribute

more than enough heat for the EMKS. When travelling to warm locations where heat will not be needed, the pellet stove can be removed from the EMKS to make the unit lighter.

Entrances to Kitchen

The EMKS will have two main entrances. The entrances to the kitchen were placed on the opposite long side of the serving window, with one entrance into each kitchen area. This was done to reduce the potential traffic within the kitchen. If an entrance was by the serving window anyone could potentially enter, or those who need to enter would not be able to do so due to the traffic outside the window. By placing the doors on the back of the unit, it is accessible to those people who need to enter. Having two entrances will also provide exits from the EMKS in case of a fire or emergency. Additionally, there will be an entrance on the backside of the kitchen to the area where the pellet stove is located. This will allow for easy access to refill the fuel.

Ventilation & Cooling

Ventilation and cooling within the EMKS will be in the form of windows and screens, as well as in ceiling vents. The doors used to enter the kitchen areas will be equipped with screens, so that the main doors could remain open to let in fresh air and light. The serving window also allows for a large area of ventilation. Having these ventilation areas on opposite sides of the container will allow for better cross breezes and air circulation. Within the kitchen there will also be ceiling vents to pull the smoke and fumes from cooking out of the kitchen. The ceiling vents will not allow any environmental elements (rain or snow) to enter the kitchen.

Countertops

We decided to incorporate stainless steel countertops in the kitchen. Metal countertops are usually a thin sheet of metal attached to a wood backing, and they are commonly used in large restaurants. Metal countertops are heat-proof and can withstand hot pots better than laminate and solid counters. They are easy to clean (though bleach will ruin the surface), durable, scratch resistant, and will not stain. We also considered laminate, solid, granite, and other stone countertops. The main drawbacks to the stone countertops were the heavy weight and high cost. Laminate countertops are the cheapest and lowest quality available. Though they are stain resistant, direct contact with a hot pan could ruin the surface. Solid countertops were also not of the same quality as the metal countertops.

All of the working spaces, including countertops, are at a standard height of 36 in and at a depth no greater than 32 in, as suggested by the measurements in Table 2. All the countertops have rounded edges in order to prevent anything from being caught on the edges and to avoid any potential hazards associated with sharp edges.

Storage

Storage for supplies is available in the form of both cabinets and shelving units both under and above counters. These storage units will be used to store all supplies necessary for cooking and serving the food, such as pots, pans, spatulas, forks, spoons, etc. There are also storage spaces for fire extinguishers near the cooking areas and pellet stoves. The cabinets will have doors on them that can latch during transport, the shelving units will have nets over the front to prevent the materials from drifting and falling during transport. Table 3 provides the various cabinets and shelving units used, as well as their sizes. Refer to Fig. 11 for locations of storage units.

Table 3. Dimensions of cabinets and shelving units

Appliance	D (in.)	W (in.)	H (in.)
Generator Cabinet 1	33.6	32.0	36.0
Shelf Above Generator	14.0	32.0	1.5
Cabinet 2	20.0	24.0	36.0
Sink Cabinet	20.0	26.0	36.0
Shelf Above Sink	14.0	26.0	1.5
Storage Cabinet	19.0	22.0	81.6
Stovetop Cabinet 3	20.0	26.0	36.0
Hinged Counter 4	20.0	22.0	1.5

Basement

The EMKS will contain a sort of basement; the bottom foot of the container will be separated from the work area by a floor. This basement area will be used for the containers for the clean water supply, gray water recycling mechanisms, septic system, and extra storage for supplies. Because it is not easy to access the center of this area due to the low clearance, there will be trap-door openings inside of the EMKS through the floor to see critical areas of the basement items. The water containers will be oriented so that the filling and draining connections are easily accessible by a hose from an edge door.

3.4 EMKS Design

We created a primary design that satisfied all of the design criteria described in Section 3.1. To illustrate this design, we used scaled sketches and CAD models created using SolidWorks. The preliminary design was in an 8 ft wide by 8 ft high by 15 ft long container. This container is equipped with two completely, independently functional kitchens. In each kitchen, there is a refrigerator, a heating cabinet, a sink, a grill top, as well as a generator, and necessary storage space for all cooking materials. Each of these kitchens has a separate access point from the outside, as well as an access point to the restroom, which is located in the center, between the two kitchens. In this design, there is also a heating system located behind the restroom, which utilizes the pellet stove system in order to supply the entire container with heat. This heating system also has an access point from the outside of the container and could be easily removed from the container in the case that it is not needed, thus providing more storage space if necessary. The following checklist illustrates how each of the design criteria were completed.

Criteria 1: The size of the kitchen should be no greater than 8'D x 20'W x 8'H.

We used an 8'D x 15'W x 8'H container for the EMKS.

Criteria 2: The weight of the kitchen must be less than 14,000 lb.

The EMKS is approximately 10,000 lb, not including any food or supplies.

Criteria 3: The kitchen must be capable of preparing 500 meals three times a day.

We exceeded the capacities for each appliance listed in the CK's minimum requirements, and have more storage for supplies and dry food.

Criteria 4: The kitchen must have a means for serving the food to the public.

The EMKS has a 74 in serving window built into the container. This serving window provides a means of transferring the food from the kitchen to the people outside the kitchen.

Criteria 5: The kitchen needs appliances that are capable of cooking three meals a day, holding warm food, and refrigerating/freezing unused food.

The EMKS has dual-temperature heating cabinets that can be used to both cook food, and hold warm food. Grill tops are also capable of cooking and reheating food. Two side-by-side refrigerators and freezers are used to keep unused food.

Criteria 6: The kitchen needs clear counters to prepare meals, under 32" in depth.

The two permanent counters have a depth of 33". Though this is deeper than the specifications, the extra inch will not be detrimental; this extra inch was necessary to completely house the generator underneath the counter. The two hinged counters have depths of 20".

Criteria 7: The kitchen must have adequate storage for necessities. ☑

In the design, there are cabinets built into every aspect of free space, trying to minimize the amount of free unused space. The EMKS has more storage space than the CK does.

Criteria 8: The kitchen must be transportable by air, land, and water. ☑

By using something like an ISO container, the EMKS will be transportable by cranes and forklifts. Since it is smaller than the CK, it will fit into the same aircraft and ships. The following two chapters also describe the EMKS's transportability as a helicopter sling load.

Scaled Drawing

In our preliminary design, the team first created scaled two-dimensional drawings. These drawings were used to create an appropriate layout for the inside of the kitchen, in order to ensure that all the necessary items would fit, as well as to ensure that the walking spaces that are necessary would be achieved. Figure 11 shows the final of these top-view layout sketches.



Figure 11 Two-dimensional layout of kitchen

The dashed lines in front of the refrigerators show how far the doors will open at 90°. A generator will be housed underneath the counters numbered 1. The storage areas will be floor to ceiling cabinets with shelving. There are additional storage cabinets underneath the grill top and sink and shelves above.

Counters 4 are hinged. They can be secured in place for more work area, or they can be unhinged to allow access to the serving area or bathroom. The two entrances to the kitchen are on the top side of the drawing between the fridge and storage (on the left) and storage and heating cabinet (on the right).

SolidWorks Design

Based on the scaled layout of the kitchen, the CAD model was created using SolidWorks. The model was created using the dimensions of the various appliances, as well as the layout of the scaled drawing. The SolidWorks model was created using ANSI standard, in the units of inches and is created on a full scale. In the three-dimensional model, there is a cylinder that is used as an approximation of a person, as is done in Thermal-Fluid Sciences problem 16-31 [38], to show general proportions. This model can be seen in Fig. 12. The space between the appliances is necessary for proper air circulation. Additional CAD images of the EMKS can be found in Appendix E.

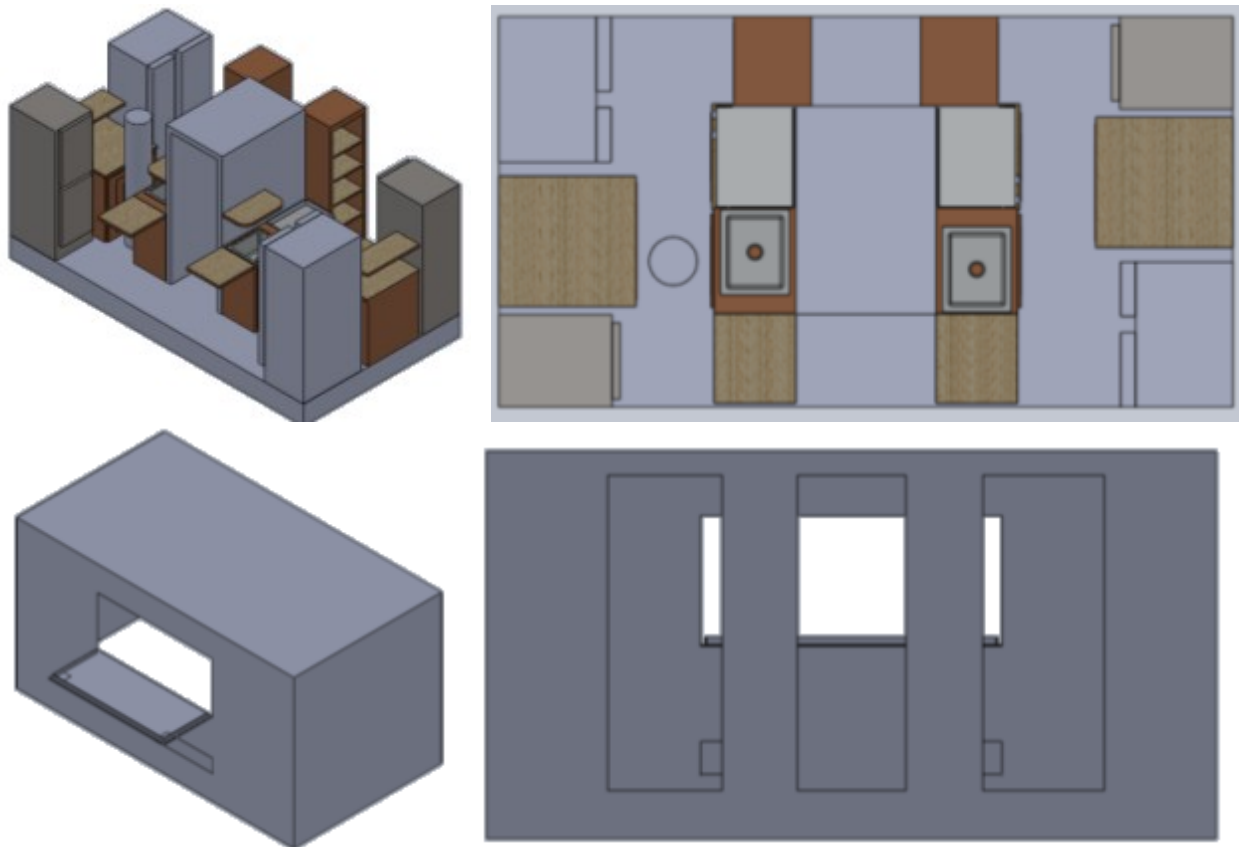


Figure 12. CAD model of EMKS inside from an isometric view (top left) and top view (top right) and outside serving window (bottom left) and outside back entrances (bottom right)

Center of Mass

To ensure that the EMKS was balanced, we calculated the center of mass of the unit with the above layout. To make this calculation, we assumed that the center of mass of each appliance was in the center. The center of mass was located exactly in the middle length-wise, a couple inches backward of the midpoint depth-wise, and several inches upward from the midpoint of the height. This location is almost ideal in that it is very close to the center of the container. A central location will help make modeling and being carried as a load easier.

This original design of the Emergency Meal Kitchen Services unit is an improvement over existing mobile kitchens. One unit has the capability to serve three hot meals a day to at least 500 people. The design is smaller, lighter, and more energy and space efficient than the existing military CK. The design is also transportable by land, water, and air vehicles, making it usable around the world to aid with any natural disaster.

CHAPTER 4. EXISTING VIBRATION MODELS

Helicopters are frequently used to transport the military's CK and other cargo containers as suspended sling loads. Both the United States military and the Australian Army have reported problems with helicopter sling loads swinging out of control, to the point where the pilot needed to release the load while still in flight to regain control and preserve the helicopter [26, 39]. This out of control swinging happened especially when travelling at high speeds.

We researched existing helicopter sling load models, as well as crane load models. A crane's suspended load experiences similar oscillations as a helicopter sling load. After studying existing models, we modeled the EMKS as a sling load, designed a control mechanism to reduce the swinging oscillations, and identified areas of stability to help address the problem of uncontrollable swinging, as described in Chapter 5. There are many methods for modeling the motion of an object, and the following chapter will give a brief summary of selected published models for both helicopter sling loads and crane loads and the mechanisms used to control or dampen the oscillations.

4.1 Helicopter Sling Load Systems

Several groups have modeled helicopters with sling loads to determine the system dynamics and stability areas. In this section, we will summarize three models, along with the types of equations used and their results. These articles were the most helpful in creating our own model for the EMKS unit as a helicopter sling load.

Roger Stuckey has published several extensive and detailed reports on modeling the system dynamics of a helicopter sling load for use by the Australian Army [26, 39]. He claims that, "several incidences have been reported by the Australian Army alone, in which possible aerodynamic excitation or dynamic instability, resulting in uncontrollable oscillations, has forced premature release of the load," [39]. By modeling the dynamics of the helicopter and load, these problems could be prevented.

Stuckey derived equations of motion of the helicopter and sling load from the Newton-Euler equations in terms of generalized coordinates and velocities. In the model, the cables are represented as elastic springs, but they can be simplified to consider inelastic cables. For simplification, the model does not consider the load and cable aerodynamics or the rotor downwash. The overall system was simplified to a two-body pendulum problem, shown in Fig. 13.

He created the Helicopter Slung-Load Simulation (HLSIM) in MATLAB to test simulations of various load weights, suspension configurations, and multiple loads. These simulations gave animations showing how the load will react to certain helicopter motions, an example of which is shown in Fig. 13.

These simulations were also used to determine the areas of stability for different frequencies and air speeds. One finding of the simulations is that an increase in load mass led to a small increase in instability.



Figure 13. Simplified pendulum model of sling load (left) and animation of helicopter and load motion (right) [26, 39]

Reddy et al. also created simulations of helicopters with sling loads to identify the operational and stability limits of CH-47D helicopters used by the Australian Army and Special Air Services [40]. This is the same type of helicopter that would likely be used to transport the EMKSS unit. Their model was based on that created by Stuckey [39], but they combined aerodynamic data on several types of loads into the model. With the additional load aerodynamics, they simulated the effects of several load parameters on the system stability, specifically on a 4000 lb CONEX container from a lateral helicopter move at 100 knots. They concluded that reducing the mass and load lift and drag coefficients reduced the oscillation amplitudes. Conversely, the load pitching moment variation, forward speed, and pilot input control magnitude all increase destabilization of the load.

Cicolani and Ehlers studied how to stabilize the side-to-side (yaw) oscillations of a 6 x 6 x 8 ft CONEX container as a UH-60 helicopter sling load. The goal was to increase the maximum travel speed of the helicopter, while minimizing the container oscillations. Most helicopters are limited in speed when carrying a sling load; by increasing the limits of stability, helicopter transport will become more efficient. They performed a flight test and found that the load on a swivel connection would rotate while the helicopter was hovering at 45 deg/sec and 120 deg/sec while traveling forwards at 60 knots. With a non-swivel connection, the container would spin back and forth (winding and unwinding) faster as the airspeed increased. For a 4000 lb CONEX container, the load was unstable when the helicopter was traveling faster than 80 kts.

To reduce the side-to-side oscillations, Cicolani and Ehlers proposed to attach a vertical fin to the container, as shown in Fig. 14. They tested this method using simulations that were based on helicopter and slung load equations of motions and aerodynamics. It models the cables as elastic and

accounts for rotor downwash. For a helicopter traveling at 60 kts, a passive fin reduced the magnitude of the oscillations until the container reached steady state and reduced the spin to 15 deg/sec. The active fin resulted in faster and more effective damping, though it required more control mechanisms than the passive fin. The stability for both passive and active fins was increased up to a travel speed of 110 kts.

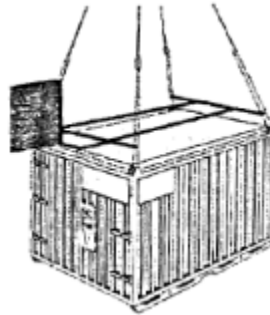


Figure 14. Proposed fin attached to the CONEX cargo container [41]

Bisgaard et al. used delayed feedback as a control mechanism to reduce and dampen sling load swinging [42]. They focused on how the control was applied to autonomous helicopters and used the AAU Corona (a 1 kg electric helicopter) and the GT-Max 100 kg helicopter for modeling and flight testing. Their control system uses input shaping feedforward and feedback loops with time delays to actively dampen the swinging. They modeled the sling load oscillations with and without the controllers on both helicopters and confirmed with flight tests that the controllers significantly reduced oscillations. Neither of these helicopters is life-size, but the methodologies and theory behind this model could be extended to full size, piloted helicopters.

4.2 Crane Dynamics

Cranes in motion induce oscillations on their loads, similar to those experienced by helicopter sling loads. Most of these oscillations are due to inertial forces from the load moving, excitations from the crane moving, and environmental forces like wind. According to Adbel-Rahman et al., “Payload pendulations/oscillations and the need to suppress them have been identified as a bottleneck in the operations of the transportation and construction industries,” [43]. Without control mechanisms, the crane operators have to stop moving the crane or try to perform counter-maneuvers to reduce the load swinging. Large oscillations can be dangerous in the close quarters of shipyards, where accurate placement and movement of loads is necessary. Loads that have large swinging motions are a danger to workers, nearby containers or object, and the crane itself. The following section will summarize several methods that have been used for modeling crane dynamics and reducing the load oscillations.

Abdel-Rahman et al. wrote an extensive review on crane dynamics and the various published methods used to model the crane and load when in motion [43]. There are two main types of crane models – distributed mass and lumped mass. The distributed mass models consider the cable as a distributed mass and the load as a point mass. The two models described in Abdel-Rahman’s summary would not pertain to our application and model for helicopter sling loads. One modeled the cable as flexible and ignored the inertia of the payload, and the second model was only valid for light loads with a mass nearly equivalent to the cable mass.

The lumped mass models are the most popular representations. Most model the load as a spherical pendulum, with a massless cable and point mass load. Extended models consider both the crane support and load in the dynamics and are more complicated. Reduced models assume that the load motions do not have a major reciprocal effect on the crane. These models are nonlinear, but many models have been reduced to simpler, linear models when assuming small oscillations. Another simplification comes from two-dimensional models assuming that there are no out-of-plane oscillations of the load. When using multiple suspension cables, the load can be modeled as a rigid body instead of a point mass. Additionally there were models specific to the design and motion of gantry, rotary, boom/tower [44], and offshore cranes. Figure 15 shows some of these types of cranes.

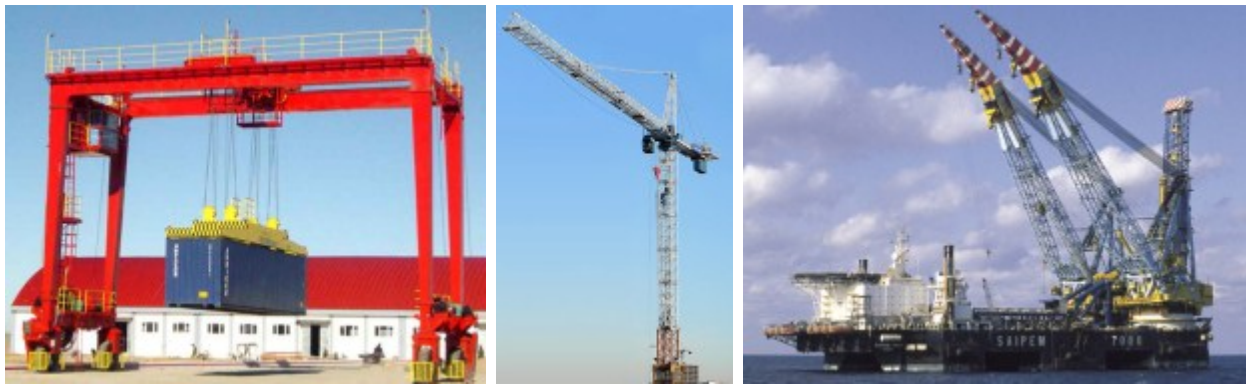


Figure 15. Gantry crane [45], tower crane [46], and a ship-mounted crane [47]

Container crane loads are usually modeled as a simple lumped-mass pendulum, but quay-side container cranes typically use four hoisting cables to suspend load, which is not in the same form as a simple pendulum. Masoud et al. modeled the container crane load as a rigid body in two-dimensions [48]. They also created a simpler model with only one cable and a point mass, as shown in Fig. 16. They used a small angle approximation to get the simpler linear equations of motion. They obtained gains and time delays for a delayed feedback controller, along with areas of stability from the linear model. The feedback controller was effective in reducing oscillations for the nonlinear model both in a computer simulation and with a scaled experimental model. Masoud et al. also used a delayed position-feedback

controller to successfully reduce rotary crane load oscillations [49]. They used a nonlinear, three-dimensional spherical pendulum as a model. Nayfeh and Baumann modeled a container crane's load as a double pendulum and used a time-delay feedback to control the load swinging [50]. As discussed, several sources have successfully used delayed feedback control to dampen out load oscillations.

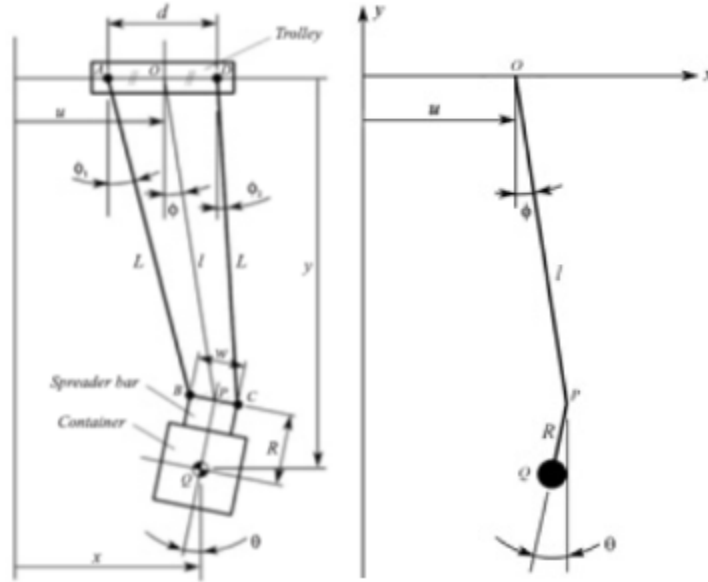


Figure 16. Quay-side container crane model and simplified pendulum model [48]

To dampen the oscillations, many of the closed-loop control mechanisms use a control force and PID controller to counter oscillations from the motion of the crane. Linear input-shaping methods, fuzzy logic, and adaptive control techniques have also been used, though these types of control mechanisms are not always simple. Input shaping is an open loop method used to control acceleration and deceleration with the goal of reducing load oscillations from inertia. Several simulations show that linear controllers do not effectively reduce large oscillations due to the nonlinearities in the load dynamics [43].

A couple other robust models allow for adjusting crane characteristics to minimize oscillations and to operate at higher speeds. Henry et al. suggested a method for adjusting the boom-luff angle on ship-mounted cranes [51]. They modeled the crane's load as a planar pendulum with rigid, massless cables, and used full nonlinear equations of motion with a delayed position-feedback for control. As with many other dynamics papers, they found regions of stability and used computer simulations and a scaled model to experimentally verify that their model was accurate. Abdel-Rahman and Nayfeh suggested changing the cable length at various speeds to reduce load pendulations [52]. The load is modeled as a spherical pendulum, both in two- and three-dimensional models (however, the two-dimensional model was not very accurate). Though changing these crane characteristics does not add

any damping to the system, it changes the crane dynamics enough to reduce and control the oscillations.

As this chapter shows, there are many ways to model moving suspended loads. The simplest models involve single pendulums that have planar swings. These are described by nonlinear equations of motion, though for oscillations less than a few degrees in amplitude, linear approximations can be made to simplify the models. More complicated models involving three dimensional, nonlinear movements of a double pendulum have also been used, though they are beyond the general scope of this project. Good models make realistic and accurate simplifications, and many of the simple models described have successfully reduced the load oscillation amplitudes. The next chapter will describe our model for the EMKS as a helicopter sling load.

CHAPTER 5. EMKS TRANSPORTATION ANALYSIS

The EMKS unit will be occasionally transported as a helicopter sling load into remote areas or terrains that are very difficult to reach by land vehicles in a short period. Both the United States and Australian militaries have experienced dynamic instability when carrying helicopter sling loads. Under wind excitations, the most sensitive parameters of the sling load system and helicopter can cause rapid energy fluctuations for the system and helicopter to leave their admissible operating boundaries. The system or helicopter responses can reach and exceed a threshold at which the damping and stiffness characteristics become too weak to operate in a sustained way. This can induce large swings and cause failures of both the helicopter and the pendulum EMKS system. The helicopter may lose its equilibrium as a result of unbalanced payload weight.

In an attempt to prevent this from occurring with the EMKS, we performed an analysis to model the motion of the container and to identify areas of instability to avoid. We must study three aspects to ensure the helicopter can maneuver with the EMKS sling load in a stable, reliable, and safe manner. First, we must understand the swing structure and its equilibria for a given payload weight of the EMKS. The second is to examine changes in the swing structure and equilibria under wind excitations. Thirdly, interpret parameter and boundary regimes for which the swing structure and equilibria do not change under wind excitations, and the pendulum EMKS system is controllable when the wind excitation becomes unevenly distributed on the helicopter and pendulum cable EMKS system.

The control strategy is understood to keep the dynamics of the helicopter and pendulum EMKS system balanced with all the forces influencing the container motion. There is no specific mechanism on the helicopter that can mechanically adjust the height and location of the payload or its attachment point. With no control mechanism, any reduction in the swinging motion of the payload rests essentially on the experience of the helicopter pilot. Movement adjustments are made manually by the helicopter pilot based upon the sense of the aerodynamic motion of the helicopter and swing structure of the payload. The pilot is thus exposed to high risk helicopter maneuvering that can result to catastrophic failure. It is therefore important to have a mechanism that can make movement adjustments during the transportation of the pendulum EMKS system.

This chapter focuses on establishing computational information that can be incorporated into the design of an improved EMKS unit and manual aerial vehicles with no possibility of failure during payload movements by preserving the regimes of stability, reliability, and safety. We will discuss each of our models, the assumptions we made, equations of motion, plots of the container motion, and phase space plots to show areas of stability. We first started with a simple pendulum model, then proceeded

to a more accurate, albeit complicated, double pendulum model. Finally, we conclude the chapter by describing a control mechanism that applies a force to translate the top pivot point of the sling load connection in the helicopter in order to dampen and reduce the load swinging.

5.1 Model Development

A CH-47D helicopter will carry the EMKS as a sling load, as shown in Fig. 17. Though this helicopter is capable securing loads with several different cable configurations (shown in Fig. 8 in Chapter 2), we chose this single point configuration because few previous analyses have used loads with this configuration, even though it is commonly used.

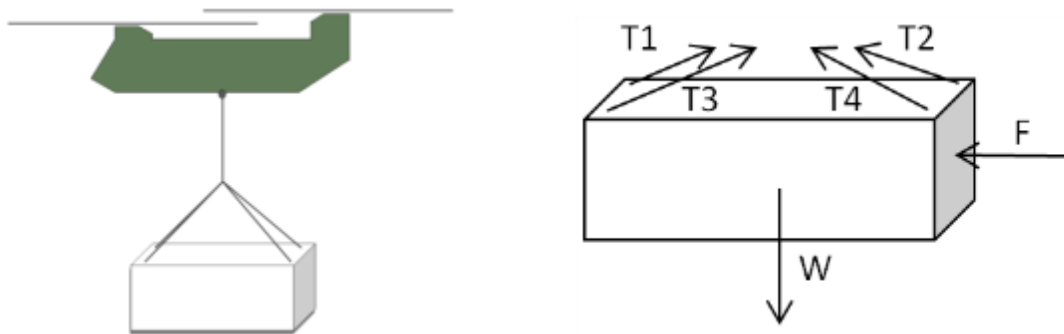


Figure 17. Sling load sketch (left) and EMKS container FBD (right)

Figure 17 also shows the free body diagram (FBD) for the container, where T_1 , T_2 , T_3 , and T_4 are the tensions on the cables, F is an externally applied force (such as wind), and W is the weight. When there is no external force ($F=0$), each of the four cables have equal tensions ($T_1 = T_2 = T_3 = T_4 = T$). The container is 8'D x 15'L x 8'H and weighs approximately 10,000 lb, with the center of mass in roughly the center of the container. Table 4 lists the parameters we used in our calculations and model. For each model, we assume that the cables were rigid and inextensible and that the connection points are frictionless. We also neglected the helicopter rotor downwash and air resistance effects.

Table 4. Parameters used in modeling the sling load

Parameter	Value
Mass _{EMKS}	10,000 lb (4535.9 kg)
Cable length (simple pend)	20 ft (6.1 m)
Mass _{hook}	50 lb (22.7 kg)
Cable L ₁ (double pend)	10.6 ft (3.23 m)
Cable L ₂ (double pend)	10 ft (3.084 m)

5.2 Simple Pendulum

The simplest model we can make from the sling load is that of a simple pendulum. As shown in Fig. 18, the simple pendulum has a single mass at the end of a massless rod (cable) connected to a pivot point. For this model, we assumed that the EMKS container is a point mass. All of the cables are rigid and inextensible, and no pivoting is allowed at the connection between the five cables. Because of this, we simplified the model to have one cable, as in a simple pendulum. In this model, we do not consider any external forces. We also assume that the load swings only in one direction without side-to-side motions. The angle θ describes the pendulum's angular displacement from the equilibrium position. L is the cable length from Table 4, m is the $mass_{EMKS}$, and the mass of the hook is neglected.

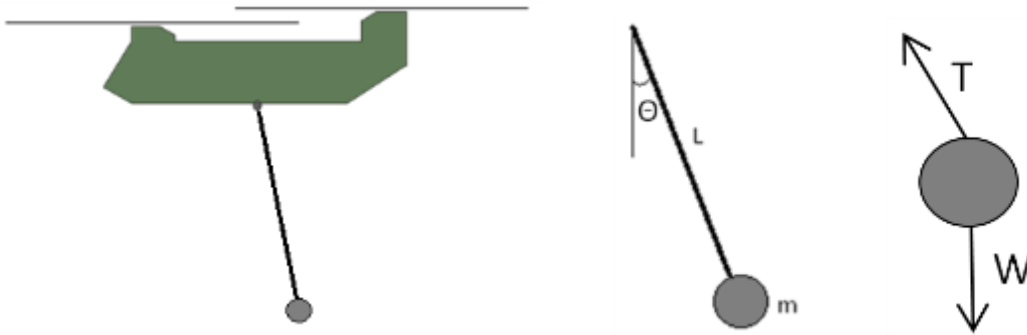


Figure 18. Simple pendulum model (left) and FDB of the container (right)

To get the equations of motion for the mass, we used Newton's Second Law for rotation,

$$\tau = I\alpha \Rightarrow -mgL\sin\theta = mL^2 \frac{d^2\theta}{dt^2}, \quad (1)$$

where τ is the torque, I is the moment of inertia, α is the angular acceleration, m is the mass, g is gravity, and L is the length of the cable. Simplifying, we get

$$\ddot{\theta} + \frac{g}{L}\sin\theta = 0. \quad (2)$$

For small angles (< 15 degrees), we can make the approximation $\sin\theta \approx \theta$. This simplification changes Eq. 2. from nonlinear to linear simple harmonic motion,

$$\ddot{\theta} + \frac{g}{L}\theta = 0. \quad (3)$$

The solution to this second order differential equation (also the desired equation of motion) is given by

$$\theta(t) = \theta_0 \cos(\omega_0 t + \varphi), \quad (4)$$

where θ_0 is the initial angle, ω_0 is the angular velocity, and φ is the phase angle. The natural frequency of the swinging is

$$\omega_0 = \sqrt{g/L}, \quad (5)$$

and the period for the undamped motion at small angles is given by

$$T = \frac{2\pi}{\omega_0} = 2\pi\sqrt{L/g}. \quad (6)$$

However, this solution and period are not accurate at larger angles. At larger angles, the sine term has a substantial contribution to the motion and must be considered. To solve for the pendulum's period, we must solve an incomplete elliptic integral of the first kind¹, as described in [53]. Starting from Eq. 1, we first multiply each side by $\dot{\theta}/mL^2$

$$\ddot{\theta}\dot{\theta} = -\omega_0^2\dot{\theta}\sin\theta. \quad (7)$$

Then multiply both sides by dt and integrate with respect to time to get

$$\frac{1}{2}\dot{\theta}^2 = \omega_0^2(\cos\theta - \cos\theta_0), \quad (8)$$

where $-\omega_0^2\cos\theta_0$ is the constant of integration. We separate the variables to get t on the left and θ on the right, then integrate each side

$$\int_0^t dt' = \int_{\theta_0}^{\theta} \frac{d\theta'}{\omega_0[2(\cos\theta' - \cos\theta'_0)]^{1/2}}. \quad (9)$$

Eq. 9 is in the form of an incomplete elliptic integral of the first kind. To get it into the typical form, we

first use the trigonometric identity of $\cos\theta = 1 - 2\sin^2(\theta/2)$, substitute in $\sin\gamma = \frac{\sin(\theta/2)}{\sin(\theta_0/2)}$ and

$\sin(\theta_0/2) = k$. We get $d\theta$ in terms of γ by differentiating the left side

$$\frac{1}{2}\cos\left(\frac{\theta}{2}\right)d\theta = \sin\left(\frac{\theta_0}{2}\right)\cos\gamma d\gamma \quad (10)$$

$$d\theta = \frac{2\sin\left(\frac{\theta_0}{2}\right)}{\cos\left(\frac{\theta}{2}\right)}\cos\gamma d\gamma. \quad (11)$$

With all of these substitutions, Eq. 7 becomes

$$t = \int_0^{\gamma} \frac{(2\sin(\frac{\theta_0}{2})/\cos(\frac{\theta}{2}))\cos\gamma'd\gamma'}{\omega_0\left[2\left(2\sin^2\left(\frac{\theta_0}{2}\right) - \sin\left(\frac{\theta}{2}\right)\right)\right]^{1/2}} \quad (12)$$

$$= \int_0^{\gamma} \frac{\cos\gamma'd\gamma'}{\omega_0\cos\left(\frac{\theta}{2}\right)\left[1 - \frac{\sin^2(\theta/2)}{\sin^2(\theta_0/2)}\right]^{1/2}} \quad (13)$$

¹ For more information on elliptic integrals of the first kind, refer to [55]

$$t = \int_0^{\gamma} \frac{d\gamma'}{\omega_0 [1 - \sin^2(\theta/2) \sin^2 \gamma']^{1/2}} \quad (14)$$

$$= \int_0^{\gamma} \frac{d\gamma'}{\omega_0 [1 - k^2 \sin^2 \gamma']^{1/2}} \quad (15)$$

To make the integration easier, we expand the integrand into a binomial series:

$$t = \frac{1}{\omega_0} \int_0^{\gamma} \left(1 + \frac{k^2}{2} \sin^2 \gamma' + \frac{3}{8} k^4 \sin^4 \gamma' + \dots \right) d\gamma' \quad (16)$$

The period of the motion is found from the time when $\gamma=2\pi$. Since one period can be divided into four equal intervals, the period is

$$T = \frac{4}{\omega_0} \int_0^{\pi/2} \left(1 + \frac{k^2}{2} \sin^2 \gamma' + \frac{3}{8} k^4 \sin^4 \gamma' + \dots \right) d\gamma' \quad (17)$$

By integrating term by term, we obtain

$$T = \frac{4}{\omega_0} \left(\frac{\pi}{2} + \frac{\pi k^2}{8} + \frac{9\pi k^4}{144} + \dots \right) \quad (18)$$

$$= \frac{2\pi}{\omega_0} \left(1 + \frac{k^2}{4} + \frac{9k^4}{72} + \dots \right) \quad (19)$$

Substituting our value of $k = \sin(\theta_0/2)$ back into Eq. 19, we find a period of

$$T = \frac{2\pi}{\omega_0} \left[1 + \frac{\sin^2(\theta_0/2)}{4} + \frac{9}{72} \sin^4\left(\frac{\theta_0}{2}\right) + \dots \right] \quad (20)$$

For small angles, we can assume that $\sin\theta \approx \theta$, then neglect the higher order terms. With this approximation, we see that the period in Eq. 20 simplifies to that predicted in Eq. 6

$$T_{small\ angles} = \frac{2\pi}{\omega_0} \left[1 + \frac{\theta_0^2}{16} + \dots \right] \approx \frac{2\pi}{\omega_0} \quad (21)$$

MATLAB Modeling

To model the simple pendulum analytically, we used MATLAB R2010b. The functions and scripts that we wrote and used are described in Table 5 and can be seen in Appendix D. For our parameters, we used the mass and length values for the simple pendulum given in Table 4. We varied the initial angle amplitude but always left the initial angular velocity as zero.

Table 5. Description of code used to model simple pendulum

Function/Script	Purpose
pendulum_large.m	Function to define non-linear, simple pendulum equation of motion
pendulum_solver_all_angles.m	Script to solve above using <i>ode45</i> and <i>ellipke</i> , compares theoretical and plotted periods to determine accuracy of <i>ode45</i> and <i>findpeaks</i> solution, shows small angle period

To put the equation of motion into MATLAB, we wrote it in state-space form. To do this, we assigned the values

$$theta1 = \theta \quad \text{and} \quad theta2 = \dot{\theta}. \quad (22)$$

Differentiating each of these, we get

$$thetadot1 = \dot{\theta} = theta2 \quad \text{and} \quad thetadot2 = \ddot{\theta} = -\frac{g}{L} \sin(theta1). \quad (23)$$

We used three different methods to determine the period of the simple pendulum. The first is the small angle approximation, given by Eq. 6. Then we calculated the theoretical period obtained from solving Eq. 9 with *ellipke*, which solves the elliptic integral of the first kind. We then solved Eq. 2 using *ODE45*, which uses a Runge-Kutta (4,5) formula to solve nonstiff ordinary differential equations. From the plot of this solution, we determined the period by taking the average of the distance between the maximum points (peaks) of the curve. These three motions were all plotted on the same axes for easy comparison.

Table 6 summarizes the different periods for initial angles of 90°, 20°, and 1°. The small angle period is the same for each because it does not depend on the initial angle; it only depends on the length, which is constant. The |Theory-Plot| values are the magnitude of the difference between the periods from the plot (calculated from *ode45*) and the theoretical periods (calculated using *ellipke*). For most other initial angles, this difference varied randomly between those given in the plot. The largest difference was approximately 0.009 s. This means that our solutions from *ode45* using *findpeaks* to obtain periods are accurate to about plus or minus one one-hundredth of a second.

Table 6. Periods for simple pendulum for different initial angles

Angle, °	Small Angle, s	Theory, s	Plot, s	Theory-Plot , s	Plot-Small , s
90	4.9546	5.8481	5.8421	0.00600	0.8875
20	4.9546	4.9926	4.9924	2.149*10 ⁻⁴	0.0378
1	4.9546	4.9547	4.9545	2.270*10 ⁻⁴	0.0001

Figure 19 shows plots of the angular displacement with the three different periods for the same initial angles in Table 6. From the $\theta_0 = 90^\circ$ plot, we can see that the small angle period does not agree well with the other two periods. This confirms that the small angle approximation should not be used for this large angle because it gives an error in the period of about 15%. For an initial angle of 20° , the small angle line coincides better with the theoretical line, but still not exactly. The error was reduced down to 0.8%, which is typically a reasonable level. An even better correlation exists for an initial angle of 1° , with an error of 0.002%. The plot shows that the small angle dashed line plots on top of the solid theoretical line so that they cannot be distinguished. This shows the importance of using the non-linear equations for the motion at angles much larger than approximately 20° .

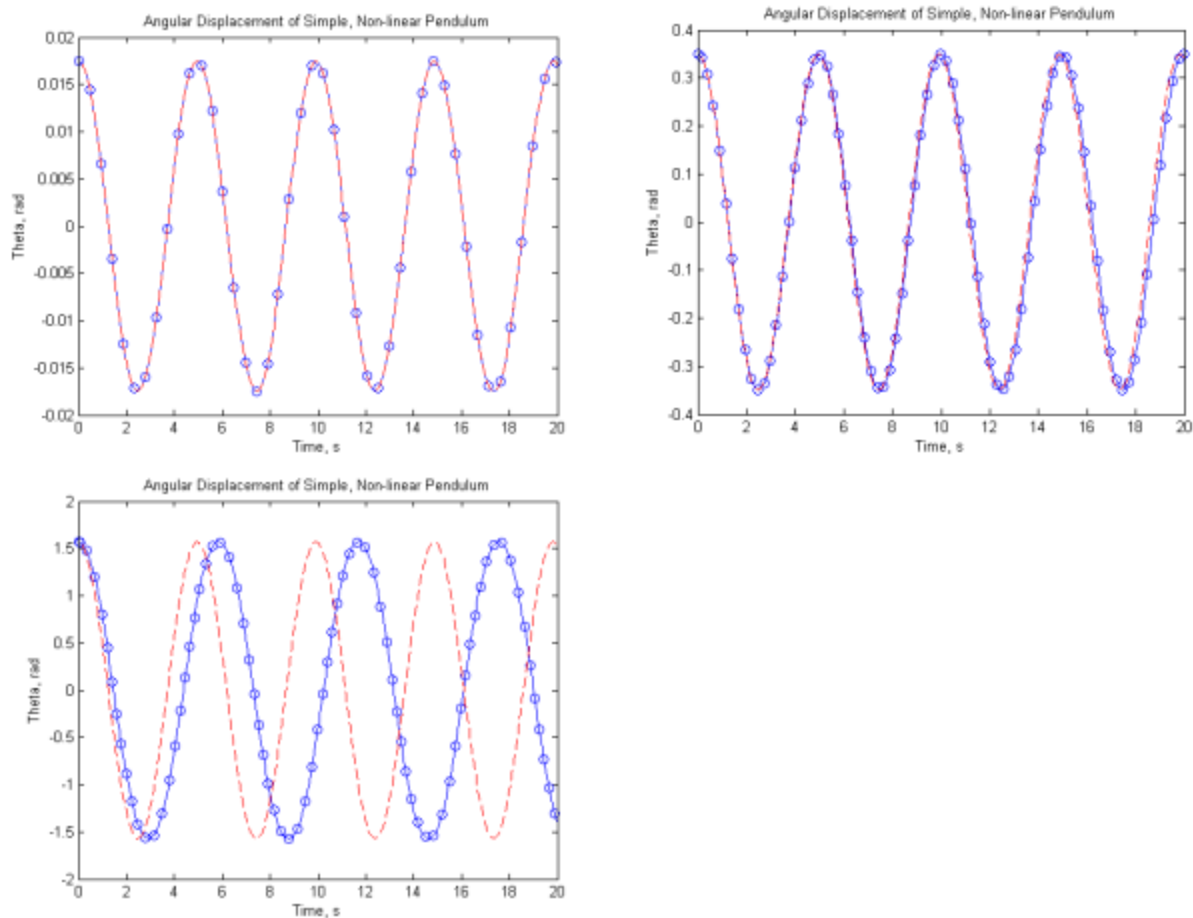


Figure 19. Plot of simple pendulum angular displacement for initial angles of 1° (top left), 20° (top right), and 90° (bottom). The blue solid line represent the *ODE45* solution, the blue \circ symbols represent the theoretical solution to the motion solved with the elliptic integral, and the red dashed line represents the motion with the small angle approximation.

The phase portraits for initial angles of 1° and 90° are shown in Fig. 20 for 50 seconds. The circular pattern starts at the right of the circle (angular velocity = 0 rad/s and position=0.0017 rad or

1.57 rad), then continues clockwise and repeats for each period of the motion. This repetition in the phase space represents stability in the pendulum's motion. Without any damping or external forces, the pendulum will continue to swing with a constant period, maintaining the stable and repetitive motion. The path for the initial angle of 90° is not a perfect circle; this is due to this very large initial angle.

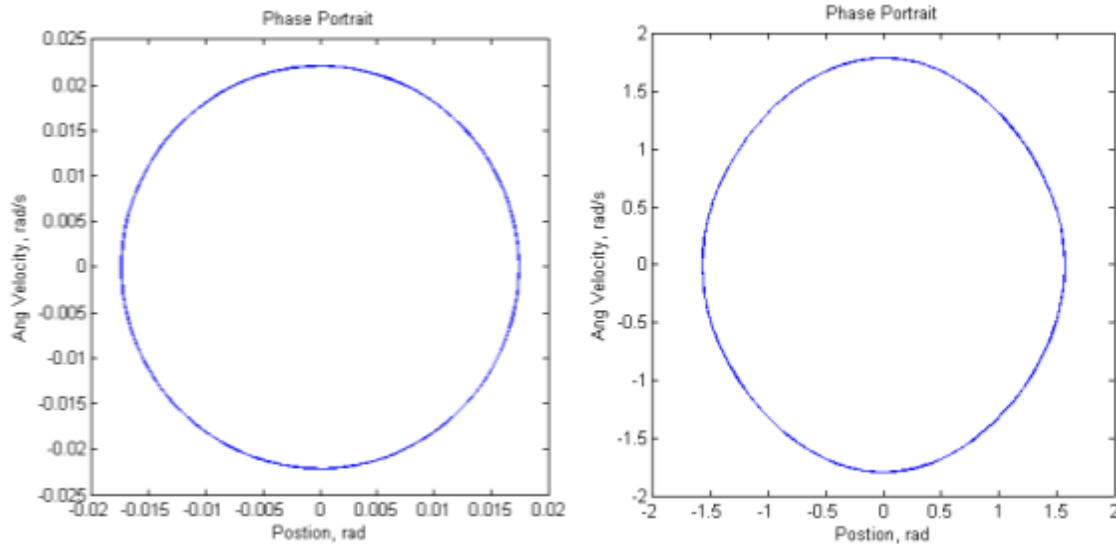


Figure 20. Phase space portraits for simple pendulum with initial angles of 1° (left) and 90° (right) for 50 seconds

5.3 Double Pendulum

A more accurate representation of the helicopter sling load is that of a double pendulum, as shown in Fig. 21. The hook that connects the four cables coming from the container to the one cable coming from the helicopter allows for frictionless motion and rotation. This is essentially a second pivot point along the pendulum's length. Our double pendulum model has two cables of length L_1 and L_2 , and the angular position is defined by angles θ_1 and θ_2 . We made similar assumptions relating to the massless cables and no damping, as in the simple pendulum model.

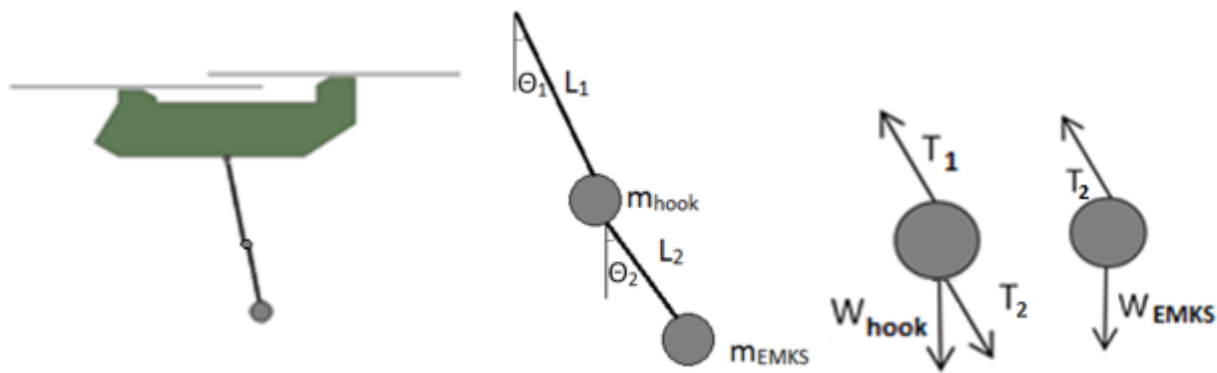


Figure 21. Double pendulum model (left) and FBDs for the hook and EMKS load (right)

To obtain the equations of motion for the pendulum, we started by writing down the total potential and kinetic energy to calculate the Lagrangian. A detailed description of obtaining the equations of motion can be found in Taylor [54]. The total potential energy of the hook and the container is given by

$$U(\theta_1, \theta_2) = (m_1 + m_2)gL_1(1 - \cos\theta_1) + m_2gL_2(1 - \cos\theta_2), \quad (24)$$

and the total kinetic energy is given by

$$T = \frac{1}{2}(m_1 + m_2)L_1^2\dot{\theta}_1^2 + m_2L_1L_2\dot{\theta}_1\dot{\theta}_2\cos(\theta_1 - \theta_2) + \frac{1}{2}m_2L_2^2\dot{\theta}_2^2. \quad (25)$$

The Lagrangian is given by

$$\mathcal{L} = T - U. \quad (26)$$

We obtain the two equations of motion for θ_1 and θ_2 with

$$\frac{d}{dt} \frac{\partial \mathcal{L}}{\partial \dot{\theta}_1} = \frac{\partial \mathcal{L}}{\partial \theta_1} \quad \text{and} \quad \frac{d}{dt} \frac{\partial \mathcal{L}}{\partial \dot{\theta}_2} = \frac{\partial \mathcal{L}}{\partial \theta_2}. \quad (27)$$

With some algebra, these simplify to two second order ordinary differential equations:

$$(m_1 + m_2)L_1\ddot{\theta}_1 + m_2L_2\ddot{\theta}_2\cos(\theta_1 - \theta_2) + m_2L_2\dot{\theta}_2^2\sin(\theta_1 - \theta_2) + g(m_1 + m_2)\sin\theta_1 = 0 \quad (28)$$

and

$$m_2L_2\ddot{\theta}_2 + m_2L_1\ddot{\theta}_1\cos(\theta_1 - \theta_2) - m_2L_1\dot{\theta}_1^2\sin(\theta_1 - \theta_2) + m_2g\sin\theta_2 = 0. \quad (29)$$

Further algebra allowed us to solve for $\ddot{\theta}_1$ and $\ddot{\theta}_2$:

$$\ddot{\theta}_1 = \frac{-g(2m_1 + m_2)\sin\theta_1 - m_2g\sin(\theta_1 - 2\theta_2) - 2m_2\sin(\theta_1 - \theta_2)[L_2\dot{\theta}_2^2 + L_1\dot{\theta}_1^2\cos(\theta_1 - \theta_2)]}{L_1[2m_1 + m_2 - m_2\cos(2\theta_1 - 2\theta_2)]} \quad (30)$$

$$\ddot{\theta}_2 = \frac{2\sin(\theta_1 - \theta_2)[\dot{\theta}_1^2L_1(m_1 + m_2) + g(m_1 + m_2)\cos\theta_1 + \dot{\theta}_2^2L_2m_2\cos(\theta_1 - \theta_2)]}{L_2[2m_1 + m_2 - m_2\cos(2\theta_1 - 2\theta_2)]}. \quad (31)$$

Rewriting Eqs. 30 and 31 into four first order, nonlinear differential equations, we get a state space representation. To do this, we first define

$$x(1) = \theta_1, x(2) = \dot{\theta}_1, x(3) = \theta_2, x(4) = \dot{\theta}_2. \quad (32)$$

Then by differentiating, we obtain:

$$\dot{x}(1) = \dot{\theta}_1 = x(2), \quad (33)$$

$$\dot{x}(2) = \ddot{\theta}_1, \quad (34)$$

$$\dot{x}(3) = \dot{\theta}_2 = x(4), \quad (35)$$

$$\dot{x}(4) = \ddot{\theta}_2. \quad (36)$$

For small oscillations, we can determine the period. For $\theta_1 \ll 1$ rad and $\theta_2 \ll 1$ rad, Eqs. 28 and 29 simplify to

$$(m_1 + m_2)L_1\ddot{\theta}_1 + m_2L_2\ddot{\theta}_2 + (m_1 + m_2)g\theta_1 = 0 \quad (37)$$

and

$$m_2L_2\ddot{\theta}_2 + m_2L_1\ddot{\theta}_1\cos(\theta_1 - \theta_2) - m_2L_1\dot{\theta}_1^2\sin(\theta_1 - \theta_2) + m_2g\sin\theta_2 = 0. \quad (38)$$

MATLAB Model

To model the double pendulum numerically, we used MATLAB R2010b, as with the simple pendulum model. The functions and scripts that we wrote and used are described in Table 8 and can be seen in Appendix E. All parameters used are given in Table 4. In this model, we varied both initial angle amplitudes and always left the initial angular velocities as zero. Our code uses *ode45* to solve Eqs. 33-36 for the angular displacement of both masses (the hook and the EMKS container). We used *ode45* because it was shown to calculate accurate solutions and periods for the simple pendulum in the previous section.

Table 7. Description of code used to model double pendulum

Function/Script	Purpose
double_pend.m	Function to define non-linear, double pendulum equations of motion
double_pend_solver.m	Script to solve above using <i>ode45</i> ; plots the load oscillations, velocities, accelerations, and phase portraits

A double pendulum has much more complicated motion than that of a simple pendulum. Double pendulums are known to have chaotic motion and are very sensitive to initial conditions. This means that a very small change in an initial angle can lead to very different motion patterns. Chaotic motion is unpredictable and does not have a regular periodicity. However, at small initial angles, the double pendulum has a regular and periodic motion. In the next sections, we look at several different initial angles and the type of motion produced.

Small Initial Angles

Figure 22 shows several plots of the hook and load angular positions, when modeled as a double pendulum with initial angles of $\theta_1=1^\circ$ and $\theta_2=2^\circ$. The top plots show θ_1 , or the hook position, and the bottom plots show θ_2 , or the EMKS container load position. For these small initial angles, the hook has an envelope that oscillates about zero with an amplitude of approximately 0.07 rad and a period of 5.2

seconds. This envelope is made up of smaller oscillations, shown in the right plot on a smaller time scale. These smaller oscillations have amplitudes of about 0.008 rad and periods of approximately 0.2 sec. The load position has an oscillating envelope about zero that is made up of smaller oscillations with shorter periods. The larger oscillations have a period that is slightly larger than the hook period, and the smaller oscillations have periods of 0.2 sec.

The load position envelope oscillations and the hook envelope oscillations are very similar in shape, amplitude, and period. Both the hook and load oscillations are very close to being in phase; however the smaller oscillations within the envelopes are out-of-phase and opposite to each other. This means that the overall motion of the load swings back and forth in a predictable manner. Throughout this large oscillation, the hook and load are oscillating on a smaller scale in opposite directions of each other.

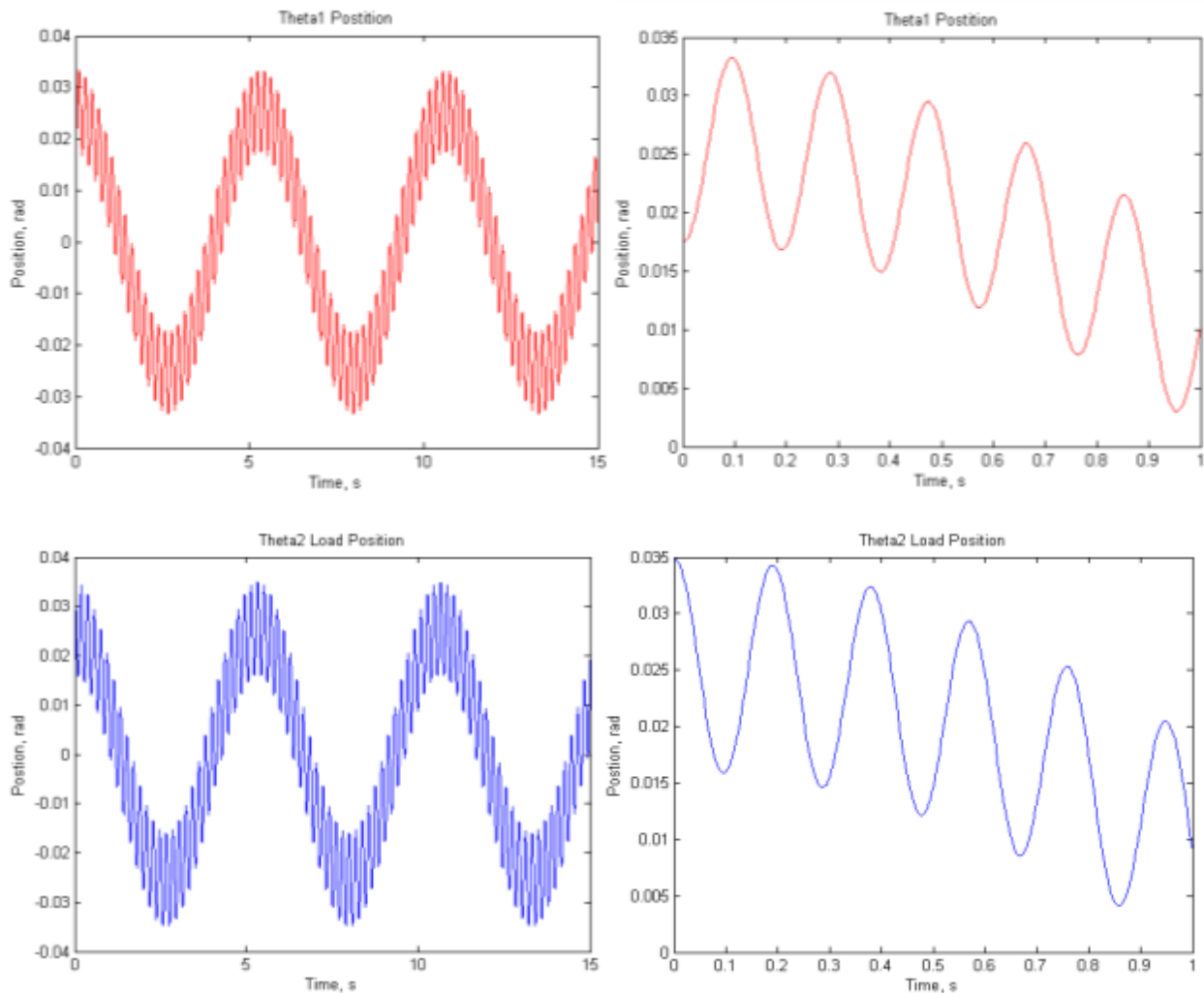


Figure 22. Angular displacement plots for initial angles of $\theta_1=1^\circ$ and $\theta_2=2^\circ$ for the hook (top) and the load (bottom)

Figure 23 shows plots of the EMKS container angular velocity and angular acceleration for the initial angles of $\theta_1=1^\circ$ and $\theta_2=2^\circ$. The load experiences oscillating angular velocities with amplitudes up to 0.35 rad/s and a period of 5.1 s. Within this larger oscillating envelope, there are smaller oscillations with amplitudes of up to 0.3 rad/s with a period of 0.2 s. The angular acceleration also has an overall periodic motion with irregularities near the peaks and troughs of the curve. The period is approximately 0.2 s. Instead of calculating the period by finding the maximum peaks, we calculated the period as the curve crossed zero rad/s^2 . This helped to eliminate the uncertainty of finding a peak with the irregular points.

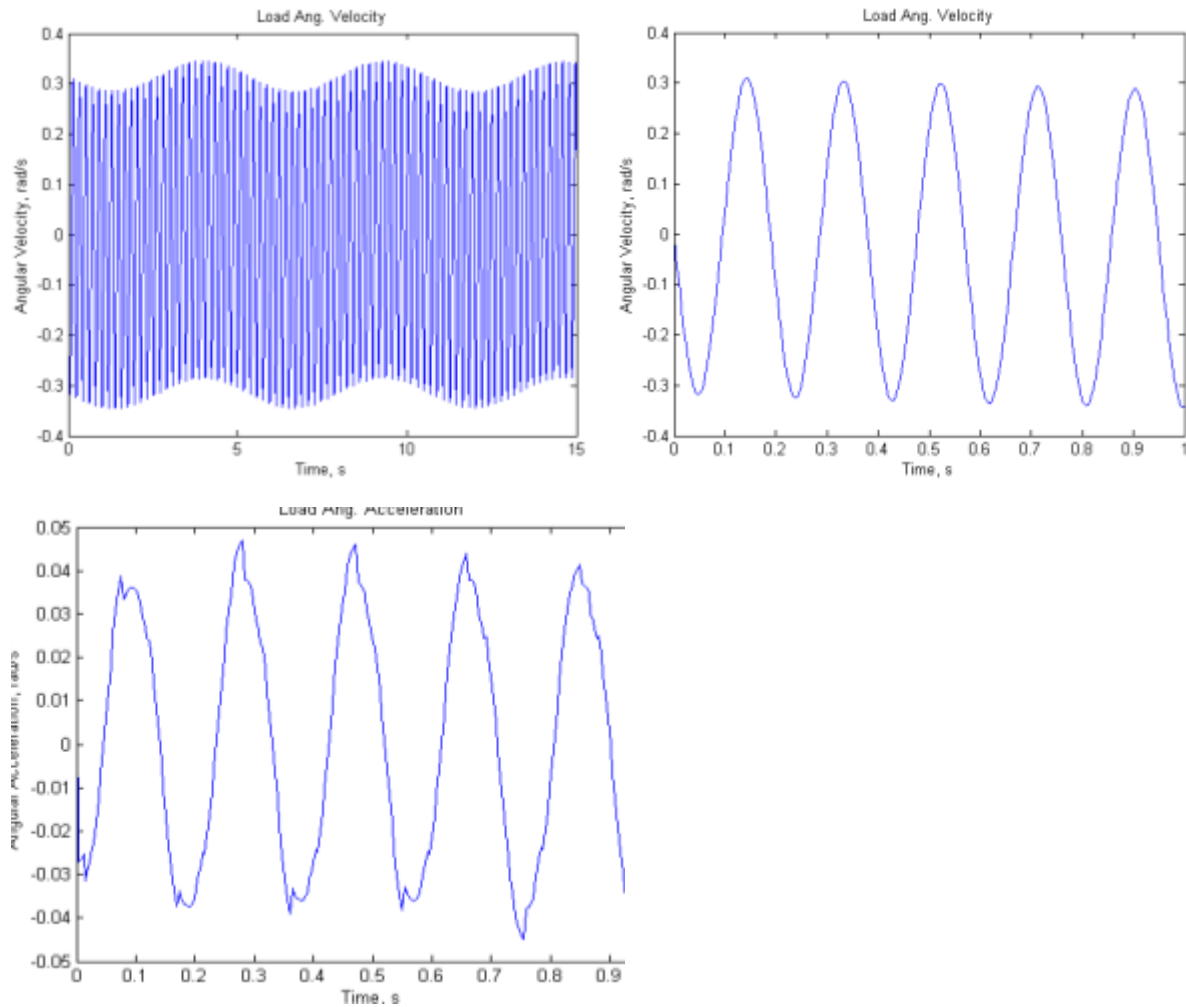


Figure 23. Load angular velocity (top) and acceleration plots (bottom) for initial angles of $\theta_1=1^\circ$ and $\theta_2=2^\circ$

The phase portrait is a type of plot that helps to identify whether the type of motion is regular (and periodic) or chaotic. Chaotic motion is not predictable and therefore does not have a well-defined period or regular motion. The phase portraits in Fig. 24 were created by plotting the load angular acceleration versus the load angular position. The right plot shows the phase space after 20 sec of

oscillations. This plot would look exactly the same for any longer period of time because it completely represents any possible combination of velocity and position that the pendulum would experience, with the small initial angles of $\theta_1=1^\circ$ and $\theta_2=2^\circ$ and zero initial angular velocities.

The left plot shows the phase space for only 1 sec, which is less than one period of the load motion. The curve starts on the right at (0.035 rad, 0 rad/s) and loops to the left. One loop represents a small oscillation (within the envelope). They are displaced from each other because the starting point of one oscillation is slightly different than the next oscillation due to the overall motion of the pendulum. If there were no smaller oscillations (i.e. no envelope in the angular position), then the loops would follow the same path and repeat on top of each other for every single oscillation. This repetition and overplotting indicates that the double pendulum with these initial conditions is stable.

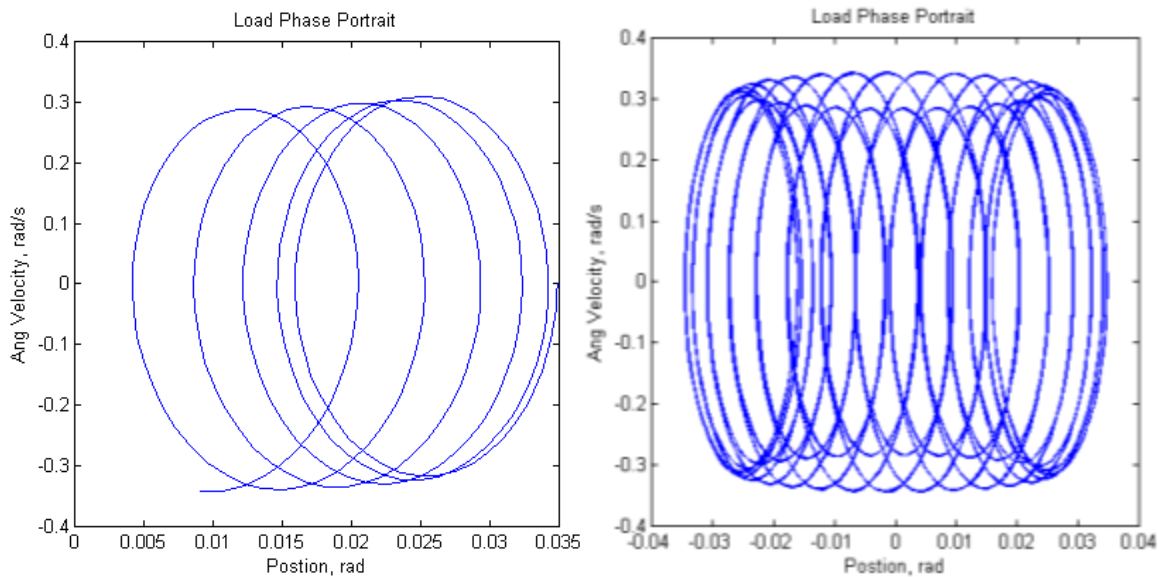


Figure 24. Load phase portraits for initial angles of $\theta_1=1^\circ$ and $\theta_2=2^\circ$ at 1 sec (left) and 20 sec (right)

Large Initial Angles

Figure 25 shows plots of the hook and load angular positions for initial angles of $\theta_1=25^\circ$ and $\theta_2=30^\circ$. These larger angles are ones that the EMKS container might experience as a sling load when the helicopter is traveling at high speeds or in windy conditions. As we will show below, this set of initial conditions results in different oscillations and motion that go beyond the simple small angle pendulum.

Similar to the smaller initial angles, the hook has an oscillating angular position with an envelope amplitude of 0.25 rad with a period of 5.7 sec (obtained from the first 25 seconds). The smaller oscillations within the envelope have amplitudes of approximately 0.04 rad and periods of 0.26 sec. The

load experiences similar, practically in-phase oscillations as the hook, with an amplitude of 0.25 rad and a period of 5.7 sec. The smaller oscillations within the envelope have amplitudes of 0.05 rad and periods of 0.26 sec. To calculate the amplitude of the smaller oscillations, we measured the difference in position for two consecutive troughs and took the average. This was a way to “flatten out” the curve and get a better value for the non-symmetrical waves. We then considered the amplitude to be the difference of the peak (between the two consecutive troughs) and the average trough value. Measurements for several peaks were averaged together to obtain the amplitude.

Compared to the smaller initial angles, the position graphs are similar, with the main difference being the amplitude of oscillations and the related periods. Larger initial angles result in larger oscillations, as expected. These two initial angle conditions showed smaller oscillations within the larger gross oscillating movement because the initial angles were similar but not exactly the same.

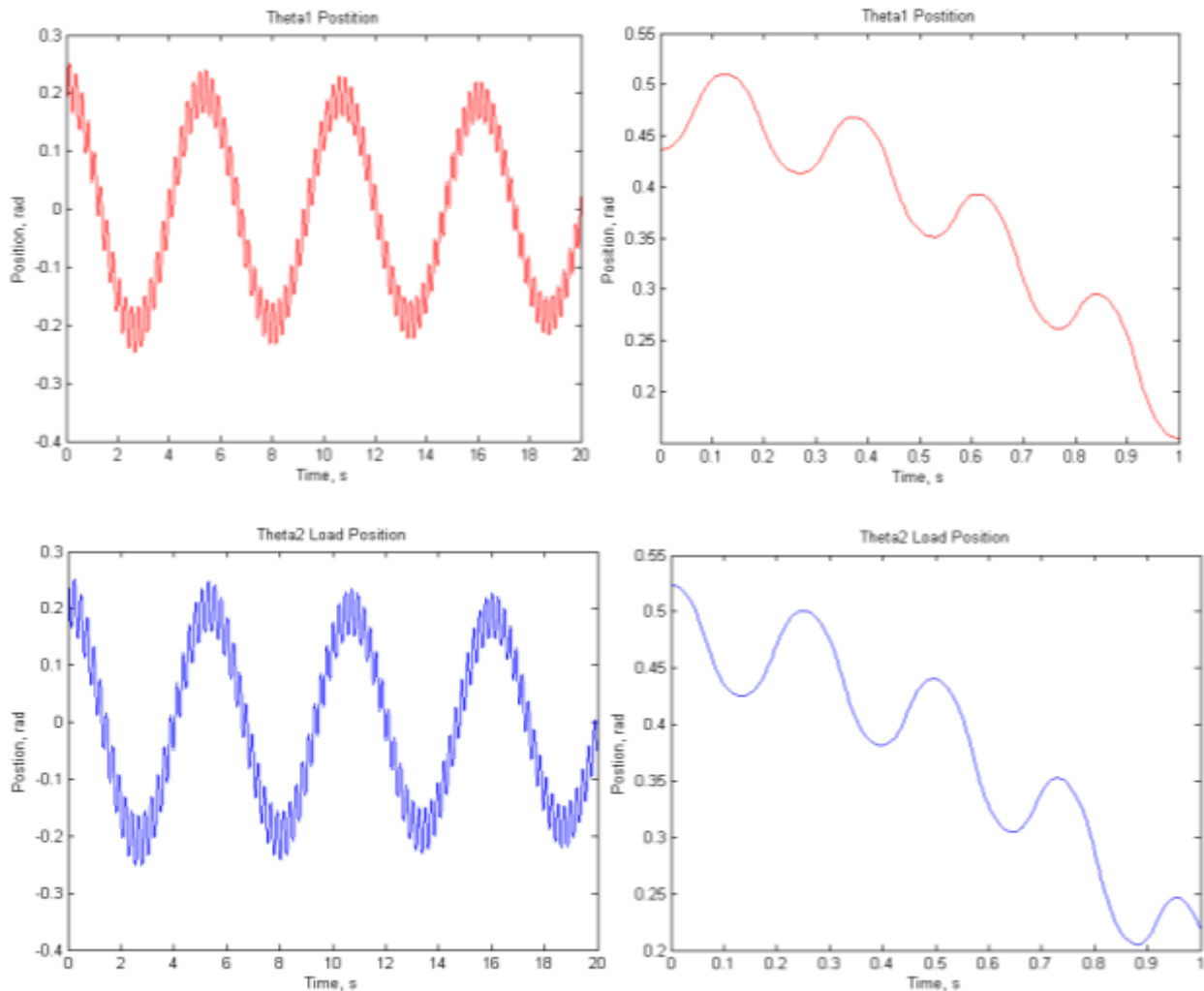


Figure 25. Angular displacement plots for initial angles of $\theta_1=25^\circ$ and $\theta_2=30^\circ$ for the hook (top) and the load (bottom)

Figure 26 shows plots for the load angular velocity and acceleration for the same large initial angles of $\theta_1=25^\circ$ and $\theta_2=30^\circ$. The overall oscillations in the angular velocity envelope have an amplitude of 0.6 rad/s, with a period of 5.6 sec. The smaller oscillations have much sharper profiles than the position curves, with an amplitude of 0.7 rad/s and period of 0.25 sec. The angular velocity oscillations have both a larger amplitude and longer period than those of the smaller initial angles from the previous section. The angular acceleration has an oscillating motion of period 0.25 sec with large irregularities near the peaks and troughs of the curve, similar to the smaller initial angles. These irregularities are more apparent and random-looking with larger initial angles.

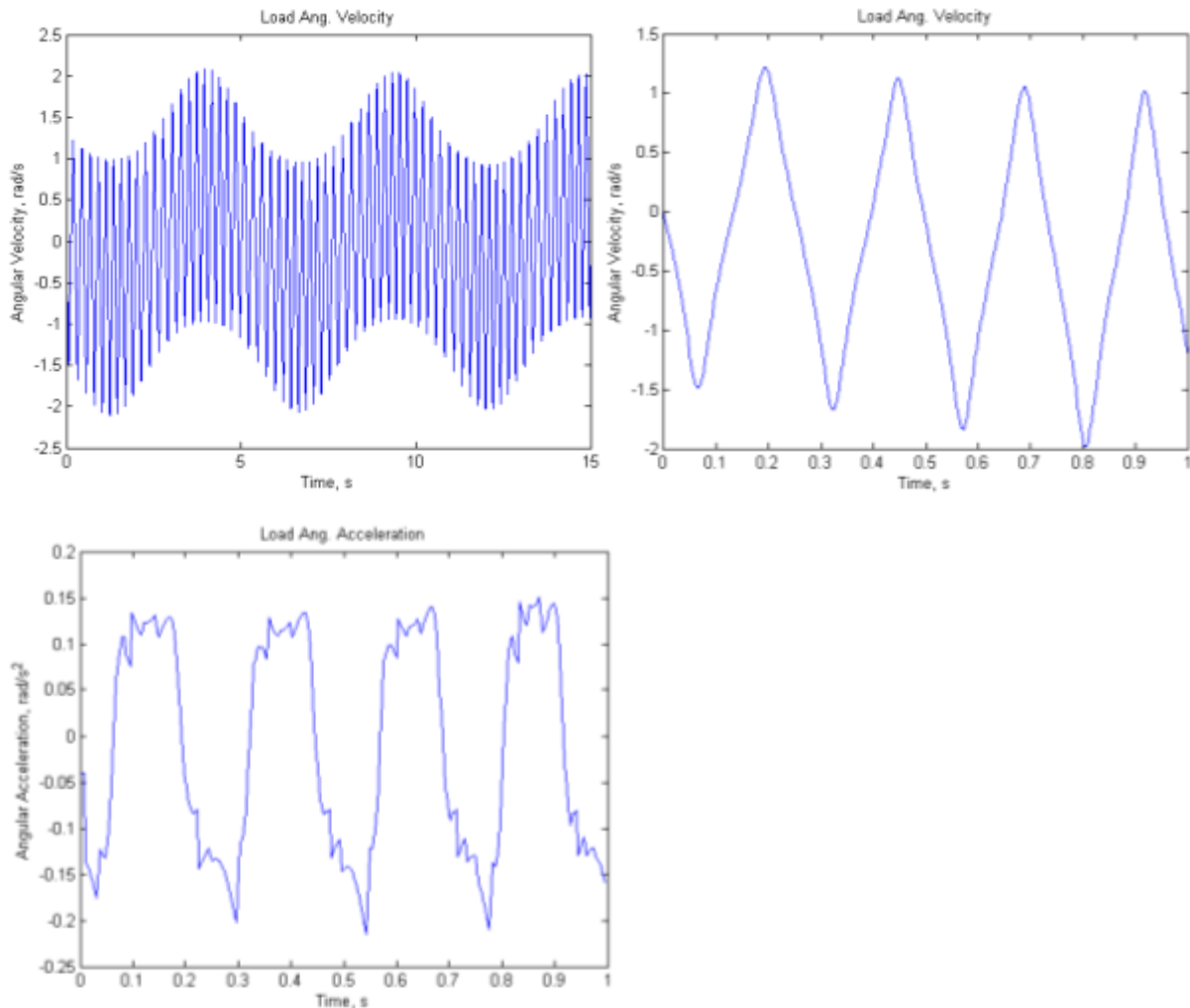


Figure 26. Load angular velocity (top) and acceleration plots (bottom) for initial angles of $\theta_1=25^\circ$ and $\theta_2=30^\circ$

Figure 27 shows the load phase portrait for the larger initial angles. The left plot shows the phase space after 25 sec (about 4 periods of motion). The curve does not repeat itself up to this point, or in the future. This lack of repetition is indicative of chaotic motion. The phase space plots also show the approximate boundaries of angular velocities and positions that the position will experience because the

motion stays within the already plotted shape. For these initial angles, the load will not have an angular velocity that exceeds 2.2 rad/s.

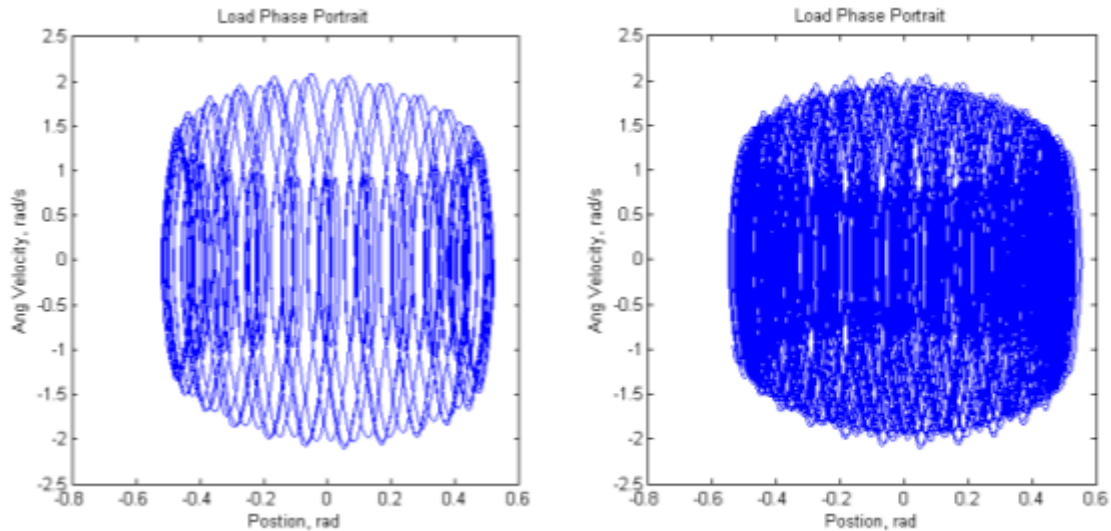


Figure 27. Phase portrait for initial angles of $\theta_1=25^\circ$ and $\theta_2=30^\circ$ at 25 sec (left) and 100 sec (right)

Equal Initial Angles

For conditions when $\theta_1 = \theta_2$, we get simpler plots for angular position, such as those shown in Fig. 28. In the case of equal initial angles, the hook will oscillate as if it were a simple pendulum with an initial angle of $\theta=15^\circ$. Similarly, the load will follow the same trajectory as the hook because it is part of the same rigid “rod” of the simple pendulum. These plots both have an oscillation amplitude of 0.26 rad and a period of 5.4 sec. No envelope of oscillation is seen because the angles are equal, unlike the previous conditions with different initial angles.

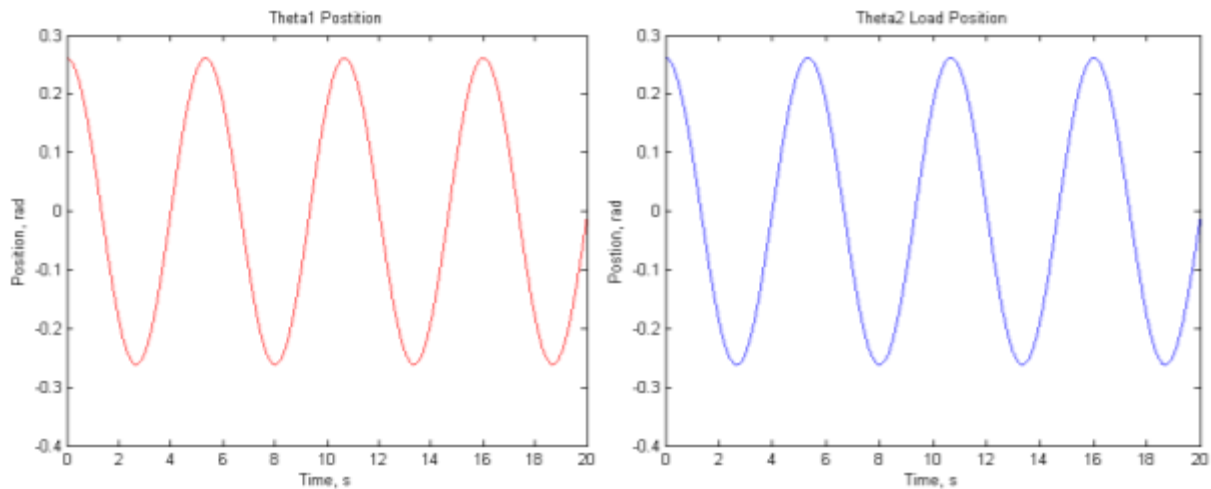


Figure 28. Angular position plots with initial angles of $\theta_1= \theta_2 = 15^\circ$ for the hook (left) and the load (right)

The angular velocity and angular acceleration both also show more “regular” oscillations with these initial angles, as shown in Fig. 29. The angular velocity has oscillations with amplitudes of about 0.15 rad/s and periods of 5.5 sec. Instead of an envelope with smaller oscillations, the angular velocity has small “bumps” with periods of 0.2 sec. When $\theta_1=\theta_2=15^\circ$, the angular acceleration has an envelope amplitude of approximately 0.005 rad/s² and a period of 5.5 sec. This envelope is made up of oscillations with periods of 0.2 sec.

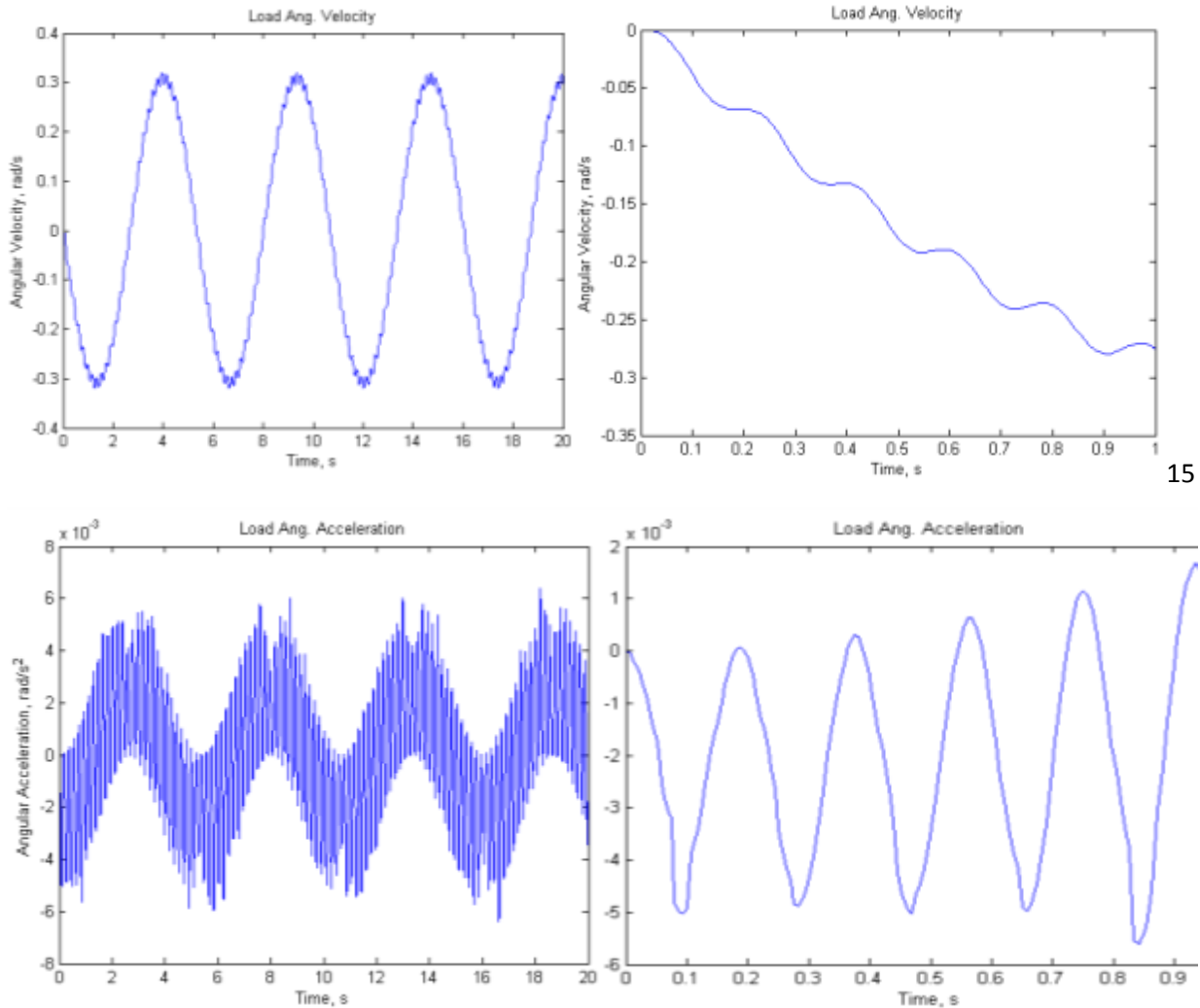


Figure 29. Load angular velocity (top) and acceleration plots (bottom) for initial angles of $\theta_1=\theta_2=15^\circ$

Figure 30 shows the phase portrait of the load for the given equal initial angles. The plot on the left shows a little more than one period of the pendulum’s motion. In the bottom right part of the pathway, a second line has started as the pendulum begins a second oscillation. The right plot shows the phase space after 30 sec. This shows another chaotic situation. The plot does not repeat the same path, but the motion always stays within the tiny ring shown in Fig. 30. The phase portrait at 100 sec looks

similar to the plot shown at 30 sec, just more “filled in” on the ring part with pathways. For smaller, equal initial angles, the motion would be more regular.

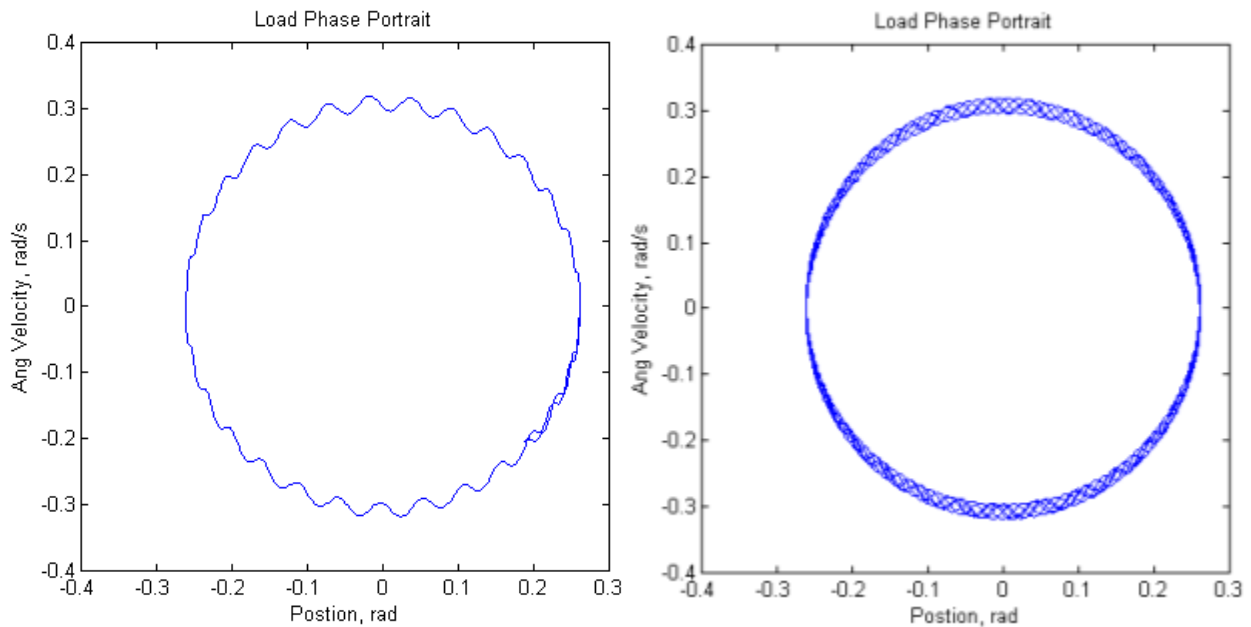


Figure 30. Load phase portrait for initial angles of $\theta_1=\theta_2=15^\circ$ at 6 sec (left) and 30 sec (right)

These three examples illustrate the types of conditions the EMKS load may experience while in flight as a sling load. Small initial angles lead to small oscillations of the load and a stable, periodic motion. These small oscillations are unlikely to throw the helicopter off balance. The problem of unsafe flight conditions occurs for larger initial angles because of the larger oscillations and instability. When the initials angles differ, smaller oscillations occur within the overall envelope of motion where the hook and load are out of phase. To increase the flight safety, the best method would be to decrease the amplitude of the oscillations, especially for larger angles. Even if the oscillations cannot be eliminated completely, a significant reduction in amplitude would result in much safer and stable conditions.

5.4 Control Strategy

In all cases, we want to avoid the load moving into the chaotic regime where we cannot predict the pendulum’s motion. In an effort to do this by reducing the oscillations experienced by the EMKS container, we created a simple design for a mechanism to be used within the helicopter. This control mechanism is composed of two perpendicular rack and pinion gear sets in a trolley that can adjust the EMKS pendulum system in horizontal and vertical directions. The trolley is gantry table slide that is mounted on a ball screw drive and placed down inside the floor of the helicopter. It is powered by a

motor with its shaft connected to a class of gears that regulate the horizontal and vertical movements. The gears are chosen and arranged in such a way that the variations in movement along the horizontal and vertical directions are independent. Essentially, as one pinion gear rotates, the rack moves in one direction, displacing the top pivot point of the pendulum. The driving shaft of the helicopter is engaged with the shaft of the motor to receive additional power from the helicopter. This direct engagement provides an opportunity for sensors to be used to estimate possible movement adjustments with the purpose of continuously maintaining the EMKS system balanced upright and ensuring stable, reliable, and safe performance equilibria.

The single connection node of the pendulum cable carrying the EMKS system is attached to the trolley. Figure 31 shows a schematic representation of a helicopter, the pendulum cable with the attachment of the EMKS system on its lower end, and the trolley mounted in the helicopter.

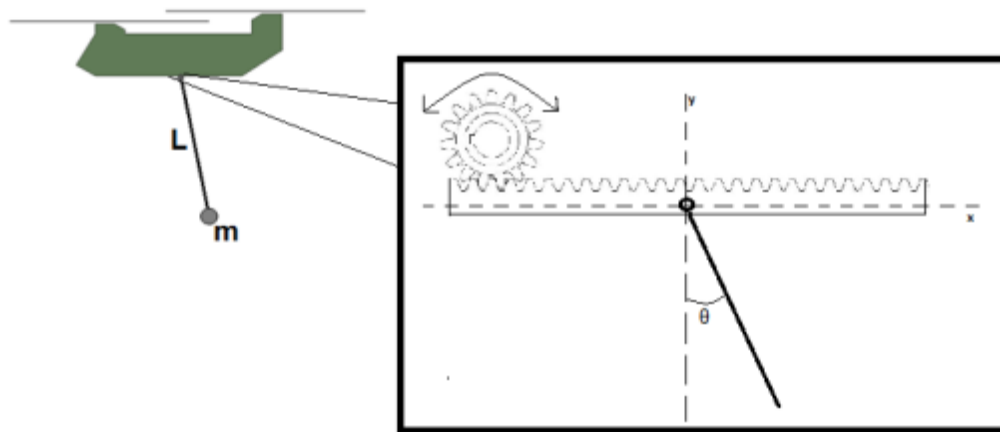


Figure 31. Schematic of control mechanism

The coordinates x and y are nonrotating fixed reference axes. The cable connected to the EMKS load is attached to the movable trolley. The mass of the trolley vehicle is m_v and its damping and stiffness characteristics are denoted by c and k , respectively. Additionally, we introduce a nonlinear damping $g(x, y)$ into the structural characteristics of the trolley vehicle and use this nonlinear damping when the wind excitation and forces acting on the pendulum cable EMKS system become large. We assume that the mass m_v of the trolley vehicle undergoes a pure translational movement along the x and y directions. The $x = X(t)$, $y = Y(t)$ equations represent the motion of the trolley vehicle. The f_v and f_{op} are the trolley vehicle and helicopter forces that are modulated by a controller feedback force u_v . The controller feedback force u_v is driven by the motors of the trolley and helicopter vehicles. The electrical current, resistance, and voltage in the motors of the two vehicles are adjusted based upon the swing structure of the pendulum EMKS system. The length of the pendulum cable is L , and its mass is assumed negligible. The mass m_k denotes the concentrated payload of the pendulum cable EMKS system that is

connected to the lower point of the pendulum cable EMKS system. The pendulum EMKS system is restrained by a torsional spring and damping coefficients k_t and c_t , respectively. Both of these torsional coefficients generate torques that would restrain the motion of the pendulum cable EMKS system.

The motion of the pendulum cable EMKS system is described by the time varying angle displacement $\theta = \theta(t)$. The motion of the trolley and pendulum cable EMKS system are coupled, and there is continuous haptic interactions among the coordinates x , y , and θ . At the height h there is potential energy that is generated by the driving force f_k and wind force f_w to induce a circular pendulum swing. The control force u_k ensures that the forces f_k , f_w , and those from the trolley and helicopter vehicles f_v , f_{op} , are balanced so as stability, reliability, and safety are attainable. The two controllers u_v and u_k in essence support all movements of the pendulum cable EMKS system regardless of the variations in the forces and payload weight on board the helicopter, trolley, and pendulum EMKS system.

To model the control mechanism, we used a damped simple pendulum that is driven by a forcing function acting on the pivot point, as shown in Fig. 32.

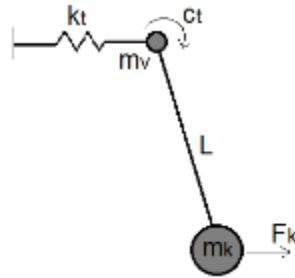


Figure 32. Simplified control mechanism and pendulum representation

The position of the pivot point is defined as

$$u(t) = X(t)\hat{i} + Y(t)\hat{j}. \quad (39)$$

The pendulum's load position is then given by

$$r(t) = u(t) + l(\sin\theta \hat{i} + \cos\theta \hat{j}), \quad (40)$$

or broken into components,

$$s_x(t) = X(t) + l\sin\theta(t), \quad s_y(t) = Y(t) + l(1 - \cos\theta(t)). \quad (41)$$

The first and second derivatives of these equations with respect to time give the corresponding velocity and acceleration, accordingly

$$v(t) = \dot{u}(t) + \dot{\theta}l(\cos\theta \hat{i} - \sin\theta \hat{j}) \quad (42)$$

$$a(t) = \ddot{u}(t) + \dot{\theta}^2l(-\sin\theta \hat{i} + \cos\theta \hat{j}) + l\ddot{\theta}(\cos\theta \hat{i} + \sin\theta \hat{j}) . \quad (43)$$

The potential energy is the sum of the energy that is stored in the translational spring of the trolley vehicle, the torsional spring, and the gravitational potential of the pendulum. This is given by

$$U(t) = \frac{1}{2}(k_x x^2(t) + k_y y^2(t)) + \frac{1}{2}k_t \theta^2(t) + m_k g h , \quad (44)$$

where the height is $h = Y(t) + l(1 - \cos\theta(t))$, k_x and k_y are the stiffness coefficients of the trolley vehicle along the x and y directions, and k_t is the stiffness of the torsional spring. The total kinetic energy is the sum of the kinetic energies of the trolley and the payload:

$$\left. \begin{aligned} T &= T_{mv} + T_{mk} , \\ T_{mv}(t) &= \frac{1}{2}m_v v^2 = \frac{1}{2}m_v(\dot{X}^2(t) + \dot{Y}^2(t)) \\ T_{mk}(t) &= \frac{1}{2}m_k((\dot{X}(t) + l\dot{\theta}(t)\cos\theta)^2 + (\dot{Y}(t) + l\dot{\theta}(t)\sin\theta)^2) . \end{aligned} \right\} \quad (45)$$

The damping and all the other applied forces are the nonconservative quantities that are given by

$$\left. \begin{aligned} W &= W_x + W_y + W_\theta , \\ W_x &= (u_v - (f_{op} + f_v))Y(t)\delta x - c\dot{X}\delta x \\ W_y &= (u_v + f_{op} - f_v)X(t)\delta y - c\dot{Y}\delta y . \\ W_\theta &= [u_k - (f_k + f_w)][\delta x + (y(t) + l\cos\theta(t))\delta\theta] - c_t\dot{\theta}\delta\theta , \end{aligned} \right\} \quad (46)$$

where δx , δy , and $\delta\theta$ are admissible translational and angular variations that enable the forces to perform work, and these variations are independent. The Lagrangian is the total kinetic energy minus the potential energy, which is given by

$$\begin{aligned} \mathcal{L} &= \frac{1}{2}m_v(\dot{X}^2(t) + \dot{Y}^2(t)) + \frac{1}{2}m_k((\dot{X}(t) + l\dot{\theta}(t)\cos\theta)^2 + (\dot{Y}(t) + l\dot{\theta}(t)\sin\theta)^2) \\ &\quad - \frac{1}{2}(k_x x^2(t) + k_y y^2(t)) + \frac{1}{2}k_t \theta^2(t) + m_k g h . \end{aligned} \quad (47)$$

For a given set of generalized coordinates, z_j , $j=1,2,3,\dots,n$ such that $z_j : X(t), Y(t), \theta(t)$ with admissible variations $\delta z_j : \delta x(t), \delta y(t), \delta\theta(t)$, Lagrange's equation is

$$\frac{d}{dt}\left(\frac{\partial \mathcal{L}}{\partial \dot{z}_j}\right) - \frac{\partial \mathcal{L}}{\partial z_j} = W_j , \quad (48)$$

or equivalently

$$\frac{d}{dt} \left(\frac{\partial T}{\partial \dot{z}_j} \right) - \frac{\partial T}{\partial z_j} + \frac{\partial U}{\partial z_j} = W_j. \quad (49)$$

This will thus yield the equations of motion governing the trolley vehicle and pendulum EMKS system. The W_j are the work done by the damping and externally applied forces given in Eq. 46. From here on, we will continue with the assumption that the trolley vehicle moves in only one direction and the pendulum EMKS system is subjected to a moveable horizontal support (in the x-direction). This is a simplification of the preceding model, eliminating the vertical control motion. By solving Eq. 49 for the horizontal-motion model, we find the equations of motion to be

$$(m_v + m_k)\ddot{X}(t) + c\dot{X}(t) + kX(t) + m_k l \ddot{\theta}(t) \cos\theta(t) - m_k l \dot{\theta}^2(t) \sin\theta(t) = u_k - (f_{op} + f_v) \quad (50)$$

$$m_k l^2 \ddot{\theta}(t) + c_t \dot{\theta}(t) + k_t \theta(t) + m_k g l \sin\theta(t) - m_k l \ddot{X}(t) \cos\theta(t) = (u_k - (f_k + f_w)) l \cos\theta(t). \quad (51)$$

By substituting the physical notations

$$\begin{aligned} 2\zeta_v \omega_{0k} &= \frac{c}{m_v}, & \zeta_v &= \frac{c}{2\sqrt{km_v}}, & \omega_{0v} &= \sqrt{\frac{k}{m_v}}, \\ 2\zeta_k \omega_{0k} &= \frac{c_t}{m_k l^2}, & \zeta_k &= \frac{c}{2\sqrt{km_k}}, & \omega_{0k} &= \sqrt{\frac{k}{m_k l^2}}, \\ a &= \frac{m_k}{m_v}, & b_1 &= \frac{g}{l\omega_{0k}}, & b_2 &= \frac{1}{l}, \end{aligned} \quad (52)$$

into Eqs. 48 and 49, we obtain the equations

$$(1 + a)\ddot{X}(t) + 2\zeta_v \omega_{0v} (1 + g(\dot{X})) \dot{X}(t) + \omega_{0v}^2 X(t) = \frac{1}{m_v} (u_v - (f_{op} + f_v)) - a l [\ddot{\theta}(t) \cos\theta(t) - \dot{\theta}^2(t) \sin\theta(t)] \quad (53)$$

$$\ddot{\theta}(t) + 2\zeta_k \omega_{0k} \dot{\theta}(t) + \omega_{0k}^2 \theta(t) + b_1 \sin\theta(t) = \frac{1}{m_k l^2} (u_k - (f_k + f_w)) l \cos\theta(t) - \ddot{X}(t) b_2 \cos\theta(t). \quad (54)$$

These equations of motion are nonlinear and can be studied for given controller functions, driving forces, and wind excitations.

Using MATLAB to solve these two coupled equations simultaneously, we could see how different driving functions would affect the motion of both the pendulum and the trolley. Appendix F shows the function and scripts we used to obtain the following plots. For zero external and driving forces and an initial angle of 0.01 rad, we obtain the pendulum motion as shown in Fig. 33. The coupled motion of the trolley has similar oscillations, though with amplitudes of under a micron and so are negligible. The phase portrait shows a ring of stable motion.

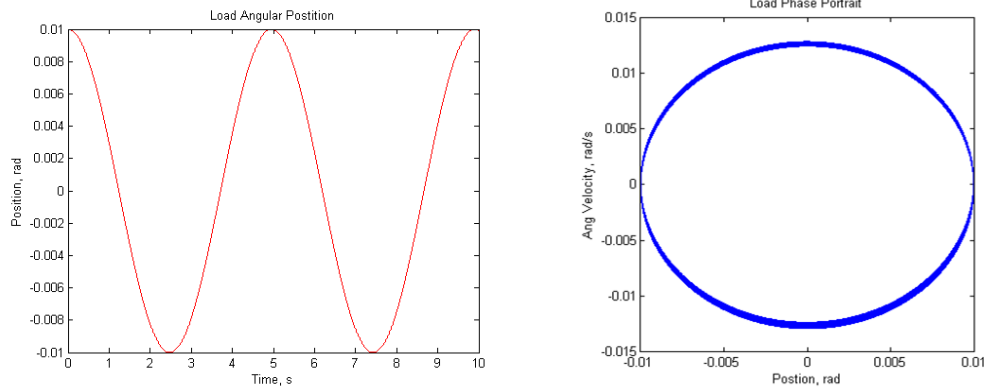


Figure 33. Plots of the load angular position (left) and phase portrait (right) for zero external forces

Figure 34 shows the motion of the pendulum EMKS system with zero external forces plus a control force. The forcing function is of the form $F_d = \theta_d \cos(\omega_f t)$, where θ_d is the forcing amplitude and ω_f is the forcing frequency. For the figure below, $\theta_d = 1000$, $\omega_f = \pi/2$, and the pendulum's initial angle was $\theta_0 = 0.01$ rad. This forcing function increased the amplitudes of oscillation of the load, which is opposite of the desired effect of reducing amplitudes. Even for smaller amplitudes of the driving function, the amplitude of oscillations increased. The phase portrait shows a complicated motion, though it is not as complex and chaotic as a similar double pendulum model would be.

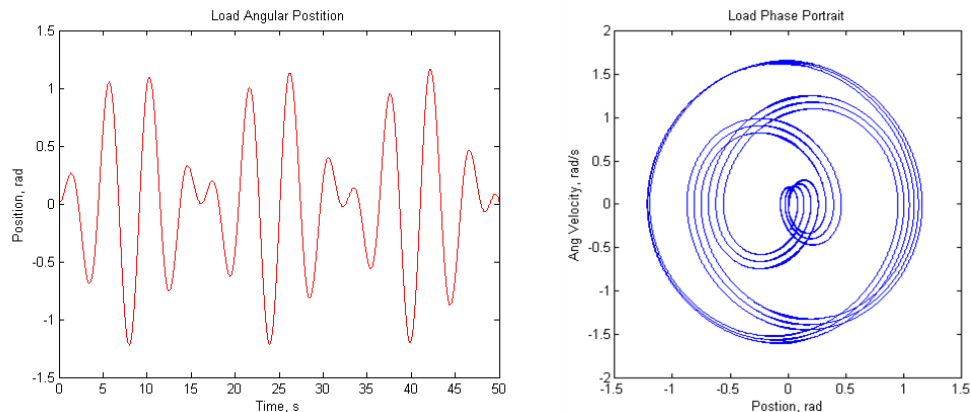


Figure 34. Plots of the load angular position (left) and phase portrait (right) with a driving force

Even with a simple nonlinear pendulum system, a driving function can induce chaotic motion. This makes it necessary to select appropriate driving amplitudes and frequencies to avoid the chaotic region. After testing several frequencies and amplitudes, it is clear that a phase delay is necessary to dampen out the load oscillations. A phase delay will allow the motion of the trolley to cancel out a portion of the load swinging motion, thereby reducing the oscillation amplitude and preventing the motion from travelling into a chaotic regime. However, due to the time limitations on this project we did not have time to complete the analysis with a phase delay.

By studying various values for the driving forces and external forces, areas of stability can be found. With proper settings and controller functions, this active control mechanism will be able to adjust the pivot point to essentially cancel out the load's swinging motion. This will help dampen out the larger oscillations of the load, resulting in a safer and more stable flight. Though this model only used a simple pendulum, a future continuation of this project could incorporate both a double pendulum and a phase delay into the control model to better represent realistic situations.

CHAPTER 6. CONCLUSIONS

The motivation behind the Emergency Meal Kitchen Service (EMKS) was to provide food and water as relief to those affected by natural disasters. The objectives of this project were to create a portable kitchen unit that could be transported worldwide by the means of air, land, and sea. This portable and compact kitchen unit would be able to supply three days' worth of food and water to at least 500 people in any disaster location. In addition to creating the design of this smaller, more compact kitchen unit, the team performed a computational and numerical analysis of the kitchen unit as a helicopter sling load and suggested a control mechanism to dampen out the swinging motions.

There is a need for a compact and easily transportable unit that dispenses food and water to many people affected in disaster areas. Through our research of current methods for distributing food in times of disaster, we learned that it can be very difficult to get to disaster areas quickly with existing mobile kitchens. Existing mobile kitchens are also very large in size and difficult to transport large distances. Other mobile kitchens that are more compact and easier to transport cannot serve large quantities of people. For disaster relief, a kitchen that is easy to transport (and is therefore relatively small) and can serve many people would be ideal. The United States Military has Containerized Kitchens (CKs) that have many of the characteristics needed for a disaster relief kitchen. The CK fits inside of a twenty foot ISO container and can feed 500 soldiers 2-3 meals per day for three days. This unit is transportable by land vehicles, ship, or aircraft such as cargo planes and helicopters.

With this background knowledge, we created an original design for the Emergency Meal Kitchen Services (EMKS) unit. We exceeded many of the basic requirements of the CK (i.e. storage space, freezer capabilities) in our design, including minimum appropriate dimensions for the functionality of a person using the kitchen. Our EMKS design is an improvement over the CK because it fits in a smaller container, weighs less, uses energy more efficiently, balances weight more evenly, and can output at least as many equivalent hot meals.

The EMKS contains appliances such as dual temperature heating cabinets for both cooking and holding warm food, dual refrigerator-freezers, and griddles, as well as sinks, preparation areas, storage, a serving window to public, and an airplane-sized restroom. These appliances were selected as the best choice based on dimensions, capacity, energy usage, and weight after extensive research of household and commercial appliances. We arranged the appliances and other items into a layout in a way to create two smaller kitchen units within the container to minimize the need for unnecessary travelling or movements within the tight quarters of the EMKS, while still providing sufficient working areas and storage spaces. The layout was also designed with symmetry as a way to balance the weight to keep the

center of mass in the middle of the container. This will also help keep the container upright and prevent tipping when carried as a suspended sling load. The two-dimensional scaled sketches were converted into a three-dimensional computer aided design model using SolidWorks software.

The biggest limitation that the team found with the layout was the space that was allotted to walk through the kitchen. In order to fit two kitchen units as well as a rest room into the fifteen foot long container, we had to cut down on the walking space in the EMKS. In future redesigns, should smaller appliances exist with similar holding capacities, we suggest that those appliances be looked at as potential replacements in order to increase the space within the kitchen. Given the proper funds, we would suggest creating a full sized model of the kitchen. This would help in determining how much (if any) the decreased walking space would affect people from being able to move around and function properly within the kitchen. If there is a great amount of inability to function, we would suggest increasing the length of the kitchen unit, as this would allow for more walking space. Another possibility to increase space would be to remove the rest room and perhaps move it to a separate unit.

The EMKS unit will likely be transported by helicopter as a sling load for difficult to reach locations. To address problem of uncontrollable swinging experienced by both US and Australian Army, we analyzed models of EMKS unit as a sling load. We created several mathematical models of the sling load as both simple and double pendulums, and numerically analyzed with MATLAB how different initial angles affect the oscillatory motion of the container. In these models, we assumed that the cables were inextensible, rigid, and massless. We did not consider any damping or frictional effects initially. Small initial angles could be described by linear equations of motion and stable, periodic oscillations. Larger initial angles needed coupled nonlinear equations to describe the chaotic and unpredictable motion. From these models, it was clear that excitations, such as wind, that create large initial angles could easily put the EMKS load into a chaotic oscillation that would cause flight instability.

This chaotic motion should be avoided at all times to ensure safety of the helicopter and load. We suggested a control mechanism involving rack and pinion gear sets mounted inside the helicopter as a way to reduce large amplitude oscillations and bring motion into a stable regime. For our mathematical model, the EMKS load was represented by a damped single pendulum with a driving control force acting to displace the pivot point. The two sets of racks and gears act independently to displace the pivot point in horizontal and vertical directions. We derived equations of motion for a purely horizontal control force, though it could easily be generalized to include a vertical control force as well.

After testing several periodic control functions with various amplitudes and driving frequencies, we concluded that a phase delay is necessary to dampen out the oscillations. Without the phase delay, the driving function increases, rather than decreases the oscillation amplitudes. A driving function can also induce chaotic motion into a simple pendulum, so it is necessary to select appropriate values for the driving amplitude and frequency. Due to time restrictions on the project, we were unable to complete the analysis using phase delays. However, with proper control forces and a phase delay, this mechanism should help dampen and reduce load swinging.

A future continuation of this project would involve a thorough study of the control mechanism for both horizontal and vertical motions. This control model could also be extended to a damped, double pendulum model for a more realistic representation. Considering three dimensional motion would increase the complexity of the equations of motion, but it would also more accurately describe the EMKS unit's motion in real life as a sling load. Ideally, a damped double pendulum driven by a periodic control force with a phase delay would be used to model the EMKS sling load system. The more realistic the model, the more predictable and exact the response of the control mechanism will be.

These EMKS units could be very valuable and helpful for disaster relief situations. Not only does this original design improve upon existing models, but it can also be transported in a more stable and safe manner in conjunction with the proposed control mechanism.

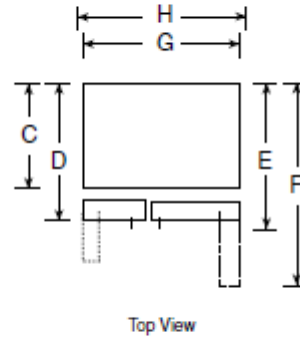
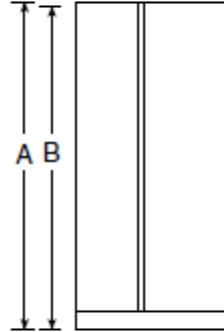
APPENDIX A. Refrigerator Spec Sheet

PSIC5RGX

GE Profile™ Counter-Depth 24.6 Cu. Ft. Side-By-Side Refrigerator

Dimensions and Installation Information (in inches)

Overall Dimensions	Height to top of hinge (in.) A	72-1/8
	Height to top of case (in.) B	71-5/8
	Case depth without door (in.) C†	23-7/8
	Case depth less door handle (in.) D†	27-1/2
	Case depth with door handle (in.) E†	28-3/4
	Depth with fresh food door open 90° (in.) F†	46
	Width (in.) G	35-3/4
Air Clearances	Each side (in.)	1/8
	Top (in.)	1
	Back (in.)	1



†Water hook-up fits in back air clearance when calculating installation depth.

If installed against a wall, allow clearance of 13-15/16" on freezer side to remove bin.

Clearance required to remove fresh food full-size pan without disassembling is 18-5/8".

Allow additional space for any necessary leveling adjustments.

PSIC5RGX

GE Profile™ Counter-Depth 24.6 Cu. Ft. Side-By-Side Refrigerator

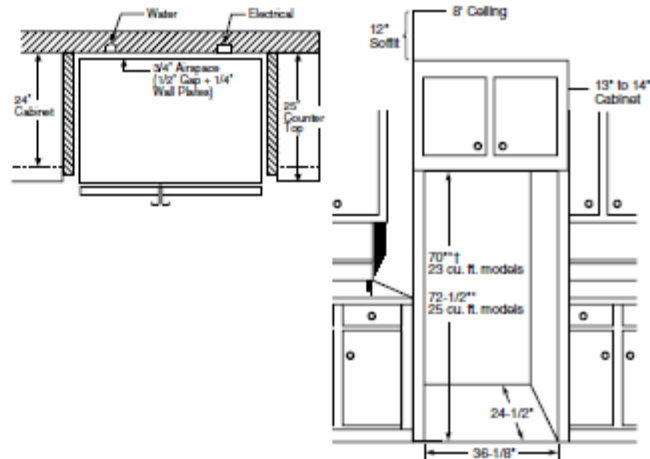
Rough-In Dimensions and Installation Information (in inches)

Installation Tips to Maximize the Built-In Look

- All wall/floor molding should be removed prior to installation.
- Water recess on rear wall recommended to prevent water line damage. 48" minimum length, 1/4" diameter water line tubing recommended.
- When possible, recess both copper water line and electrical outlet. (See local codes)
- Front and rear leveling legs are adjustable for the built-in look. (See owner's manual)

*The rough-in dimensions of 70" for 23 cu. ft. models and 72-1/2" for 25 cu. ft. models are minimum and measured from the finished floor to top of opening (or the underside of the overhead cabinets). For Models with Trim Kit: If frameless style cabinets are planned for above the refrigerator, you may need to consider adding a maximum of 1/4" (70-1/4") to height of opening for 23 cu. ft. models and 1/8" (72-5/8") for 25 cu. ft. models to allow for additional clearance between the cabinet doors and the top of refrigerator trim when the cabinet doors are in open position.

†Model PSDW3YGX is 71-3/4"



For answers to your Monogram®, GE Profile™ or GE® appliance questions, visit our website at ge.com or call GE Answer Center® service, 800.626.2000.



imagination at work



Specification Revised 5/08

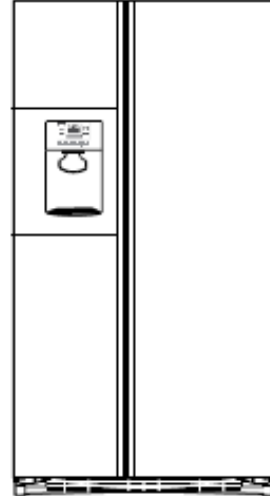
210226

PSIC5RGX

GE Profile™ Counter-Depth 24.6 Cu. Ft. Side-By-Side Refrigerator

Features and Benefits

- Counter-Depth Design - Offers a built-in look without the built-in expense
- ClimateKeeper2™ System - Keeps food garden fresh longer, while protecting ice from odor transfer, with its unique dual-evaporator system
- Quick Ice™ Option - Makes ice up to 50% faster than normal settings-ideal for entertaining
- TurboCool™ Setting - Cools the refrigerator quickly after frequent door openings
- Integrated Ice™ System - Frees up valuable freezer space; It tilts down, providing easy access to bulk ice
- Integrated Shelf Support System - Provides strong, yet flexible support
- Adjustable ClearLook™ Door Bins - Hold gallon-size containers with style and ease
- Adjustable Slide-Out, Spillproof Glass Shelves - Raised edges help contain spills and slide-out shelves make clean up quick and easy
- GE Water Plus Filtration System - Delivers clean, great-tasting water and ice through the LightTouch™ Dispenser with indicator light
- FrostGuard™ Technology - Protects frozen items from freezer burn by monitoring freezer door openings and defrosting only when needed
- Premium Quiet Design - GE's most advanced sound control system
- Model PSIC5RGXBV - Black on black
- Model PSIC5RGXWW - White on white
- Model PSIC5RGXCV - Bisque on bisque



imagination at work

Specification Revised 5/08

210226

APPENDIX B. Heating Cabinet Spec Sheet



DWI7 & DPWI7
7 pans



DWI18 & DPWI18
18 pans

**Insulated holding
cabinets**

*"Superior quality product
at an affordable price!"*

Insulated Holding Cabinets

FEATURING DWI & DPWI Series

- Body construction of .063 aluminum, one piece extended base and solid extruded aluminum frame
- Fully insulated holding cabinet keeps prepared foods at serving temperature (180°F - 85°C)
- Versatile, can be used as a proofer or holding cabinet with or without moisture (DPWI7 & DPWI18 only)
- Powerful, efficient even airflow heating system
- Removable stainless steel bottom power assembly for easy cleaning and maintenance
- Easy to read thermometer and thermostat
- Heavy duty 3" (7.6 cm) non-marking swivel casters (2 with brakes)
- Reinforced brushed aluminum doors with heavy duty pull handles; standard with right hand hinges, left hand hinges upon request
- All construction is riveted and welded
- ETL listed
- One year parts and labor limited warranty

OPTIONAL

- Perimeter bumpers
- Moving handle
- Corner bumpers
- Stainless steel body construction

Holding Cabinets from Doyon

Doyon Hot holding cabinets can be used for holding various cooked products at serving temperature and moisture level.

www.doyon.qc.ca

OVERALL DIMENSIONS

DW17 & DPW17

22 3/4" W X 29" D X 35 1/2" H
(57.8 cm) X (73.7 cm) X (90.2 cm)

DW118 & DPW118

22 3/4" W X 29" D X 69" H
(57.8 cm) X (73.7 cm) X (175.3 cm)

INTERIOR DIMENSIONS

DW17 & DPW17

18 1/2" W X 28 3/4" D X 21 1/4" H
(47 cm) X (73 cm) X (54 cm)

DW118 & DPW118

18 1/2" W X 28 3/4" D X 54" H
(47 cm) X (73 cm) X (137.2 cm)

Shelf spacing 3" (7.6 cm)

ELECTRICAL SYSTEM

DW17 & DW118

120V - 1PH - 11.5A - 1.4 kW - 60Hz - 2 wires NEMA 5-15P

DPW17 & DPW118

120V - 1PH - 16A - 1.9 kW - 60 Hz - 2 wires NEMA 5-20P

208V - 1PH - 12A - 2.5 kW - 60 Hz - 2 wires NEMA 6-15P

240V - 1PH - 10A - 2.4 kW - 60 Hz - 2 wires NEMA 6-15P

250V - 1PH - 10A - 2.3 kW - 50 Hz - 2 wires NEMA 6-15P

WATER ENTRY

DW17 & DW118

N/A

DPW17 & DPW118

Manual

CAPACITY

DW17 & DPW17

7 standard sheet pans 18" X 26" (45.8 cm X 66 cm)

DW118 & DPW118

18 standard sheet pans 18" X 26" (45.8 cm X 66 cm)

FINISH

Aluminum

SHIPPING INFORMATION

DW17 200 lbs (91 kg)

DPW17 235 lbs (107 kg)

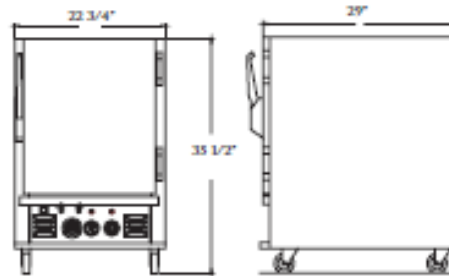
DW118 300 lbs (136 kg)

DPW118 300 lbs (114 kg)

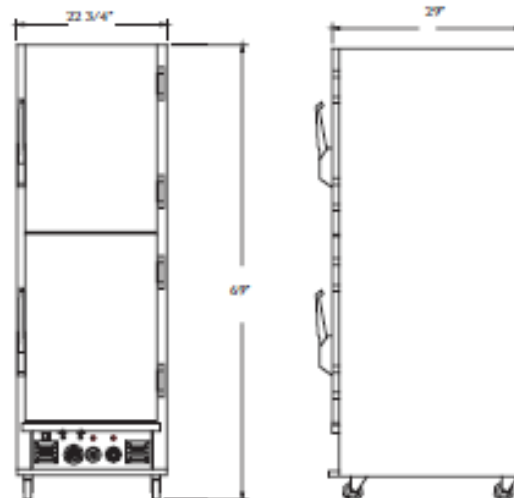
Electrical service connection located at the back of the unit.

Specifications and design subject to change without notice.

DW17 & DPW17



DW118 & DPW118



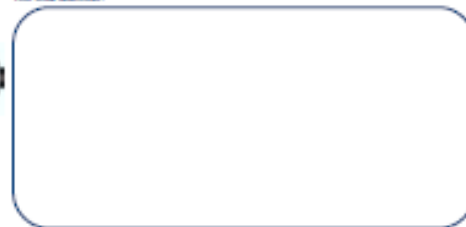
1255, rue Principale
Lafite, Beauport, Québec, Canada G0M 1J0

Telephone: 418-685-3431
Canada: 1-800-463-1636
E-mail: doyon@doyon.qc.ca

Fax: 418-685-3948
U.S.: 1-800-463-4273
Internet: http://www.doyon.qc.ca



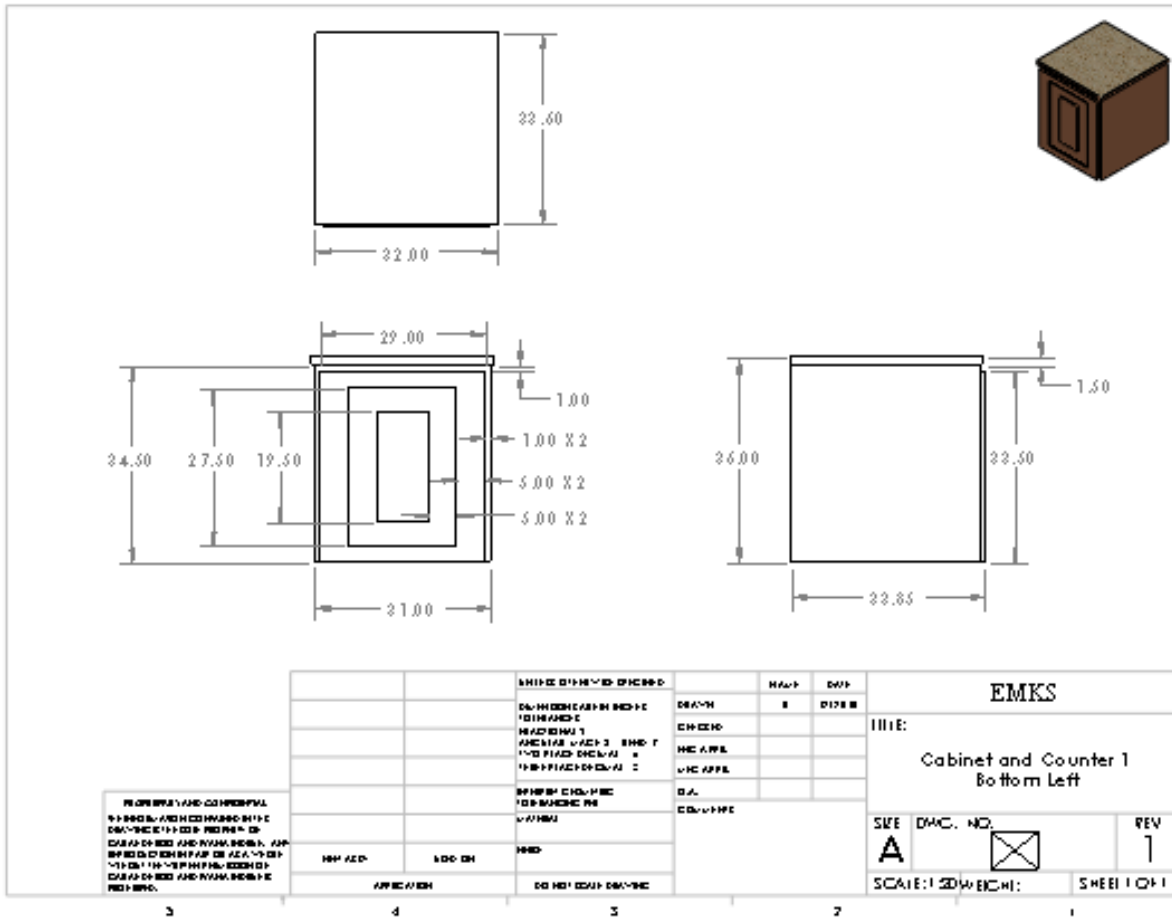
Your local distributor:

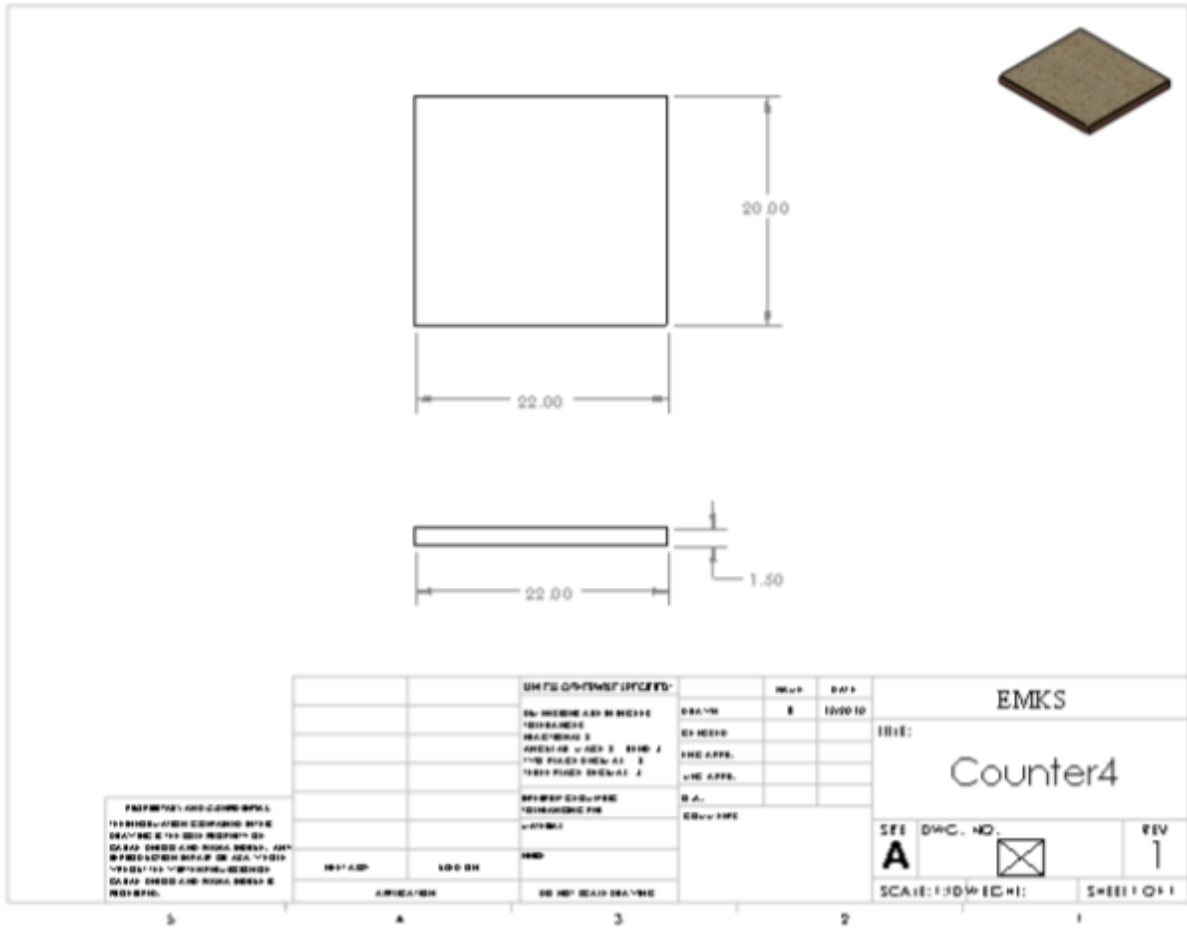


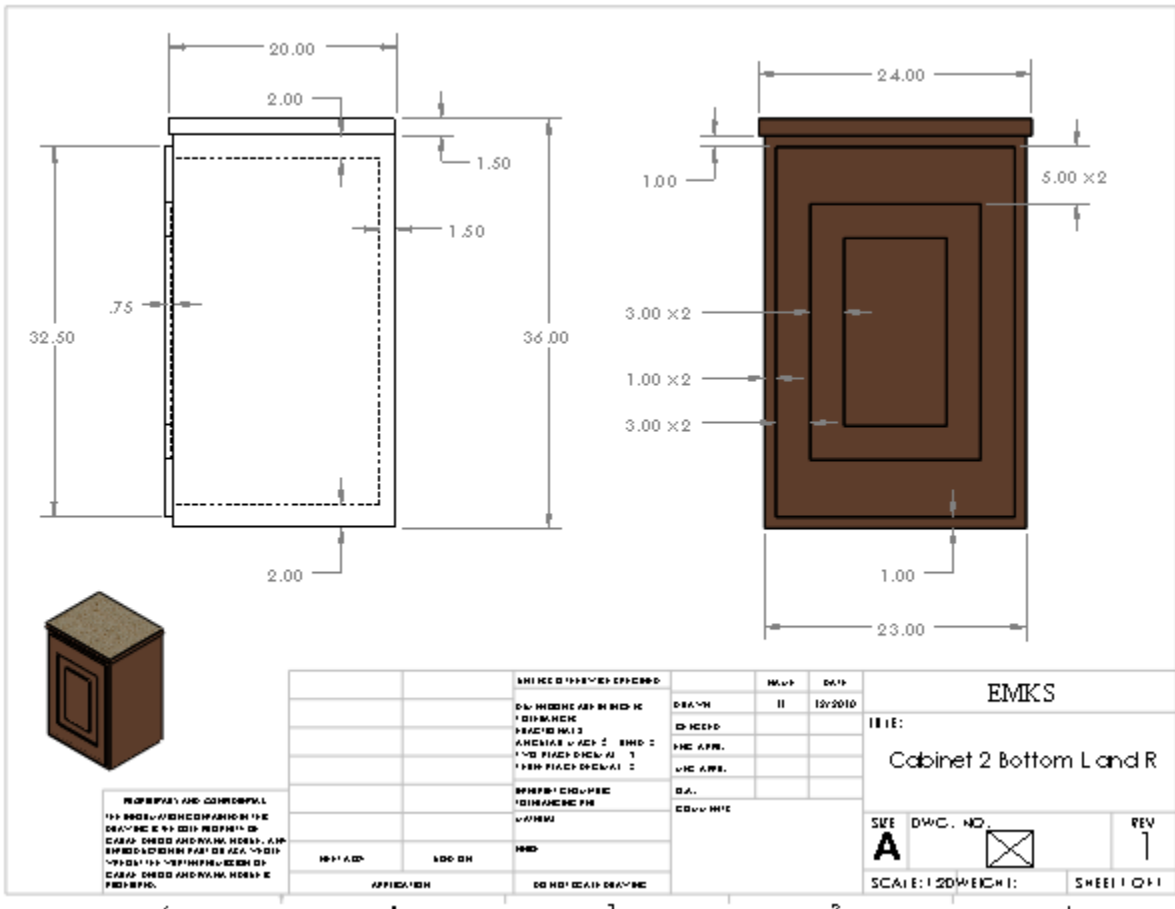
Printed in Canada Rev. 1.2010.02

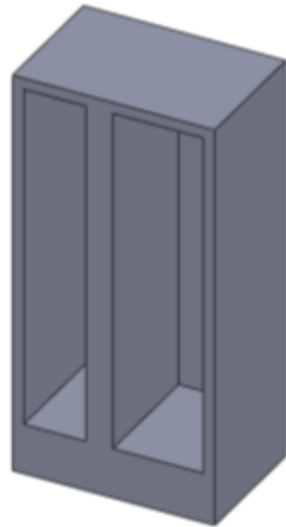
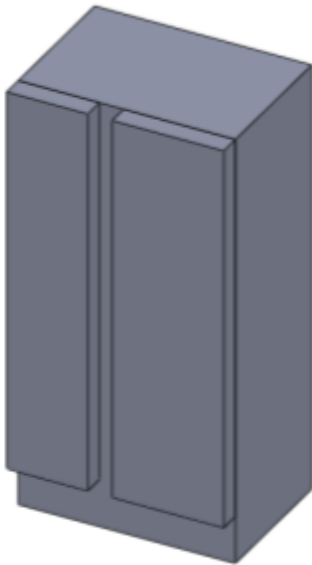
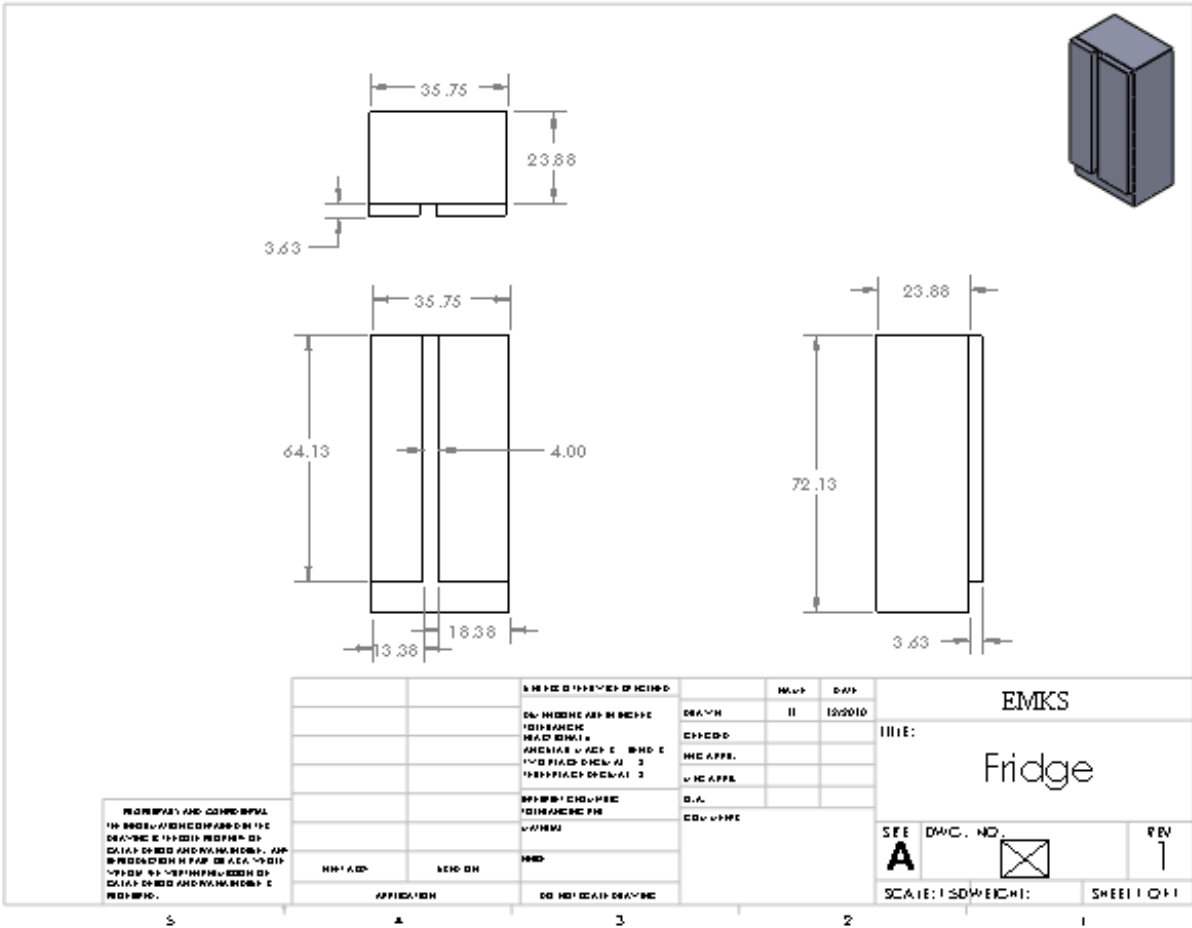
www.doyon.qc.ca

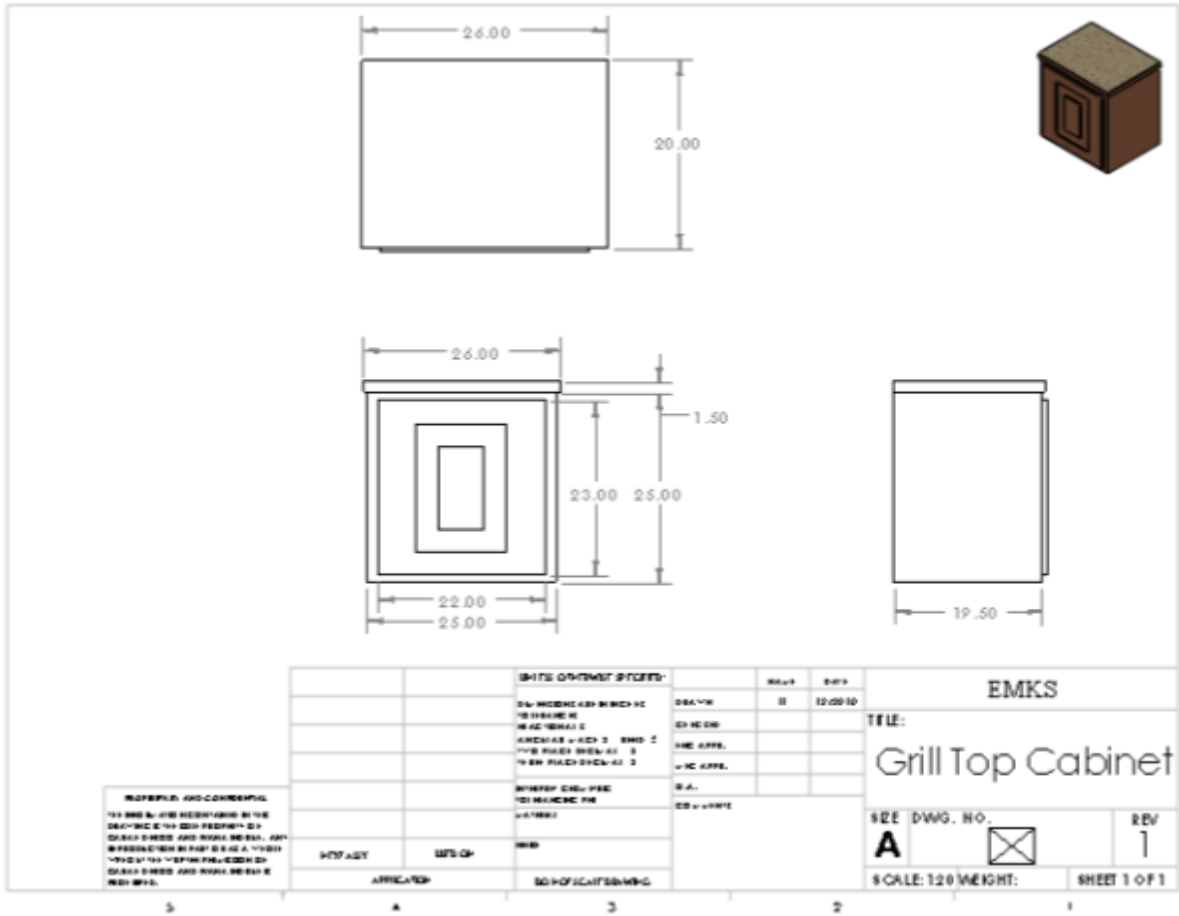
APPENDIX C. SolidWorks Drawings and Models

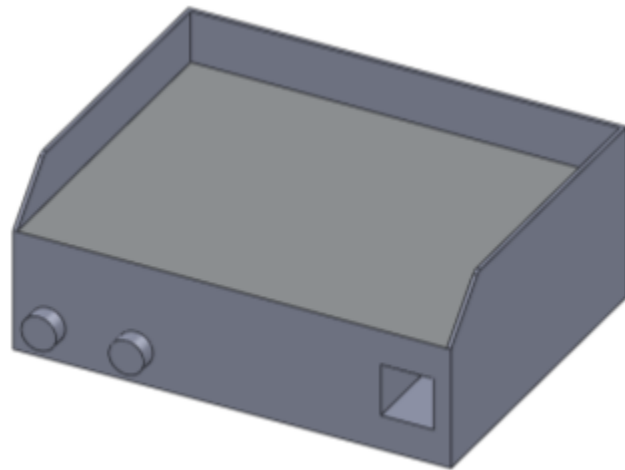
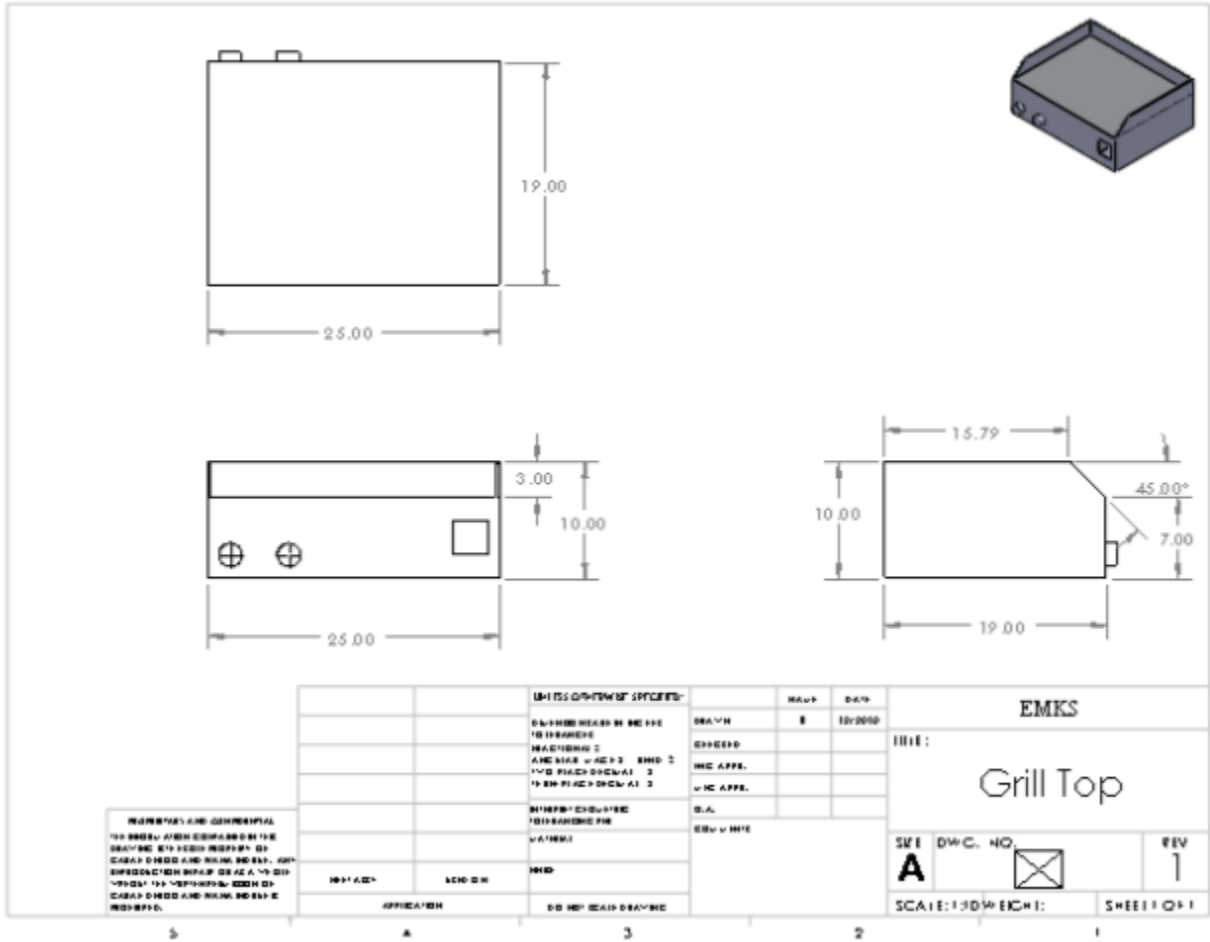


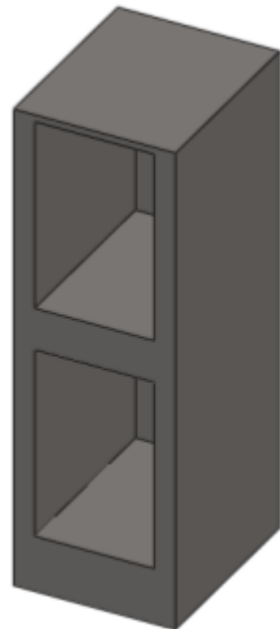
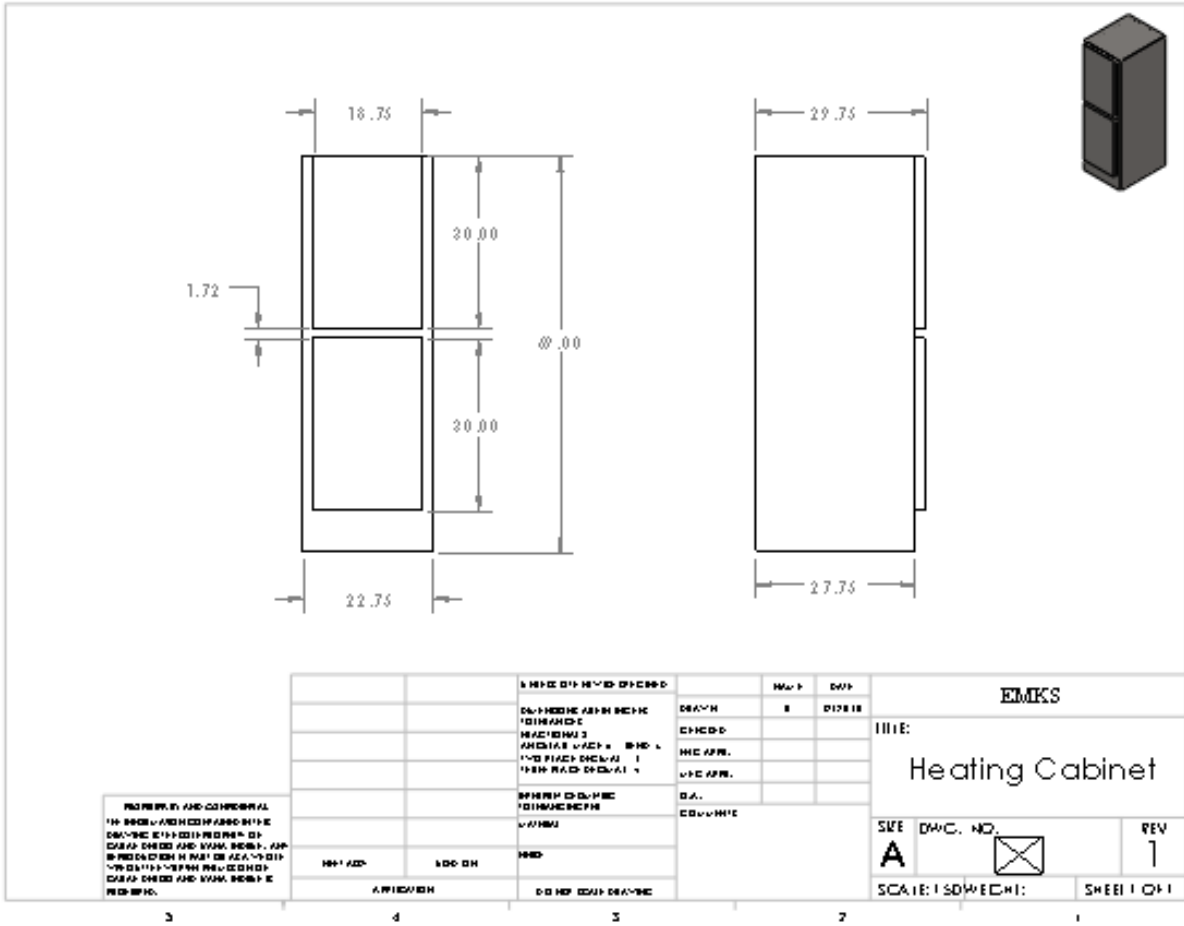


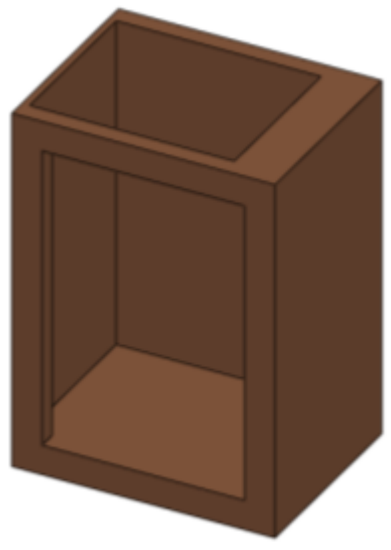
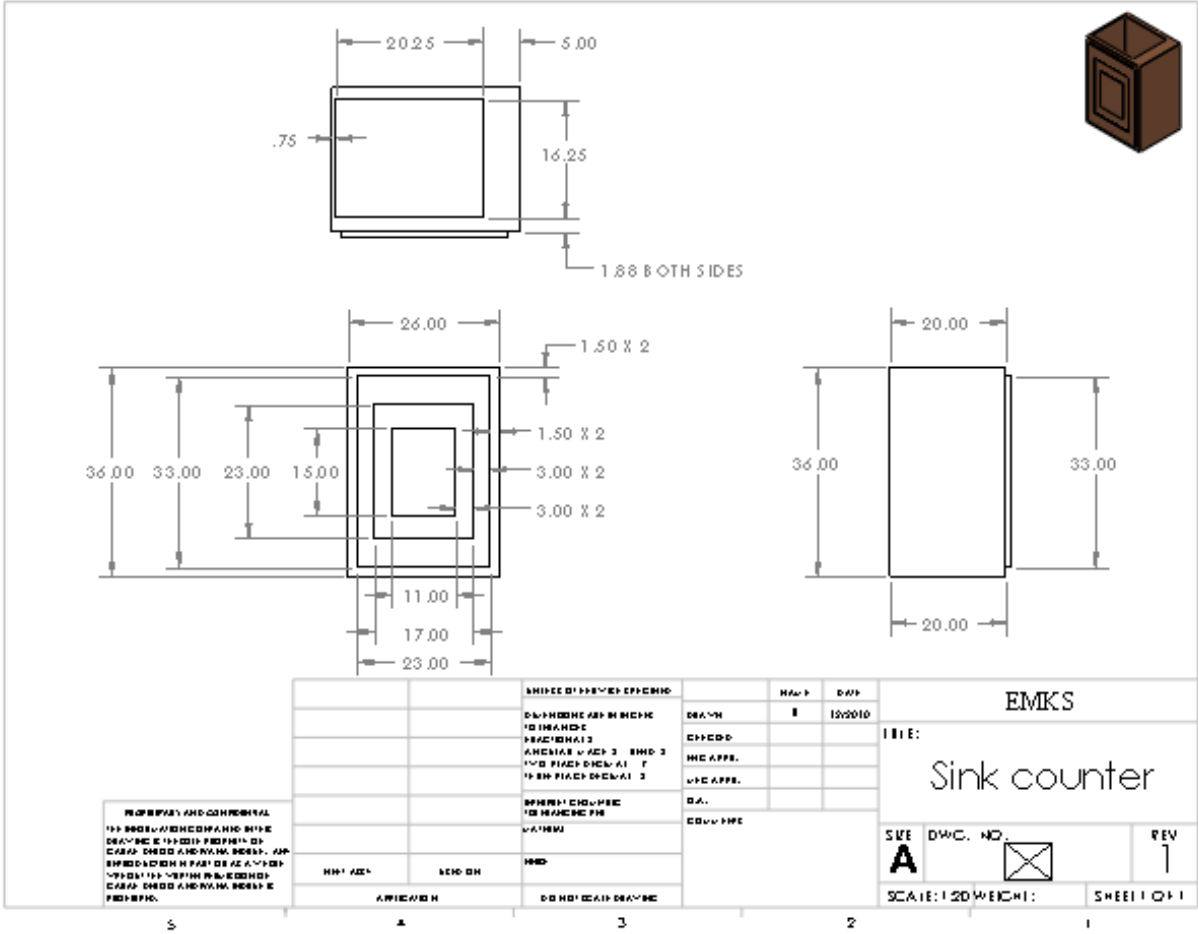


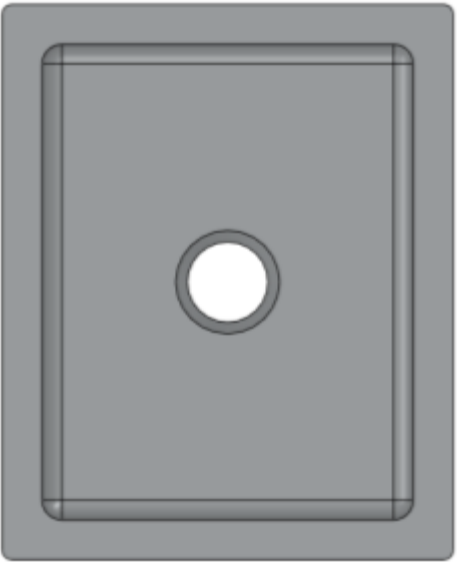
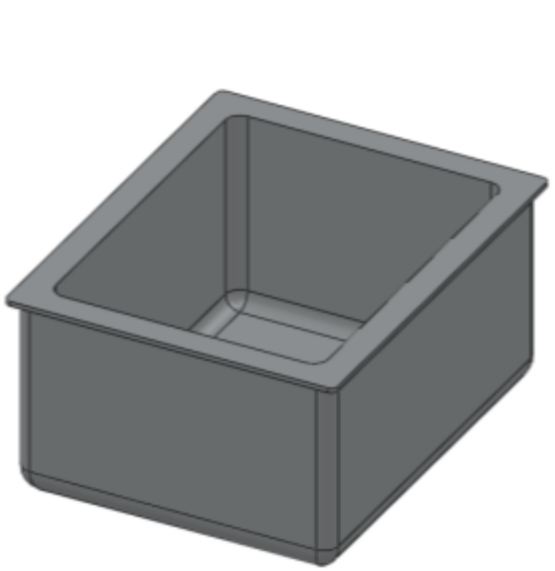
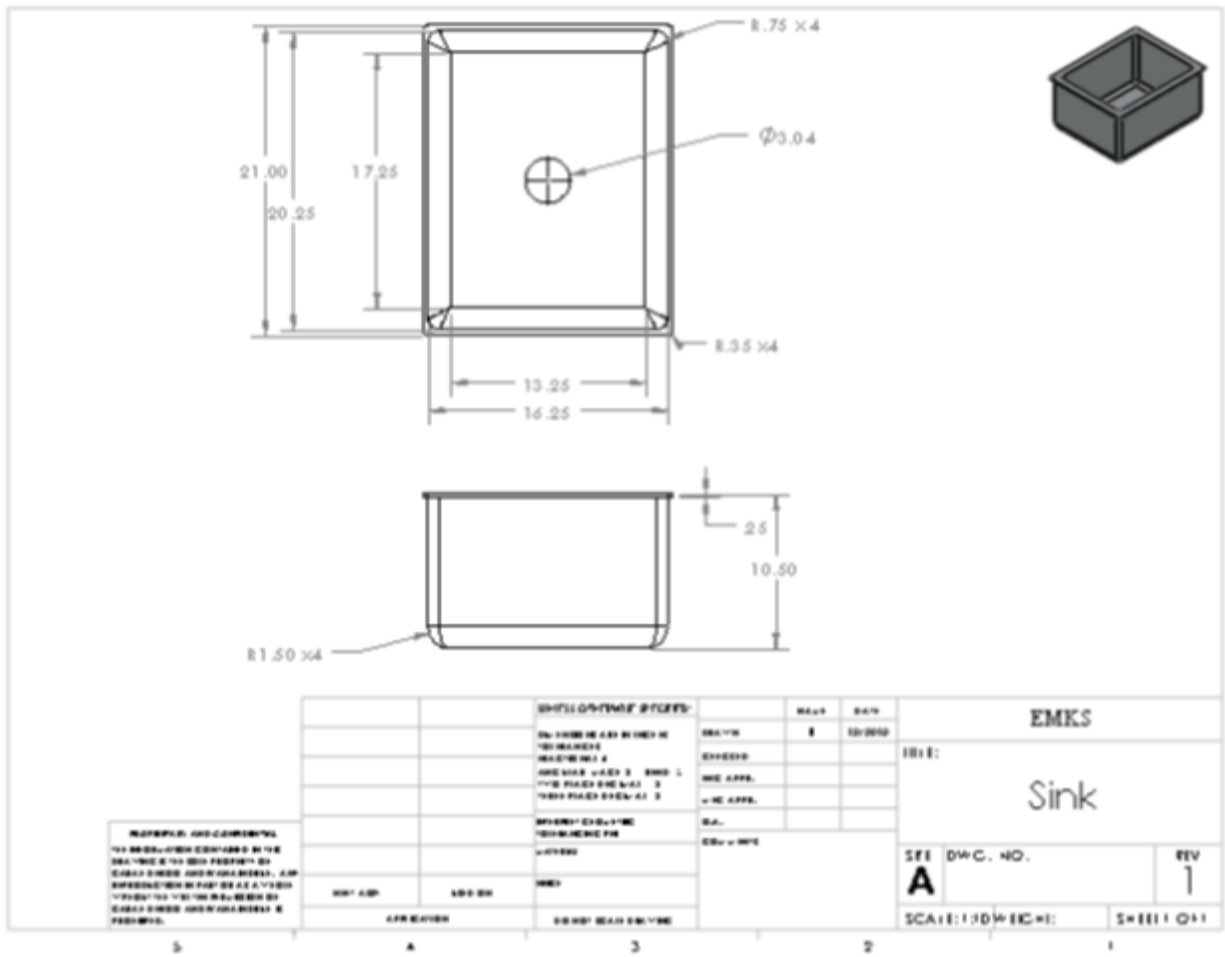


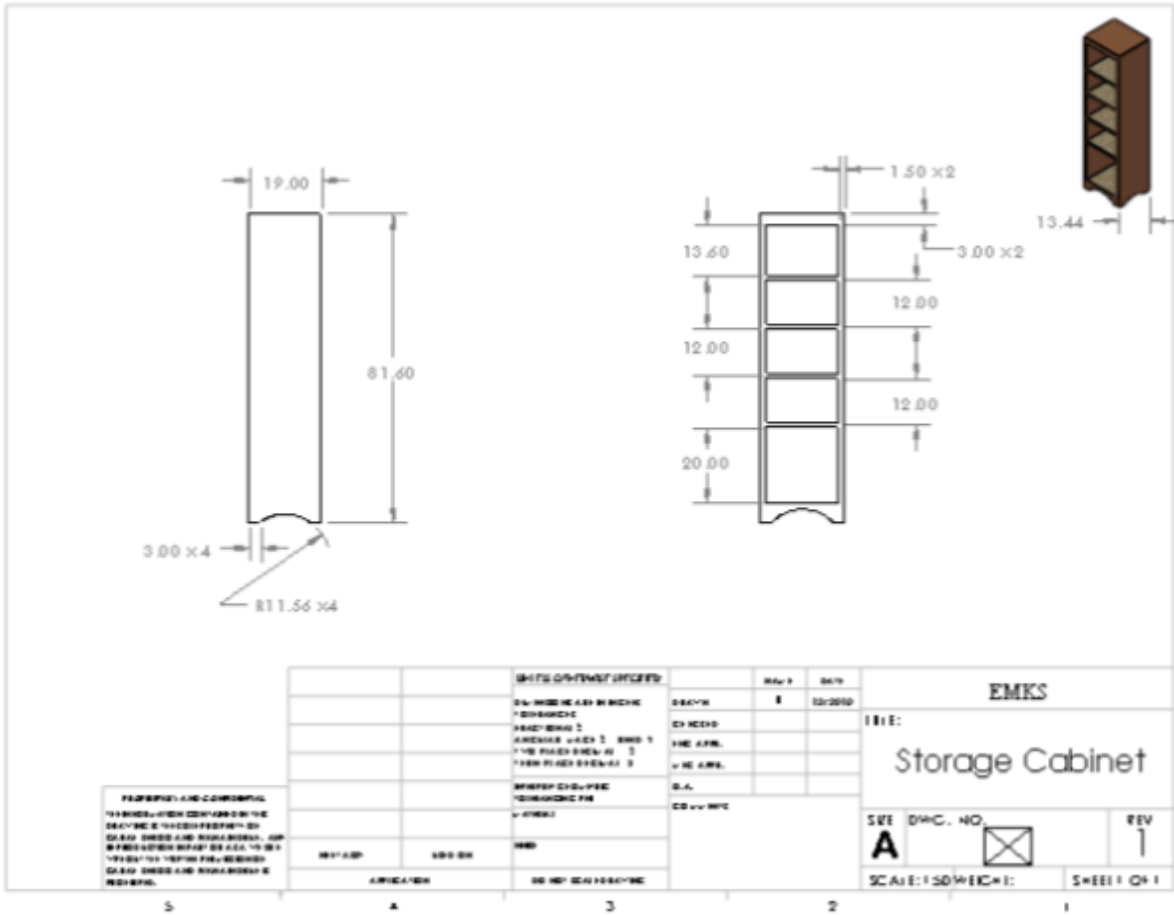


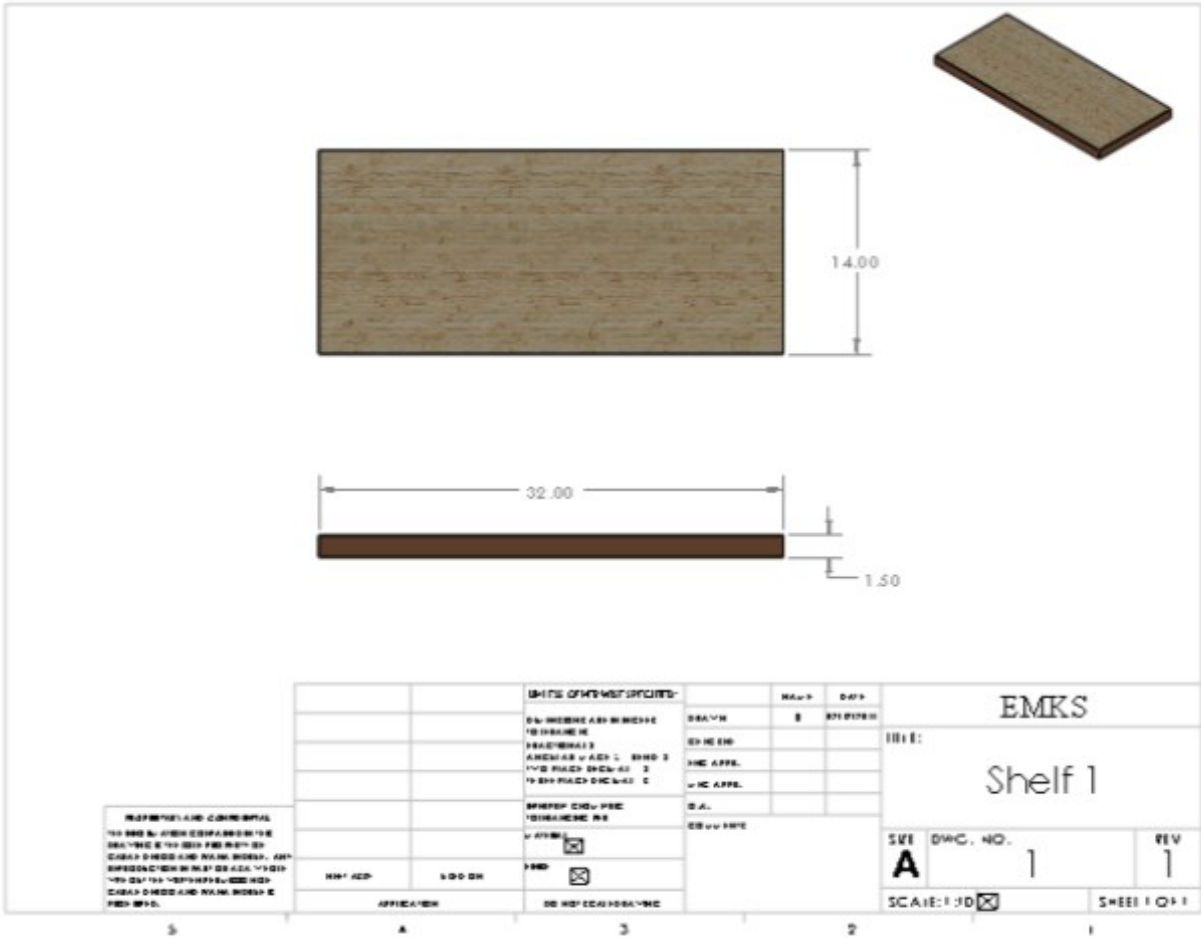


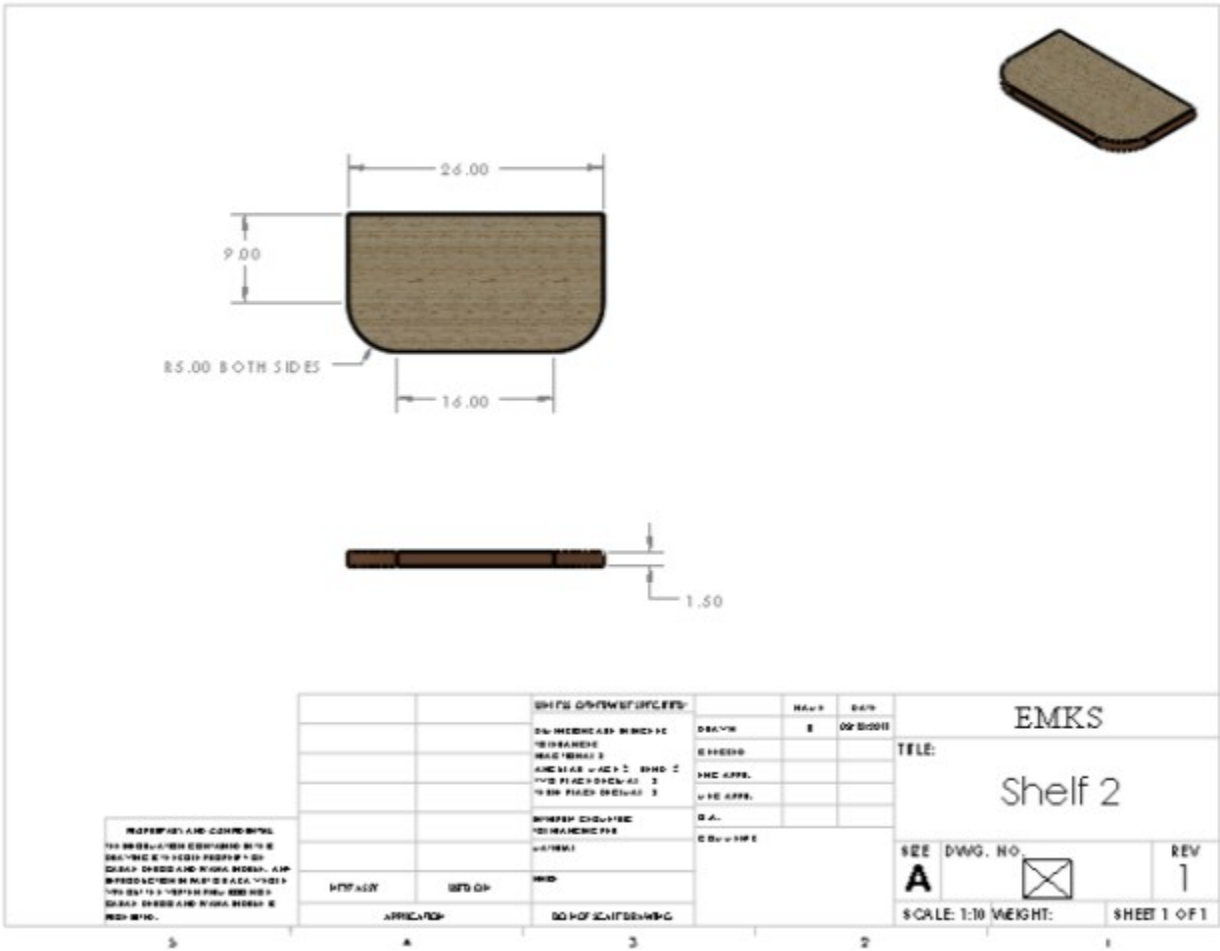


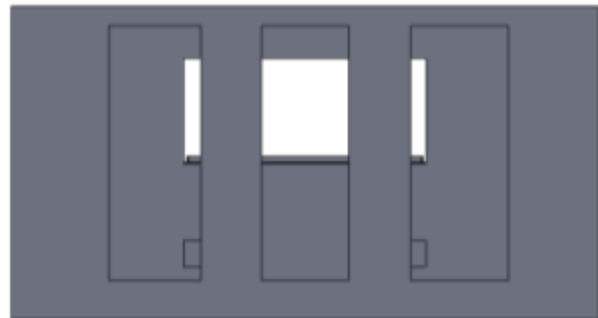
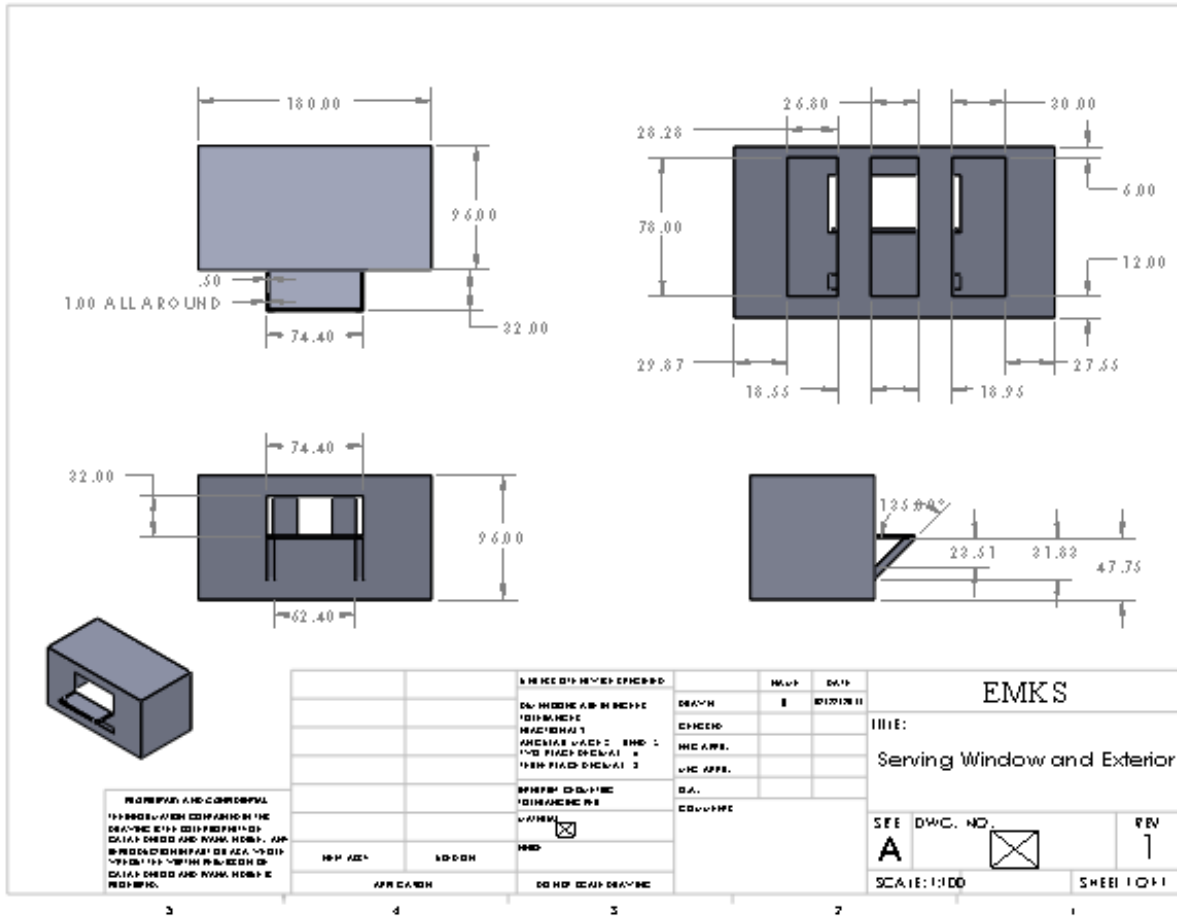


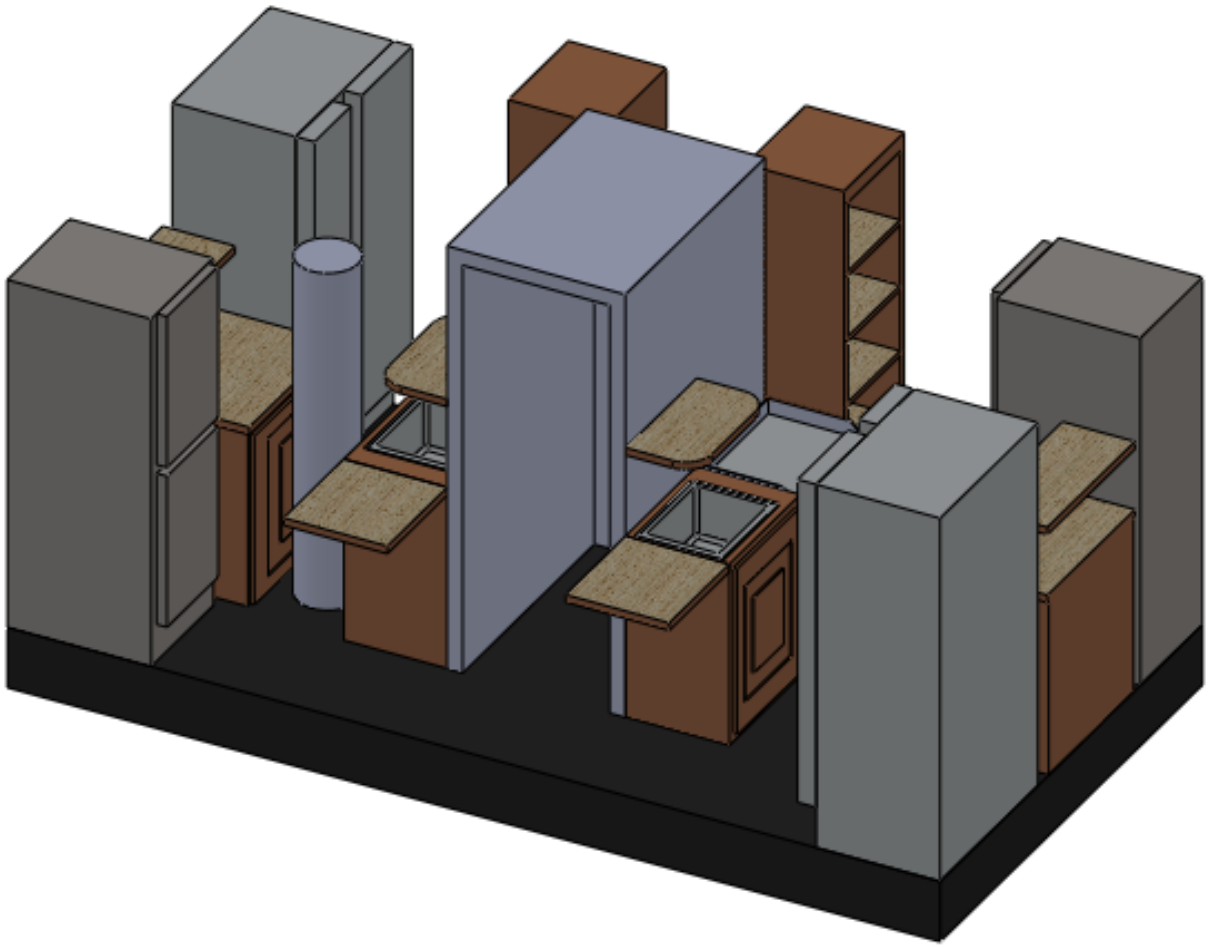












Appendix D. Simple Pendulum MATLAB Code

```
5      % accuracy of ode45 solution), as
6      % and phase portrait.
7      %
8      %Written by Cailah DeRoo & Ivana
9  -   clear all;
10 -   close all;
11
12 -   totaltime=20;           %time, [s]
13 -   g=9.81;                %gravity, [m
14 -   L=6.1;                 %pendulum :
15
16 -   theta0=pi/2;          %Initial ang:
17 -   omega0=sqrt(g/L);     %Natural fre:
18 -   T0=2*pi/omega0        %Simple pendu:
19
20   %Theoretical Non-linear period u:
21 -   k=sin(theta0/2);
22 -   m=k.^2;
23 -   Ttheory=ellipke(m)*T0*2/pi %Peri:
24
25   % Numerical solution of the pend:
26 -   options = odeset('RelTol',1e-6);
27 -   [t,theta1] = ode45(@pendulum larg
```

Continued on the next page...


```

32
33 - for n=1:numel(Tplot)-1
34 -     Ttest(n)=Tplot(n+1)-Tplot(n);
35 - end
36
37 - Tavg=(sum(Ttest)+Tplot(1))/numel(Tplot)    %average period from plot
38
39 % Difference between theory and numerical solutions
40 - Tdiff=Ttheory-Tavg
41
42 % Theoretical solution of the non-linear pendulum
43 - [sn,cn,dn] = ellipj(ellipke(m)-omega0*t,m);
44 - theta_theory=2.0*asin(k*sn);
45
46 %Simple pendulum solution (good only for small angles)
47 - theta_smallang=theta0*cos(omega0*t);
48
49 % Comparison of all solutions
50 - theta_theory_sparse=theta_theory(1:10:length(theta_theory));
51 - t_sparse=t(1:10:length(theta_theory)); %sparsed out for easy comparison
52
53 - plot(t,theta(:,1),'-',t_sparse,theta_theory_sparse,'bo',t,theta_smallang,'r--')
54 -     title('Angular Displacement of Simple, Non-linear Pendulum');
55 -     xlabel('Time, s');
56 -     ylabel('Theta, rad');
57 -     %legend('ODE45 solution','Theoretical Solution','Location');
58 - figure
59 - plot(theta(:,1),theta(:,2))
60 -     axis square
61 -     xlabel('Position, rad');
62 -     ylabel('Ang Velocity, rad/s');
63 -     title('Phase Portrait');

```

```

1  function dtheta = pendulum_large( t, theta )
2  %PENDULUM_LARGE.m
3  % Defines equation of motion for non-linear, simple pendulum. Valid for
4  % all angles.
5  % Solution of equation and period is done in PENDULUM_SOLVER_ALL_ANGLES.
6
7  - g=9.81;    %gravity, [m/s]
8  - L=6.1;    %penulum length, [m]
9
10 - dtheta = zeros(2,1);
11 - dtheta(1) = theta(2) ;
12 - dtheta(2) = -g/L*sin(theta(1));
13
14 - end

```

Appendix E. Double Pendulum MATLAB Code

```
1 function xdot = double_pend( tm, x )
2 %DOUBLE_PEND
3 %Differential equations of motion for a double pendulum, valid at all
4 %angles
5 %Written by Cailah DeRoo & Ivana Indruh, March 2011
6 %
7 % tm      time vector
8 % x      [theta1, theta1 dot, theta2, theta2 dot]
9 % xdot   solution
10
11 g=9.81;      % gravity, [m/s^2]
12 m1=22.7;    % mass 1 (top, hook), [kg]
13 m2=4535.9;  % mass 2 (bottom, load), [kg]
14 L1=3.81;    % length1 (top), [m]
15 L2=3.23;    % length2 (bottom), [m]
16
17 xdot=zeros(4,1);
18
19 xdot(1)=x(2);
20
21 xdot(2) = (-g*(2*m1+m2)*sin(x(1))-m2*g*sin(x(1)-2*x(3))-2*(L2*x(4)^2+...
22         L1*x(2)^2*cos(x(1)-x(3)))*m2*sin(x(1)-x(3)))/...
23         (L1*(2*m1+m2-m2*cos(2*x(1)-2*x(3))));
24
25 xdot(3)=x(4);
26
27 xdot(4) = (2*sin(x(1)-x(3))*(x(2)^2*L1*(m1+m2)+g*(m1+m2)*cos(x(1))+...
28         x(4)^2*L2*m2*cos(x(1)-x(2)))/...
29         (L2*(2*m1+m2-m2*cos(2*x(1)-2*x(3))));
30
31 end
32
```

```

1 %DOUBLE_PEND_SOLVER.m
2 % Solves equations of motion for double pendulum using ode45 and creates
3 % plots of load oscillations, velocities, accelerations, and phase
4 % portraits.
5 %
6 % Written by Cailah DeRoo & Ivana Indruh, March 2011
7 - clear all; close all;
8
9 - totaltime=20; % time, [s]
10 - g=9.81; % gravity, [m/s^2]
11 - m1=22.7; % mass 1 (top, hook), [kg]
12 - m2=4535.9; % mass 2 (bottom, load), [kg]
13 - L1=3.81; % length1 (top), [m]
14 - L2=3.048; % length2 (bottom), [m]
15 - theta1_0=0.01745; % Initial angle of theta1, [rad]
16 - theta2_0=0.01745; % Initial angle of theta2, [rad]
17
18 % Numerical solution of the double pendulum equations
19 - options = odeset('RelTol',1e-4);
20 - [t,x] = ode45(@double_pend,[0 totaltime],[theta1_0 0 theta2_0 0],options);
21 - xdot4=diff(x(:,4)); %load angular acceleration
22
23 %Plot solutions
24 - plot(t,x(:,1),'r-')
25 - xlabel('Time, s');
26 - ylabel('Position, rad');
27 - title('Theta1 Position');
28 - figure
29 - plot(t,x(:,3),'-')
30 - xlabel('Time, s');
31 - ylabel('Postion, rad');
32 - title('Theta2 Load Position');
33 - figure
34 - plot(t,x(:,4),'-')
35 - xlabel('Time, s');
36 - ylabel('Angular Velocity, rad/s');
37 - title('Load Ang. Velocity');
38 - figure
39 - plot(t(1:numel(t)-1),xdot4,'-')
40 - xlabel('Time, s')
41 - ylabel('Angular Acceleration, rad/s^2');
42 - title('Load Ang. Acceleration');
43 - figure
44 - plot(x(:,3),x(:,4),'-')
45 - axis square
46 - xlabel('Postion, rad');
47 - ylabel('Ang Velocity, rad/s');
48 - title('Load Phase Portrait');

```

APPENDIX F. Driven Pendulum MATLAB Code

```

1  function ydot = control_pend_new( tm, y )
2  %CONTROL_PEND_NEW
3  %Differential equations of motion for a simple damped pendulum, with a
4  %driving force acting on the pivot point
5  %Written by Cailah DeRoo & Ivana Indruh, April 2011
6  %
7  %   tm       time vector
8  %   y        [x pos, xpos dot, theta, theta dot]
9  %   ydot     solution
10
11 - mv=45;           % trolley mass, [kg, approx 100 lb]
12 - mk=4535.9;      % container mass, [kg]
13 - L=6.096;       % length, [m]
14 - c=0.085;       % trolley damping (values of 0.01-0.085)
15 - ct=0.085;      % helicopter damping
16 - k=1e9;         % torsional stiffness [estimated from steel, A=0.1m^2, L=2m]
17 - kt=1;         % helicopter stiffness
18 - Fp=0;         % Force acting on pivot
19 - uk=1e3;       % Control force amplitude
20 - Fk=0;         % External forces acting on container
21 - g=9.81;       % Gravity, [m/s^2]
22 - T=4;         % Period
23 - omega=2*pi/T; % Driving frequency
24
25 - a=mv+mk;
26 - b=mk*L*cos(y(3));
27 - d=mk*L^2;
28 - e=Fp+mk*L*y(4)*y(4)*sin(y(3))-c*y(2)-k*y(1);
29 - f=uk*cos(tm*omega+0.5*T)-Fk*cos(y(3))-mk*g*L*sin(y(3))-ct*y(4)-kt*y(3);
30
31 %Define coupled equations of motion for trolley position and load angular
32 %displacement
33 - ydot=zeros(4,1);
34
35 - ydot(1)=y(2);
36
37 - ydot(2)=(f*b-e*d)/(b*b-a*d);
38
39 - ydot(3)=y(4);
40
41 - ydot(4)=(-a*f+e*b)/(b*b-a*d);
42
43 - end

```

```

1 %CONTROL_PEND_SOLVER_NEW.m
2 % Solves equations of motion for simple, damped pendulum using ode45 and
3 % creates plots of load oscillations and phase portraits.
4 %
5 % Written by Cailah DeRoo & Ivana Indruh, April 2011
6 - clear all; close all;
7
8 - totaltime=50; % time, [s]
9 - xpos_0=0; % Initial trolley position, [m]
10 - theta_0=0.01; % Initial angle, [rad]
11
12 % Numerical solution of the pendulum equations of motion
13 - options = odeset('RelTol',1e-4);
14 - [t,y]=ode45(@control_pond_new,[0 totaltime],[xpos_0 0 theta_0 0],options);
15
16 %Plot solutions
17 - plot(t,y(:,1),'r-')
18 - xlabel('Time, s');
19 - ylabel('Position, m');
20 - title('Trolley Postition');
21 - figure
22 - plot(t,y(:,3),'r-')
23 - xlabel('Time, s');
24 - ylabel('Position, rad');
25 - title('Load Angular Postition');
26 - figure
27 - plot(y(:,3),y(:,4),'-')
28 - axis square
29 - xlabel('Postion, rad');
30 - ylabel('Ang Velocity, rad/s');
31 - title('Load Phase Portrait');

```

REFERENCES

- [1] American Red Cross, 2010, "Bringing Help, Bringing Hope: The American Red Cross Response to Hurricanes Katrina, Rita and Wilma," .
- [2] American Red Cross, 2010, "The American Red Cross," **2011**(01/23) .
- [3] Anonymous 2011, "Disaster Relief Organizations," **2011**(02/2011) .
- [4] Danals, D., 2008, "US Navy 080912-N-8907D-170," **2011**(02/05/11) .
- [5] Anonymous 2000, "Heavy Flooding Hits Miami," **2011**(02/01) .
- [6] American Red Cross, 2006, "A Year of Healing: The American Red Cross Response to Hurricanes Katrina, Rita and Wilma," .
- [7] Salvation Army, 2006, "Salvation Army Reflects on Largest Disaster Response Ever at One-Year Anniversary of Hurricane Katrina," .
- [8] Bertuca, D. J., 2010, "Indian Ocean Tsunami Disaster December 26, 2004 and Reconstruction," **2011**(02/02) .
- [9] Green Flash Production Sound, "Hurricane Katrina," **2011**(02/02) .
- [10] Brunner, B., 2007, "Tsunami Factfile," **2011**(02/02) .
- [11] Calstate L.A. Geology Office, "Environmental Geology of Developing Nations," **2011**(02/02) .
- [12] Department of Defense, 2009, "DoD Humanitarian Daily Rations," **2011**(01/29) pp. 2.
- [13] Anonymous "Enduring Freedom Humanitarian Aid to Afganistan," **2011**(02/01) pp. 1.
- [14] Basashi-san, M., "Haiku Duel," **2011**(02/01) .
- [15] Nationwide Mobile Kitchens, "Mobile Kitchens," **2011**(02/03) .
- [16] Deployed Resources LLC, 2011, "Containerized Kitchen Unit," **2011**(02/03) .
- [17] Campbell, B.J., 2008, "Manufacturability and Reliability of a Transportable Containerized Kitchen," .
- [18] Natick Research, Development and Engineering Center, 1998, "Performance Specifications: Containerized Kitchen," US Army, MIL-PRF-32026(GL), .

- [19] Witherspoon, D. A., 2006, "Cooks Put New Mobile Kitchen to Test," Military.Com, pp. 02/02/11.
- [20] Casem, G., 2010, "Blackhorse Cooks Rewarded for Frying Competition," **2011**(02/02) .
- [21] W&K Container, 2009, "Specifications and Shipping," **2011**(02/03) .
- [22] Campbell, K., 2009, "Airbus Search Operation Now a Stern Routine," Creamer Media's Engineering News Online, .
- [23] Anonymous 2009, "Pegasus Sling Loads," **2011**(02/01) .
- [24] Hornyak, T., 2010, "Wobble-Proof Navy Crane can Unload Cargo at Sea," pp. 02/01/11.
- [25] Global Security, 2006, "CH 47D - CHINOOK Specifications," **2011**(02/03) .
- [26] Stuckey, R.A., 2008, "Helicopter Slung-Load Simulation Toolbox for use with MATLAB," Australian Government Department of Defense, DSTO-TN-0855, .
- [27] Guillory, G., 2011, "Different, Yet the Same," **2011**(02/03) .
- [28] Flight International, 2006, "Airbus A380 Clears European and US Certification Hurdles for Evacuation Trial," **2011**(02/03) .
- [29] Catering:Airline, "Links between Kitchen and Service Areas," **2010**(11/22) .
- [30] Catering:Airline, "Receive and Store Stock," **2010**(11/22) .
- [31] Food and Drug Administration, 2009, "Food Code," U.S. Public Health Service, .
- [32] General Electric Company, 2011, "GE Profile PSIC5RGXBV 24.6 Cu. Ft. Side-by-Side Refrigerator," **2011**(02/09) .
- [33] Doyon, 2007, "DPWI18 Insulated Holding Cabinet," **2011**(02/09) .
- [34] Builders Square, 2010, "Uniworld UGR-3E 25 Inch H.D. Griddle," **2011**(02/09) .
- [35] Generac, 2010, "GP Series 5500 Watt," **2011**(02/09) .
- [36] Plumbers Surplus, L., 2011, "Just Deep Single Bowl Stylist Group," **2011**(02/09) .
- [37] JetBlue Airways, 2011, "Our Planes," **2011**(02/10) .

- [38] Yunus A. Cengel, Robert H. Turner, John M. Cimbala, 2008, "Fundamentals of Thermal-Fluid Sciences," Mc-Graw Hill, New York, NY 10020, pp. 625-646.
- [39] Stuckey, R. A., 2002, "Mathematical Modelling of Helicopter Slung-Load System," **2011**.
- [40] Reddy, K. R., Truong, T. T., Stuckey, R. A., 2007, "Dynamic Simulation of a Helicopter Carrying a Slung Load," .
- [41] Cicolani, L. S., and Ehlers, M. G. E., 2002, "Modeling and Simulation of a Helicopter Slung Load Stabilization Device," Anonymous American Helicopter Society International, .
- [42] Bisgaard, M., la Cour-Harbo, A., and Dimon Bendtsen, J., 2009, "Swing Damping for Helicopter Slung Load Systems using Delayed Feedback," .
- [43] Abdel-Rahman, E., Nayfeh, A. H., and Masoud, Z. N., 2003, "Dynamics and Control of Cranes: A Review," Journal of Vibration and Control, **9**(7) pp. 863-908.
- [44] Chin, C., 2001, "Nonlinear Dynamics of a Boom Crane," Journal of Vibration and Control, **7**(2) pp. 199-220.
- [45] Smith, R., 2011, "Container Gantry Crane," **2011**(02/18) .
- [46] Nebrot, 2008, "Tower Crane," **2011**(02/21) .
- [47] ENI Saipem, 2004, "Saipem 7000," **2011**(02/21) .
- [48] Masoud, Z. N., Nayfeh, A. H., and Nayfeh, N. A., 2005, "Sway Reduction on Quay-Side Container Cranes using Delayed Feedback Controller: Simulations and Experiments," Journal of Vibration and Control, **11**(8) pp. 1103-22.
- [49] Masoud, Z. N., Nayfeh, A. H., and Al-Mousa, A., 2003, "Delayed Position-Feedback Controller for the Reduction of Payload Pendulations of Rotary Cranes," Journal of Vibration and Control, **9**(1-2) pp. 257-77.
- [50] Nayfeh, N. A., and Baumann, W. T., 2008, "Nonlinear Analysis of Time-Delay Position Feedback Control of Container Cranes," Nonlinear Dynamics, **53**(1-2) pp. 72-85.
- [51] Henry, R. J., Masoud, Z. N., Nayfeh, A. H., 2001, "Cargo Pendulation Reduction on Ship-Mounted Cranes Via Boom-Luff Angle Actuation," Journal of Vibration and Control, **7**(8) pp. 1253-1264.
- [52] Abdel-Rahman, E., and Nayfeh, A. H., 2002, "Pendulation Reduction in Boom Cranes using Cable Length Manipulation," Nonlinear Dynamics, **27**(3) pp. 255-69.

[53] Arthur, Wallace & Fenster, Saul K., 1969, "Mechanics," Holt, Rinehart and Winston, Inc, New York, .

[54] Taylor, J.R., 2005, "Classical Mechanics," University Science Books, Sausalito, CA, .

[55] Weisstein, E. W., 2011, "Elliptic Integral of the First Kind," **2011**(03/28) .